

Utah State University

DigitalCommons@USU

---

All Graduate Theses and Dissertations

Graduate Studies

---

12-2008

## Dechlorinating and Iron Reducing Bacteria Distribution in a Trichloroethene Contaminated Aquifer

Carmen Lourdes Yupanqui Zaa  
*Utah State University*

Follow this and additional works at: <https://digitalcommons.usu.edu/etd>

 Part of the [Environmental Engineering Commons](#), and the [Microbiology Commons](#)

---

### Recommended Citation

Yupanqui Zaa, Carmen Lourdes, "Dechlorinating and Iron Reducing Bacteria Distribution in a Trichloroethene Contaminated Aquifer" (2008). *All Graduate Theses and Dissertations*. 41.  
<https://digitalcommons.usu.edu/etd/41>

This Thesis is brought to you for free and open access by the Graduate Studies at DigitalCommons@USU. It has been accepted for inclusion in All Graduate Theses and Dissertations by an authorized administrator of DigitalCommons@USU. For more information, please contact [digitalcommons@usu.edu](mailto:digitalcommons@usu.edu).



DECHLORINATING AND IRON REDUCING BACTERIA DISTRIBUTION IN A  
TRICHLOROETHENE CONTAMINATED AQUIFER

by

Carmen Lourdes Yupanqui Zaa

A thesis submitted in partial fulfillment  
of the requirements for the degree

of

MASTER OF SCIENCE

in

Civil and Environmental Engineering

Approved:

---

Darwin L. Sorensen  
Major Professor

---

R. Ryan Dupont  
Committee Member

---

Jeanette M. Norton  
Committee member

---

Joan E. McLean  
Committee Member

---

Byron R. Burnham  
Dean of Graduate Studies

UTAH STATE UNIVERSITY  
Logan, Utah

2008

## ABSTRACT

Dechlorinating and Iron-Reducing Bacteria Distribution in a Trichloroethene-  
Contaminated Aquifer

by

Carmen Lourdes Yupanqui Zaa, Master of Science

Utah State University, 2008

Major Professor: Dr. Darwin L. Sorensen

Department: Civil and Environmental Engineering

The Operable Unit 5 (OU 5) area of Hill Air Force Base currently has two trichloroethene-contaminated groundwater plumes underneath residential areas in Sunset and Clinton, Utah. Bioremediation by biological reductive dechlorination can be an important mechanism for the removal of chlorinated compounds from the plumes. The presence of suitable bacteria to carry on reductive dechlorination is the key in the bioremediation process. The goal of this study was to determine the distribution and population density of the 16S rRNA genes of *Bacteria*, *Dehalococcoides ethenogenes*, *Desulfuromonas michiganensis*, *Geobacter spp* and *Rhodoferrax ferrireducens*-like bacteria, as well as the functional genes trichloroethene reductive dehalogenase (*tceA*) and vinyl chloride reductase gene (*vcrA*). This study also evaluated the influence of the physical-chemical properties of the OU 5 aquifer material on the observed bacterial distribution.

Twenty OU 5 soil cores were obtained from a 14-ha area that included a trichloroethene (TCE) plume. DNA was extracted from each core. Molecular analysis with qRT-PCR was used to quantify the densities of the mentioned 16S rRNA and functional genes. Separately, total arsenic and iron in the II and II+III oxidation states were extracted by two methods (HCl and hydroxylamine HCl in HCl) in each core. Concentrations of TCE, cis-dichloroethene (cis-DCE), vinyl chloride (VC) and ethane in well water were included.

*Dehalococcoides* population density was low and its distribution was uneven with densities lower than  $3.2 \times 10^4$  copies/g (detection limit of  $2.5 \times 10^3$ ). *D. michiganensis* distribution was not uniform but was clustered near the TCE-source area with densities of  $7.9 \times 10^3$ - $1 \times 10^5$  copies/g (detection limit of  $6.3 \times 10^3$ ). *Geobacter* spp. distribution was uneven but broader, with densities of  $4 \times 10^3$ - $1.6 \times 10^6$  copies/g (detection limit of  $3.2 \times 10^3$ ). The *vcrA* gene distribution was relatively uniform and broad. Densities were the lowest measured (detection limit of 63 copies/g). *TceA* was measured in two cores with densities close to detection limit of  $1.6 \times 10^3$  copies/g. *Rhodoferrax ferrireducens*-like bacteria had a broader distribution with the highest densities of  $1.6 \times 10^6$ - $1.3 \times 10^8$  copies/g (detection limit of  $7.9 \times 10^3$ ). Total *Bacteria* were measured in all cores with densities  $3.2 \times 10^4$ - $3.2 \times 10^6$  copies/g (detection limit of  $1 \times 10^3$ ).

Three multivariate statistical methods were used to determine the effect of physical-chemical properties on the target gene distributions. Cluster and discriminant analysis selected five properties (pH, sand and silt content,  $\text{NO}_3^-$ -N and  $\text{NH}_4^+$ -N) as the most discriminating factors among thirty-one physical-chemical properties. However, no effect in the bacterial distribution was observed. The tree classification method identified

nine variables that described higher or lower densities of the target genes. Variables such as *Bacteria*, Fe(II+III) (by hydroxylamine HCl in HCl), organic matter and cis-DCE were selected by the method.. All methods agreed on the selection of pH and sand content as the physical/chemical factors most influencing in the bacterial distribution.

Based on the findings of low densities of dechlorinating bacteria and dechlorinating-associated functional genes, low available carbon donor and sandy mineral composition, the partial TCE-dechlorination at this site can be ascribed to the nature of the site and incomplete set of required factors for complete reductive dechlorination.

(242 pages)

## ACKNOWLEDGMENTS

I want to dedicate this thesis to my parents for their encouragement, moral support, and patience as I worked my way from the initial proposal through writing this final document.

I want to make special thanks to my advisor, Dr. Darwin Sorensen, for all his guidance, help, and patience during the development of this thesis. Also, I want to express my gratitude to all my committee members, Joan McLean and Drs. Jeanette Norton and Ryan Dupont, for their advice and encouragement throughout the entire process. Also, I want to thank them for giving me the opportunity to work at the Utah Water Research Laboratory, being part of their research group.

Thanks to all the people who worked with me at the Lab and to Andrejus Parfionovas for his advice and help in the statistical part of this research.

Carmen Yupanqui

## CONTENTS

	Page
ABSTRACT .....	ii
ACKNOWLEDGMENTS .....	v
LIST OF TABLES .....	viii
LIST OF FIGURES .....	x
CHAPTER	
1. INTRODUCTION .....	1
2. HYPOTHESES AND OBJECTIVES .....	3
3. LITERATURE REVIEW .....	5
In Situ Anaerobic Reductive Dechlorination of Chloroethenes .....	5
Dehalorespiring Microbial Communities .....	7
Reductive Dehalogenase Enzymes .....	9
Iron Inhibition in TCE-Reduction .....	10
Dissimilatory Iron-Reducing Bacteria in OU 5 Sediment .....	12
Iron Forms in Aquifer Systems .....	12
Groundwater Bioremediation in OU 5 .....	13
Effect of Physical and Chemical Factors on Dehalorespiring Microorganisms .....	14
Molecular Biology Techniques to Determine the Presence of Dechlorinating and Iron- Reducing Bacteria .....	15
The OU 5 Area of Hill Air Force Base .....	26
Site Characterization of OU 5 .....	27
4. MATERIALS AND METHODS .....	31
Aquifer Sampling in OU 5 Area of HAFB .....	31
Sample Collection, Handling and Storage .....	34
Soil DNA Extraction of OU5 Aquifer Core Samples .....	35
Real-Time PCR Detection of the Target	

	DNA in the OU 5 Soil Cores.....	35
	Physical and Chemical Analysis of the OU 5 Aquifer Material.....	40
	TCE and Dissolved Oxygen Concentrations in the OU5 Study Area.....	41
	Arsenic and Iron Extraction Methods from the OU 5 Aquifer Material.....	41
	QRT-PCR Quality Control Criteria.....	43
5.	ANALYSIS OF THE DATA .....	47
6.	RESULTS.....	51
	Gene Limits of Quantitation.....	51
	Gene Distribution and Population Density .....	52
	Physical and Chemical Properties of the OU 5 Aquifer Material.....	63
	Concentration of TCE and Other Chlorinated Compounds in the Study Area .....	66
	Iron and Arsenic Reducible Forms .....	67
	Dissolved Oxygen Concentration in the OU 5 Study Area.....	70
	Clustering Analysis.....	70
	Discriminant Analysis.....	70
	Regression Tree Classification.....	75
7.	DISCUSSION.....	80
8.	CONCLUSIONS.....	85
9.	ENGINEERING SIGNIFICANCE.....	88
10.	FUTURE STUDIES.....	90
	REFERENCES.....	91
	APPENDICES.....	97
	Appendix A: Tolerance Limits of the Studied 16S rDNA Primers.....	98
	Appendix B: qRT-PCR Results of the Target 16S rDNA Primers in the Soil Core Samples .....	114
	Appendix C: Iron and Arsenic Data in the OU 5 Aquifer Core Samples .....	222
	Appendix D: Discriminant Analysis and ANOVA results.....	227

## LIST OF TABLES

Table	Page
3.1	Cycle Parameters in the PCR Procedure..... 17
4.1	Primer List for Organisms and Functional Genes Quantified in This Study..... 36
4.2	Twenty Possible Bacteria Amplified in qRT-PCR by <i>Rhodoferax</i> 16S rDNA Primer Set ..... 36
4.3	Source of the Standard DNA Material Used in This Study ..... 37
4.4	QRT-PCR Program Used in This Study ..... 39
4.5	Optimized Annealing Temperatures (T <sub>m</sub> ) ..... 39
4.6	Assigned Closest Well to Each Sampling Point in the Study Area and the Sampling Data of TCE, cis-DCE, and VC Concentrations..... 36
5.1	All Measured Variables Included in Each Multivariate Method..... 48
6.1	Tolerance Limit of 16S rDNA Primers..... 51
6.2	Density of Bacteria in the Study Area of OU 5 in DNA Copies per g Dry Soil ..... 53
6.3	Frequency of Quantifiable, Positive Not Quantifiable, and Negative Results for <i>Dehalococcoides</i> sp in the OU 5 Study Area..... 55
6.4	Frequencies of Quantifiable, Positive Not Quantifiable, and Negative Results for <i>D. Michiganensis</i> in the OU 5 Study Area.. ..... 56
6.5	Frequency of Quantifiable, Positive Not Quantifiable, and Negative Results for <i>Geobacter</i> sp. in the OU 5 Study Area..... 58
6.6	Frequency of Positives, Positive Not Quantifiable, and Negative Results for <i>Rhodoferax ferrireducens</i> -like Bacteria in the OU 5 Study Area. .... 59
6.7	Frequency of Positives, Positive Not Quantifiable, and Negative Results for <i>vcrA</i> Functional Gene in the OU 5 Study Area.. ..... 61
6.8	Frequency of Positives, Positive Not Quantifiable, and Negative

	Results for <i>tceA</i> Functional Gene in the OU 5 Study Area.....	62
6.9	ICP Analysis for Total Element Composition of the OU 5 Core Aquifer Samples .....	64
6.10	Physical and Chemical Properties of the OU 5 Core Aquifer Samples .....	65
6.11	Concentration of TCE, 1,1-DCE, 1,2-cisDCE and VC in the OU 5 Study Area .....	66
6.12	Mean of the Discriminating Variables in Each Clustering Group.....	73
6.13	P+PNQ Results of the Target Genes in Each Cluster Group .....	74

## LIST OF FIGURES

Figure		Page
3.1	Sequential reduction of PCE to ethene by anaerobic reductive dechlorination with H <sub>2</sub> as the electron donor.....	6
3.2	Three steps of the polymerase chain reaction .....	18
3.3	Linear view of amplification curves of six-serial dilutions and threshold line at 102 RFU.....	21
3.4	Melting temperature curves of eight standard serial-dilutions obtained from <i>Bacteria</i> (iQ5 Optical System Software).....	23
3.5	Regression line of seven serial dilutions of a DNA template with known standard quantity concentration.....	25
3.6	Location of the two OU 5 plumes flowing northwestly from the source area and their respective source of contamination. ....	28
4.1	Transect sampling across TARS plume with nine sampling points done in October 2005.....	31
4.2	Location of the study area in OU 5 of Hill Air Force Base.....	32
4.3	Twenty sampling locations in the study area of the OU5 plume with three different TCE concentrations .....	33
4.4	Distribution of the samples in the 96 well-plate.....	38
6.1	Bacteria distribution in the OU 5 study area .....	54
6.2	Maximum <i>Dehalococcoides</i> bacteria distribution in the OU 5 study area.....	56
6.3	Maximum <i>Desulfuromonas michiganensis</i> 16S rRNA gene distribution in the OU 5 study area.....	57
6.4	Maximum <i>Geobacter</i> sp. bacteria distribution in the OU 5 study area.....	59
6.5	Maximum <i>Rhodoferax ferrireducens</i> -like bacteria distribution in the OU 5 study area.....	60
6.6	Distribution of <i>vcrA</i> functional gene in the OU 5 study area,.....	62

6.7	Distribution of <i>tceA</i> functional gene in the OU 5 study area .....	63
6.8	TCE distribution in the OU 5 study area.....	67
6.9	Fe (II+III) by two extraction methods: HCL and HA-HCl + HCl. Released Fe (II).....	68
6.10	Total arsenic by two different extraction methods. ....	69
6.11	Dissolved oxygen concentrations (mg/L) in the OU 5 study area. ....	71
6.12	Hierarchical tree classification plot of the OU 5 soil core samples.....	71
6.13	Canonical plot of the discriminant analysis showing three different clusters with the 95 % confidence interval.....	72
6.14	Location of the three clusters in the OU 5 study area. ....	74
6.15	Regression tree classification using <i>Dehalococcoides sp.</i> , P+PNQ results as the dependent variable. ....	76
6.16	Regression tree classification using <i>D. michiganensis</i> P+PNQ results as the dependent variable.....	76
6.17	Regression tree classification using <i>vcrA</i> functional gene P+PNQ results as the dependent variable .....	77
6.18	Regression tree classification using <i>Geobacter</i> P+PNQ results as the dependent variables. ....	78
6.19	Regression tree classification using <i>Rhodoferax ferrireducens</i> -like bacteria as the dependent variable .....	78
6.20	Regression tree classification using <i>tceA</i> functional gene P+PNQ results as the dependent variable .....	79

# CHAPTER 1

## INTRODUCTION

Engineered bioremediation technologies are considered one of the least expensive in situ techniques to treat TCE contaminated groundwater (AFCEE and NFESC, 2004). The greatest advantage of these technologies is their relatively low cost of operation compared to other in situ remediation technologies. The efficiency of a given technology will vary with many factors including the abundance of indigenous, dechlorinating microorganisms and the availability of electron donors. Consequently, the potential for natural attenuation of any TCE contaminated plume needs to be evaluated in treatability studies. These studies may require long periods of monitoring making this technology less cost-effective. Decision making about using natural attenuation by indigenous bacteria at a site may also be based on monitoring the contaminated aquifer for the presence of known dehalorespiratory bacteria and the presence of required reductive dehalogenase enzymes.

The Tooele Army Rail Shop (TARS) located in the Operable Unit 5 (OU 5) of Hill Air Force Base (HAFB), Utah, is currently the source of two TCE-contaminated groundwater plumes that extend underneath the cities of Clinton and Sunset. Groundwater and soil in the off-base parts of OU 5 contain TCE and other contaminants of concern above the drinking water Maximum Contaminant Level (MCL) of 5 µg/L (National Primary Drinking Water Regulation, 2002). Effective remediation technologies are needed in the entire OU 5 area. Field observation of vinyl chloride in some monitoring wells located down-gradient of an aeration curtain on the western side of the

OU5 TCE source area suggested that complete dehalogenation of TCE may be possible, at least in some locations, at OU 5.

The scope of this study was to determine the spatial distribution and density of selected bacteria capable of TCE reductive dechlorination as well as the distribution of the vinyl chloride reductase A (*vcrA*) and trichloroethene reductase A (*tceA*) genes in the study area. In addition, the presence of selected iron reducing microorganism as one kind of possible competitors with dechlorinating microorganisms was determined in an OU5 study area. Work by Hendrickson et al. (2002) suggested that chlorinated ethene reducing bacteria are widely distributed in nature and that demonstrating their presence or absence is evidence of the potential effectiveness of bioremediation via biostimulation for reductive dehalogenation.

The present study evaluated the effect of the physical and chemical properties of the OU5 aquifer material on the selected dechlorinating and iron reducing bacteria distribution. This evaluation included parameters such as dissolved oxygen, soil organic carbon,  $\text{NO}_3^-$ -N,  $\text{NH}_4^+$ -N, bioavailable Fe(III), Fe(II), water soluble elements, chlorinated compounds, soil texture, pH, electrical conductivity and elemental composition. The evaluation was performed using multivariate statistical analysis methods

## CHAPTER 2

## HYPOTHESES AND OBJECTIVES

Hypothesis 1: The distribution of detectable 16s rRNA genes of the dechlorinating bacteria *Dehalococcoides ethenogenes* and *Desulfuromonas michiganensis* and the dechlorinating functional genes *tceA* and *vcrA* in the OU5 aquifer material will depend on certain physical and chemical properties of the OU5 aquifer material.

Hypothesis 2: The distribution of the 16s rRNA genes of the iron reducing bacteria *Geobacter* sp. and *Rhodoferrax ferrireducens*-like bacteria in the OU5 sediment will also be influenced by certain physical and chemical properties.

Hypothesis 3: The concentration of the target dechlorinating bacteria and their functional genes at the OU 5 study area are very low and not uniformly distributed.

In order to test the above hypotheses, this study accomplished the following objectives:

Objective 1: Determine the limits of quantitation in Real Time Polymerase Chain Reaction (qRT-PCR) of the bacterial genes to be enumerated.

Objective 2: Estimate the distribution and population density of the following 16S rRNA genes and selected functional genes in the OU 5 aquifer material: *Bacteria*, *D. ethenogenes*, *D. michiganensis*, trichloroethene reductive dehalogenase gene (*tceA*), vinyl chloride reductase gene (*vcrA*), *Geobacter spp.*, and *Rodoferrax ferrireducens*-like bacteria.

Objective 3: Evaluate the influence of Fe(II) and bioavailable Fe(III) in the aquifer material of OU 5 in the dechlorinating and iron-reducing bacteria distribution in the OU 5 plume.

Objective 4: Evaluate the soil texture, water soluble elements, elemental composition, pH, electrical conductivity, dissolved oxygen in well water, organic carbon,  $\text{NO}_3^-$ -N,  $\text{NH}_4^+$ -N, TCE, cis-dichloroethene and vinyl chloride in the OU 5 aquifer material and their influences on the dechlorinating and iron reducing bacteria distribution.

## CHAPTER 3

## LITERATURE REVIEW

**3.1 In situ Anaerobic Reductive  
Dechlorination of Chloroethenes**

In situ anaerobic reductive dechlorination has been documented as a remediation and contaminant removal process at various groundwater sites in the United States. This is a process of sequential reductive dechlorination (Lu et al., 2006) that is carried on in place without the removal of soil and/or water (Hyman and Dupont 2001). The reductive dechlorination reaction, also known as dehalorespiration, is the biological pathway where bacteria can derive useful energy from the reductive dechlorination of chlorinated solvents using hydrogen as an electron donor and yielding chlorine and ethene as degradation products (Lee et al., 1998). The reductive dechlorination of chlorinated compounds happens in sequential reactions where a chlorine atom is removed and replaced with hydrogen at each reaction step. Figure 3.1 shows that the dechlorination reactions of the transformation of perchloroethene (PCE) to ethene usually produce cis-DCE, however, it may produce other DCE isomers such as trans-DCE and 1,1-DCE. Maymó-Gattell et al. (1999) demonstrated that trans-DCE is the intermediate product between cis-DCE and VC, however trans-DCE is formed by cometabolic reactions which are catalyzed by chemical reactions that include either poorly substrate-adapted enzymes or constituents in the cell. The study also showed that cis-DCE is the precursor of 1,1-DCE in a PCE-grown inoculum of *Dehalococcoides ethenogenes* strain 195 and its chlorinated product is VC.

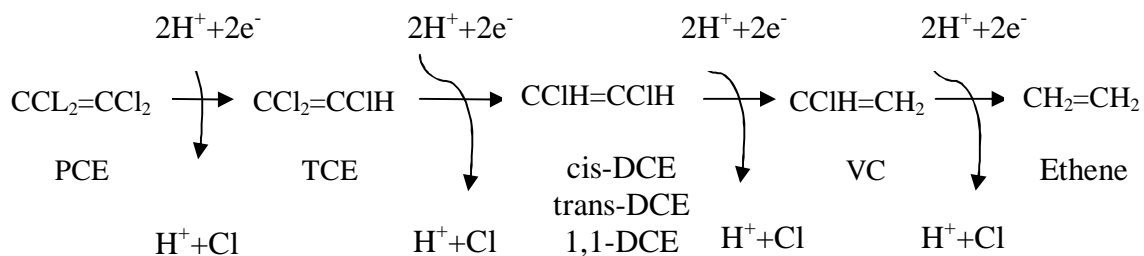


**FIGURE 3.1 Sequential reduction of PCE to ethene by anaerobic reductive dechlorination with H<sub>2</sub> as the electron donor.**

Other studies reported the formation of 1,1-DCE by aerobic chemical reactions from TCE (Kästner, 1991) and from 1,1,1-trichloroethene under methanogenic conditions (Vogel and McCarty, 1987).

Anaerobic dechlorination occurs in the absence of oxygen. Chlorinated compounds are the electron acceptors and hydrogen is the electron donor. In organic matter-rich anaerobic environments, fermentation reactions are the principal source of hydrogen (Bitton, 2005). The initial fermentation is done by acidogenic-fermentative bacteria, which convert sugars, amino acids and fatty acids to organic acids, alcohols, acetate, CO<sub>2</sub> and H<sub>2</sub>. The next fermentation reaction is done by acetogenic bacteria, which convert fatty acids and alcohols into acetate, H<sub>2</sub>, and CO<sub>2</sub> in low hydrogen concentrations. Then, methanogenic bacteria use CO<sub>2</sub> and H<sub>2</sub> to produce methane gas and water. Furthermore, acetogenic bacteria and methanogens build a symbiotic relationship around the amount of hydrogen being produced and consumed; methanogens maintain the low hydrogen tension required by acetogenic bacteria to convert fatty acids (Bitton, 2005). After acetate and hydrogen has been produced by acetogenic bacteria, they both are available to be used by denitrifiers, iron reducers, sulfate reducers, methanogens and

dechlorinating bacteria. After oxygen has been depleted, electron acceptors such as  $\text{NO}_3^-$ ,  $\text{Fe(III)}$ ,  $\text{SO}_4^{2-}$ , and  $\text{CO}_2$  are often present in groundwater systems (Bitton, 2005).

Oxidation-reduction reactions in groundwater systems are the source of energy for anaerobic respiration. These energy-yielding processes start with nitrate as the electron acceptor in the absence of oxygen by denitrifying bacteria. After nitrate has been depleted and fermentation products start to accumulate, competition for hydrogen utilization begins between manganese and iron reducer microorganisms followed by sulfate and methanogenic microorganisms. The competition for the hydrogen is influenced by the greater energy yield reactions taking place in anaerobic conditions as well as by the enzymatic preference for hydrogen. One example of competition is when sulfate reducers dominate the use of hydrogen over methanogens, they are able to grow up more with higher hydrogen utilization rates. After sulfate has been consumed, the hydrogen concentration starts increasing and methanogens are the dominant population in the use of hydrogen (Prescott et al., 2002).

Past studies demonstrate that dechlorinating bacteria such as *Dehalococcoides* only utilize hydrogen ( $\text{H}_2$ ) as a direct electron donor for reductive dechlorination (Maymó-Gatell et al., 1997). Consequently, hydrogen constitutes the most important electron donor for dechlorinating and methanogenic microorganisms. For this reason, hydrogen competition among bacteria is an important consideration in situ reductive dechlorination of PCE of groundwater plumes.

### **3.2 Dehalorespiring Microbial Communities**

Dehalorespiring microorganisms are able to use fermentation products such as  $\text{H}_2$  and organic acids as the electron donors in reductive dechlorination reactions. They are

divided into four phylogenetic groups: Low G+C Gram-positive bacteria,  $\epsilon$ -Proteobacteria,  $\delta$ -Proteobacteria and Green non-sulfur bacteria or chloroflexi (Krajmalnick-Brown, 2005).

One lineage group of low G+C gram-positive bacteria is formed by *Desulfitobacterium* sp. strain PCE1, Viet1 and PCE-s.; *Desulfitobacterium frappieri* sp. strain TCE1; *Dehalobacter restrictus* strain PERK-23 and TEA; and *Clostridium bifermentans* strain DPH1. The final dechlorinating product is cis-DCE for the majority of this group but TCE is the end product for *Desulfitobacterium* sp. strain PCE1 and Viet1. All organisms of this group use H<sub>2</sub> as the only electron donor (Gerritse et al., 1996,1999; Löffler et al., 1997; Miller et al., 1997; Holliger et al., 1998; Wild et al., 1996; Chang et al., 2000).

The organisms in the  $\delta$ -Proteobacteria subdivision are *Desulfuromonas chloroethenica* strain TT4B and *Desulfuromonas michiganensis* strain BB1 and BRs1. Cis-DCE is the chlorinated end product of the metabolism and acetate is the major electron donor (Krumholz 1997; Sung et al., 2003). The  $\epsilon$ -Proteobacteria subdivision contains *Dehalosporillum multivorans* including *D. multivorans* strain PCE-M2. This group does dechlorination to cis-DCE by using H<sub>2</sub> as the electron donor (Krajmalnick-Brown, 2005).

The final group is the chloroflexi or green non-sulfur bacteria, which includes *Dehalococcoides* sp. strain FL2 and BAV1 and *Dehalococcoides ethenogenes* strain 195. This group is known for carrying on full dechlorination of PCE via TCE, cis-DCE, and VC to ethene using H<sub>2</sub> as the electron donor. Strain 195 and FL2 reduce PCE to VC and then VC is reduced by cometabolism. Strain BAV1 is so far the only organism capable of

reducing PCE to ethene through direct metabolism (Maymo-Gatell et al., 1997, 2001; He et al., 2003, 2005; Holliger et al., 1999).

### 3.3 Reductive Dehalogenase Enzymes

Reductases are the key catalysts in reductive dehalogenation reactions (Krajmalnick-Brown, 2005). Enzymes mediating dechlorination from PCE to DCE have been purified from cells of different dechlorinating microorganisms such as *Desulfitobacterium* strain PCE-S, *Dehalobacter restrictus*, *Dehalospirillum multivorans* and *Dehalococcoides ethenogenes* (Holliger et al., 1999).

*Dehalococcoides* organisms have been identified as those responsible for successful dechlorination at different TCE-contaminated sites. For that reason environmental distribution of the reductase genes from *Dehalococcoides* organism is a relevant consideration in TCE bioremediation of contaminated plumes. The present study focused on the trichloroethene reductive dehalogenase (*tceA*) identified in *Dehalococcoides ethenogenes* strain 195 (Magnuson et al., 2000) and the vinyl chloride reductase (*vcrA*) from *Dehalococcoides* sp. strain VS (Müller et al., 2004).

The *tceA* reductase enzyme mediates the catalysis of TCE to vinyl chloride and was cloned and sequenced by Magnuson et al. (1998). The authors also showed the catalysis of VC by *tceA* in *D. ethanogenes* 195 culture, but the reduction rate of VC was less than 1% of the TCE to c-DCE reduction rate.

The VC reductive dehalogenase was partially purified by Müller et al. (2004). The authors identified and characterized the encoding gene *vcrAB*. The study found the presence of the homologous *vcrAB* genes in groundwater samples which came from a chlorinated ethene aquifer where complete dechlorination to ethene was achieved by

indigenous microorganism. Furthermore, the study suggested that the presence of the *vcrAB* sequence in environmental samples indicated the potential dechlorination of VC at TCE-contaminated sites (Müller et al., 2004).

### **3.4 Iron Inhibition in TCE-reduction**

Iron (III) minerals are often the most abundant electron acceptors in subsurface environments and groundwater systems. Previous studies (Lovley, 1995) demonstrated that Fe(III) reduction was the main terminal electron-accepting process carried out by pure culture and natural microbial communities in sediments. It was proposed that the majority of the catalyzed Fe (III) reduction in anaerobic sedimentary environments is due to microorganism that can completely oxidize acetate to carbon dioxide by using Fe(III) as the sole electron acceptor (Lovley, 1995).

The availability of carbon donor in TCE-contaminated groundwater sediments stimulates microbial energy capturing reactions using different terminal electron acceptors (TEAs), including TCE and Fe(III). Since H<sub>2</sub> is the ultimate electron donor for dehalorespiring microorganisms, iron-reducer communities, among other microbial communities compete with *Dehalococcoides* species for H<sub>2</sub> and may inhibit the dechlorination process in TCE contaminated aquifers (Lu et al., 2001).

This effect on TCE reduction has been hypothesized by Dupont et al. (2003) based on results from a microcosm study which used OU5 aquifer material from HAFB amended with three different carbon sources. The microcosm study observed very limited TCE dechlorination and significant releases of Fe(II) and arsenic in the microcosms with the carbon donor addition. Based on this observation, it was proposed that inhibition of

TCE dechlorination was likely due to a large bioavailable iron (III) pool present in the OU5 sediment systems (Dupont et al., 2003).

Lu et al. (2001) have noted that PCE/TCE dechlorination by microbial communities occurred in similar or lower hydrogen concentration ranges (0.6-0.9 nM H<sub>2</sub>) as manganese and Fe(III) reduction reactions (0.1-2.0 nM and 0.1 -0.4 nM H<sub>2</sub>, respectively). The study also demonstrated that cis-DCE and VC required hydrogen concentration values close to those for methanogenesis and sulfate reduction reactions.

Evans and Koenigsberg (2001) also conducted an evaluation of 13 PCE/TCE-contaminated sites across the United States. At all sites, experimental pilot testing with Regeneration Hydrogen Release Compounds (HRC) was used to enhance dechlorination of TCE, PCE or/and the chlorinated daughter products. The evaluation of the data showed inhibition of cis-DCE reduction and/or VC production where there was production of Fe(II) in nine of the 13 sites. Only one site was not consistent with the inhibition hypothesis showing dechlorination of cisDCE to VC with Fe(II) production. Five of the nine sites showed the production of VC after the production of Fe(II) stopped. Three of the nine sites showed VC production with little or no Fe(II) production.

Therefore, the influence of bioavailable iron (III) in the microbial TCE dechlorination at the OU 5 site is an important consideration in the development of the present study. Furthermore, dissimilatory iron reducing bacteria (DIRB) are the key factor in the reduction of Fe(III) and knowing their distribution in the OU 5 sediments helps to describe the potential for their reduction of bioavailable iron (III) and potential inhibition of TCE-reduction.

### **3.5 Dissimilatory Iron-Reducing Bacteria in OU 5 Sediment**

The presence of two DIRB, *Geobacter* spp and *Rhodoferrax ferrireducens*-like bacteria, that are anticipated to be important at the OU 5 site were evaluated in the study in order to test the potential reduction of bioavailable iron in the OU 5 aquifer material. The reasons why these organisms were selected were: first, a clone library of 16S rRNA genes of bacteria in an OU 5 sediment sample showed 56 out of 255 clones (22%) resembled *R. ferrireducens* with 93% similarity (Zhou, 2008). Second, microorganisms of the genus *Geobacter* have been shown to be prominent members of the microbial community that carry on dissimilatory metal-reducing reactions (Lovley, 1995). *Geobacter* sp. are able to completely oxidize organic compounds to CO<sub>2</sub> by using either Fe(III) or humic substances as the only electron acceptor in the reductive reaction. Some *Geobacter* sp. can also reduce nitrate and fumarate depending on their availability in natural systems, while other *Geobacter* sp. are known to have the ability to oxidize monoaromatic compounds (Coppi et al., 2001).

### **3.6 Iron Forms in Aquifer Systems**

Fe(III) oxides can be found in several chemical forms, from poorly crystalline Fe(III) to highly crystalline iron structures such as goethite and hematite oxides (Lovely and Phillips, 1987). The availability of those forms of iron as well as the degree of crystallinity, particule size, available surface area, reactivity and oxidation state define the rate and extent of Fe(III) reduction in sedimentary environments. Poorly crystalline iron oxides are considered to be the principal source of microbial Fe(III) reduction in soils and sediments because of their greater accessibility and faster reduction rates (Lovley, 1991;

Roden and Zachara, 1996). Work done by Roden and Zachara (1996) demonstrated Fe(III) reduction in highly crystalline oxides (like goethite) by Fe(III) reducing microorganism grown on syntetic geotite media but at lower reduction rates than in non crystalline iron (III) oxides

Hydroxylamine hydrochloride extraction is the method of preference to count specifically for the poorly crystalline Fe(III) oxides in sediment samples. Lovley and Phillips (1987) showed the usefulness of this method by using fresh-and brackish water aquatic sediments and core sediment samples. The authors showed a strong relationship between the amount of Fe(III) extracted by the hydroxylamine extraction method and the extent of microbial Fe(III) reduction. This method utilized 1 g of wet sediment in 5 ml of hydroxylamine hydrochloride in HCl. Under this acidic, reducing condition all extractable Fe(III) is converted to Fe(II). The extraction of Fe(II) was performed by the same procedure but HCl alone was the extractant. Hydroxylamine-reducible Fe(III), called bioavailable Fe(III) in the present study, was calculated by subtracting the Fe(II) released by the HCl extraction from that released in the HA-HCL extraction.

### **3.7 Groundwater Bioremediation in OU5**

The bioremediation process is the natural remediation of contaminated sites catalyzed by microorganisms and enzymes. Bioremediation in the OU5 area was reported by Dupont et al. (2003). The study demonstrated that TCE dechlorination at OU5 can be achieved only by amendment with a high dose of carbon donor and microbial inoculum. The study showed complete TCE dechlorination occurred in the amended microcosms in an 80-day period of incubation. The most effective enhancement of dechlorination was achieved in the presence of emulsified oil and a known dechlorinating microbial

community. Also, the addition of the microbial inoculum mitigated arsenic and iron releases. Consequently, this investigation suggested that there was potential for complete dechlorination in the OU 5 area if there was biostimulation of indigenous microorganisms present at the site plus bioaugmentation as well.

### **3.8 Effect of Physical and Chemical Factors on Dehalorespiring Microorganisms**

As has been reported, *Dehalococcoides* sp. is a strict anaerobic microorganism which can only use hydrogen as its electron donor. *Dehalococcoides* sp. can not use nitrate, nitrite, fumarate, ferric iron, sulfate, sulfite, thiosulfate, sulfur or oxygen as electron acceptors, it can only use chlorinated organic compounds (Maymó-Gattel et al., 1997; He et al., 2003; Adrian et al., 2000). Furthermore, competition for H<sub>2</sub> as the electron donor may happen among iron reducers, sulfate reducers, methanogens and dechlorinators (Lee et al., 1998). Consequently, the availability of H<sub>2</sub> and the presence of different electron acceptor compounds greatly affect the growth of *Dehalococcoides* sp. (Lu et al., 2006).

The relationship between geochemical parameters and the occurrence of *Dehalococcoides* DNA in contaminated aquifers has been reported by Lu et al. (2006). This study found, with a 95% confidence level, that the distribution of NO<sub>3</sub><sup>-</sup> plus NO<sub>2</sub><sup>-</sup>-N, oxidation reduction potential (ORP) and CH<sub>4</sub> concentrations were statistically different between water with *Dehalococcoides* DNA and the water without it. Other geochemical parameters that did not show a significant relationship to the presence or absence of *Dehalococcoides* DNA were O<sub>2</sub>, H<sub>2</sub>, Fe(II), SO<sub>4</sub><sup>-2</sup>, TOC, Cl<sup>-</sup>, BTEX compounds, alkalinity, electrical conductivity, pH and temperature. The study found,

statistically, that ORP is the most important factor affecting the growth of *Dehalococcoides* (Lu et al., 2006).

### **3.9 Molecular Biology Techniques to Determine the Presence of Dechlorinating and Iron-Reducing Bacteria**

The polymerase chain reaction (PCR) amplifies specific target DNA sequences and is one of the most popular molecular biology techniques applied in the engineered bioremediation of contaminated soil and groundwater sites. Using this technique, bacteria, including dechlorinating microorganisms, can be detected and quantified in terms of presence or absence as well as numbers of copies of a specific DNA molecule per gram of soil. The present study applied quantitative Real Time Polymerase Chain Reaction (qRT-PCR) methodology to determine the population density of the target bacteria and functional genes in units of copy number of DNA molecule per gram of soil.

#### **3.9.1 Structure of DNA Molecules**

A DNA molecule contains two chains of polynucleotides bound together by hydrogen bonds. The long DNA molecule is twisted forming a double helix. DNA strands contain nucleotides that are made up of one base (purine or pyrimidine), one sugar (ribose or deoxybose) and one phosphate molecule (the backbone). The purine bases are adenine and guanine and the pyrimidine bases are thymine and cytosine. Each base is connected with its complementary base, thus adenine pairs with thymine by two non-covalent hydrogen bonds and guanine pairs with cytosine by three hydrogen bonds. The pairing between bases allows the formation of two complementary DNA strands. As the purine and pyrimidine bases are in the middle of the DNA chain, the phosphoric acid

molecules are at the outside of the DNA chain connecting two adjacent deoxyribose sugars. The phosphodiester molecule connects the upper with the lower sugar by positioning between the 3'-hydroxyl group and the 5'-hydroxyl position of the upper and lower sugar, respectively (Prescott et al., 2002).

During this study, the DNA of dechlorinating and iron-reducing microorganisms was amplified by the qRT-PCR. The DNA from these organisms is called the template for the qRT-PCR reaction.

### **3.9.2 Polymerase Chain Reaction**

The Polymerase chain reaction (PCR) is a molecular biology technique for replicating a DNA fragment by using an enzyme called polymerase. This technique has become very valuable within engineered bioremediation because it allows the determination of the presence or absence of low concentrations of bacteria of interest in environmental samples.

The PCR procedure is an in vitro amplification carried out by enzymes. Living cells carry out a DNA replication process. The most studied is the replication of *Escherichia coli* DNA where DnaA and DnaB proteins unwind the double-stranded DNA at an initiation site and throughout the double helix DNA chain. After that, two strands are generated, the leading and the lagging strand. DNA polymerase starts to synthesize a new copy of DNA in the leading strand by moving from its 5' to 3' direction so as DNA is unwound a new copy of DNA is extended to its 3' direction. In parallel, the lagging strand is synthesized discontinuously because all fragments replicate from the 5' to the 3' direction. A special RNA primer is synthesized so that DNA polymerase can build from

it a new target DNA copy. The actual duplicate is formed by 100s of fragments which are then joined to form the entire DNA copy (Prescott et al., 2002).

In vitro amplification or PCR is a similar process to the DNA replication in living cells. The basic principle of the PCR procedure is that DNA polymerases build a new DNA sequence along the DNA template based on a primer. The primer defines the starting point in the DNA template where DNA polymerases begin to synthesize complementary DNA along the template. Primers usually contain a sequence of 20-25 nucleotides. The entire reaction can be described in three sequential steps as shown in Table 1 (Cantor and Smith, 1999).

DNA polymerase starts amplification in the 5' to 3' direction while reading the DNA template in the 3' to 5' direction. In the first step, the DNA template is heated at 92-96 °C to denature and separate it into two strands as shown in Figure 3.2. Then, the primer anneals along the DNA template as the temperature drops to 55-60 °C to allow primers to hydrogen bond to the DNA template. Since the double-stranded DNA was separated, two DNA strands are available for amplification. The primers anneal with both DNA strands. In the final step, DNA polymerase extends the primers along the DNA template and starts synthesizing copies of the DNA template by using the deoxyribonucleoside triphosphates. At the end of the first cycle, the reaction ends with two copies of double stranded DNA that are exact copies of the original DNA template.

**TABLE 3.1 Cycle Parameters in the PCR Procedure**

Step	Rx Optimum Temperature	Time
1) DNA denaturation	92-96 °C	60 sec
2) Primer annealing	55-60 °C	30 sec
3) Chain Extension	72 °C	60 sec

Finally, the cycles are sequentially repeated between 30 to 40 times as shown in Figure 3.2 If the efficiency of the PCR is 100%, the final DNA product would have an exponential growth of  $2^n$  where n is the total number of cycles carried out in the PCR (Prescott et al., 2002). During the sequential steps of each cycle, the DNA polymerase enzyme is constantly heated from lower to higher temperatures. Consequently, this enzyme must be very resistant to continuous changes in temperature in order to carry out efficiently the PCR amplification. Hence, the most widely used enzyme is Taq polymerase because of its good resistance to the heating and cooling in the sequential steps of the PCR (Cantor and Smith, 1999).

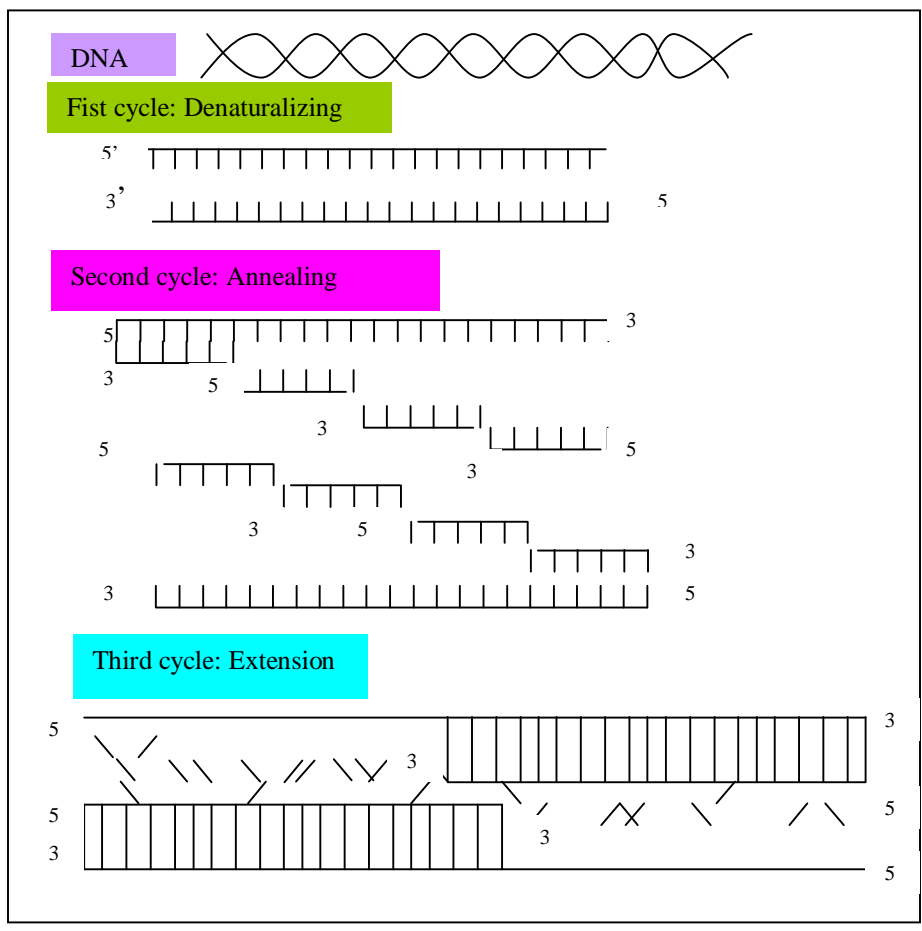


**FIGURE 3.2 Three steps of the polymerase chain reaction (Cantor and Smith, 1999).**

Finally, an additional laboratory technique is used to determine the presence or absence of the target gene in the PCR amplification. This technique is gel electrophoresis. It can show qualitatively the existence of the DNA of interest that has been amplified from the original sample.

The principle of the technique is that negatively charged DNA molecules migrate through a polymer matrix due to an electric field. The matrix, a gel material made with agarose, buffer and ethidium bromide, is submerged in a salt buffer solution that can conduct electricity from the negative to the positive electrode. DNA molecules travel through the pores of the gel toward the anode. Smaller molecules can travel further than larger DNA molecules with time due to less resistance through the matrix material. Thus, they can be separated by size according to the extent of the migration. DNA molecules are mixed with a loading dye and transferred to a well located inside the matrix. The loading dye, containing glycerol or sucrose, makes the DNA solution more dense and viscous so it is easier to load into the well and see it with the naked eye. As electricity is passed through the solution, the smallest DNA molecules migrate faster toward the anode, then the DNA samples can be visualized by ethidium bromide staining under the ultraviolet light. A photograph of the gel is taken to see the migration of the DNA molecules in the sample. Molecular weight markers are used to estimate the DNA size of all DNA molecules in the sample. They are usually located on one side of the gel along the DNA samples. The markers are visualized under the ultraviolet light to generate a ladder of known size DNA molecules to which the DNA fragments in the sample can be compared (MoBio Laboratories, 2008).

### **3.9.3 Real-Time Polymerase Chain Reaction (qRT-PCR)**

A tutorial published by Applied Biosystems (2006) clearly indicates the main difference between PCR and qRT-PCR; namely that qRT-PCR allows reporting the starting quantity of DNA at the beginning of the exponential phase of the amplification process. In PCR, the amount of DNA, which is visualized by the agarose gel electrophoresis method, is the total DNA accumulated during 30-40 cycles of amplification. This point is called the end-point because the reaction ends at the non-exponential plateau phase.

During the exponential phase of the PCR, the amplification of the DNA doubles the amount of the DNA in every cycle if the efficiency is 100%. In the linear phase of the PCR, the reaction components become limited as the amplification increases. Finally, the reaction stops at the end point because of lack of reactants.

The qRT-PCR instrument takes fluorescence measurements of the amplified DNA throughout the amplification process showing an amplification curve from the initial amplification until it reaches the plateau of the curve at the maximum cycle number. The high sensitivity of this method is based on the instrument's capability to measure a fluorescent signal emitted by a fluorescent molecule. The chemistry of this molecule contains a DNA-binding dye called SyberGreen which binds to all double-stranded DNA present in the sample. This DNA-binding dye bonds to more DNA as the cycle number increases and the fluorescence signal increases as more DNA is amplified in the reaction.

An example of the qRT-PCR amplification fluorescent measurements is shown in Figure 3.3. This figure is a linear view of the amplification reaction of six serial dilutions

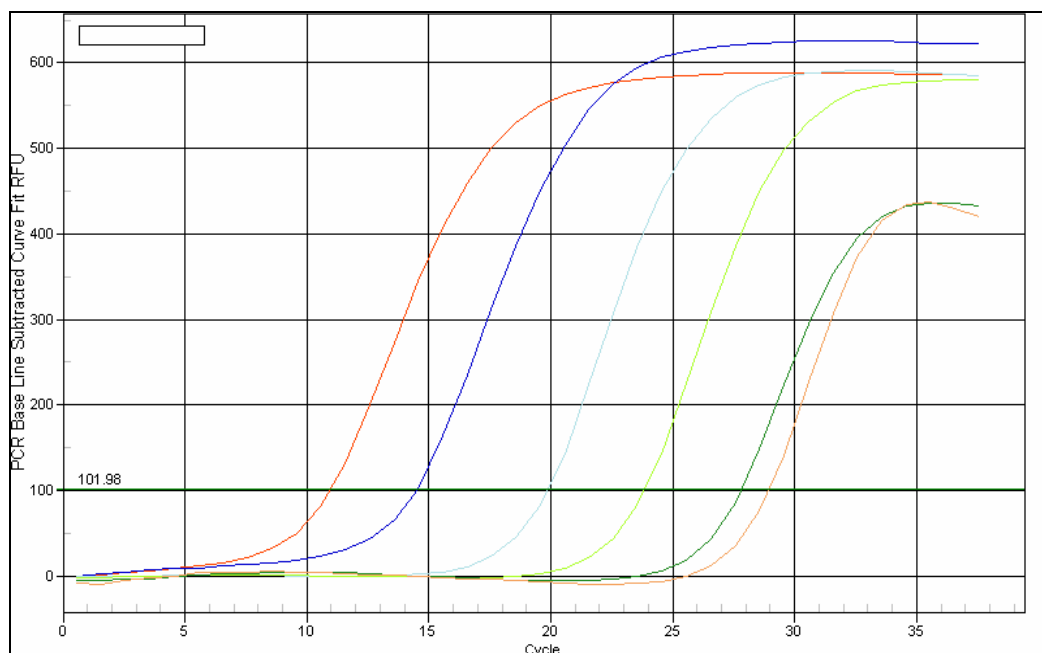


**FIGURE 3.3 Linear view of amplification curves of six-serial dilutions and threshold line at 102 RFU. Amplification curves show a growth-equation of 2cycle from cycle 0 to the beginning of plateau. Amplification in earlier cycles can not be seen at linear scale plot (iQ5 Optical System Software).**

of a DNA template. The exponential amplification phase usually happens from cycle 10-15 to a maximum cycle of 25-35. The actual range of the exponential phase of the PCR depends on the initial amount of DNA in the sample. For that reason, the qRT-PCR instrument defines its working range by defining two parameters: the Threshold Cycle and the Efficiency of the PCR.

The technical qRT-PCR manual by Bio-Rad Laboratories (2004b) refers to the threshold cycle as a Ct value which is the cycle number where DNA amplification becomes measurable by the instrument. Amplification before the Ct value is not enough to be detectable by the instrument due to the small amount of DNA in the starting material. Thus, if the sample contains a low amount of DNA initially, the Ct value is higher compared to a sample with a high DNA concentration at the beginning of the

reaction because the instrument system needs more cycles to develop a fluorescent signal that is significantly above the background level. The instrument defines a threshold line that crosses the amplification curves at their corresponding Ct value. The threshold line is shown in Figure 3.3 as the horizontal line located at 101.98 relative fluorescence units (RFU).

It is important to note that the three sequential steps used in the PCR amplification reaction are the same in the qRT-PCR procedure except for the reaction time in each step. The reaction temperatures in qRT-PCR are also similar to PCR.

After DNA amplification, a qRT-PCR instrument system offers a melting curve step analysis, where all double stranded DNA is melted at temperatures ranging from 55 °C to 95 °C in 1 degree increments and is held for a few seconds at each temperature. The melting curve analysis is used to confirm that the amplified DNA corresponds to the target DNA in the sample. This analysis shows the change in RFU of all DNA molecules versus the change in temperature from 55 to 95 °C. All target DNA must melt faster in a narrow range of temperatures showing a significant decrease in RFU with time compared to other non-specific products. Figure 3.4 shows a melt temperature chart as it appears in the IQ 5 Optical System software. The first derivative of the RFU with time (T) is on the Y axis and the temperature is on the X axis.

#### **3.9.4 Characteristics of the Bio-Rad iCycler iQ Instrument**

The Bio-Rad iCycler Thermal Cycler instrument was used to carry out the qRT-PCR detection for this study. The instrument includes two optical modules: the excitation system and the detection system.

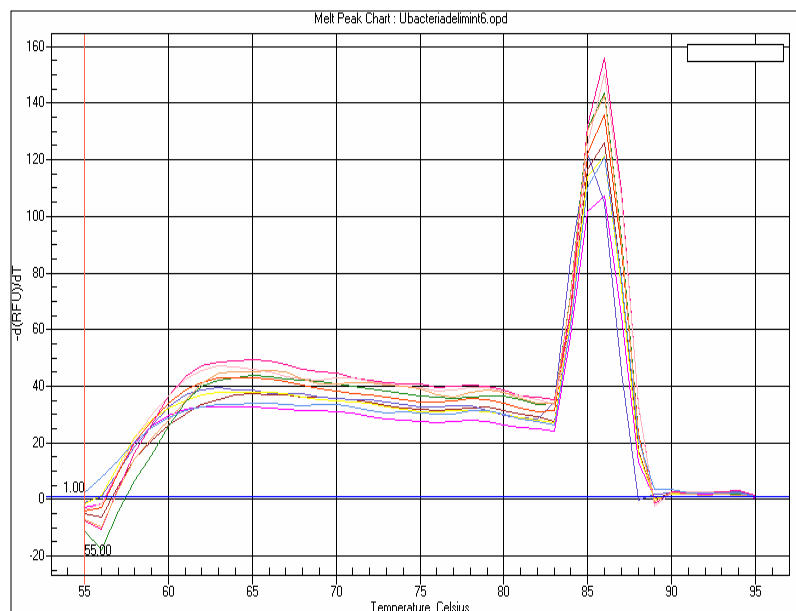


**FIGURE 3.4** Melting temperature curves of eight standard serial-dilutions obtained from *Bacteria* (iQ5 Optical System Software).

The excitation system contains a fan-cooled, 50-watt tungsten halogen lamp, a heat filter made with infrared absorbing glass, a six-position excitation filter wheel, and two mirrors above the sample plate to allow simultaneous illumination of the plate. On the other side, the detection system includes a six-position emission filter wheel, an image intensifier and a photoelectric charge-coupled device (CCD) detector (Bio-Rad Laboratories, 2004a).

The light emitted by the tungsten lamp passes through IR absorbing glass, then through one optical filter, depending on the dye type, to the mirrors where the light is reflected toward the 96-well plate. In the plate, the light activates the SyBR Green molecules which fluoresce intensely when they bind double stranded DNA. Finally, the fluorescent light goes through the selected emission filter and then to the intensifier to increase the fluorescent light. The CCD receives the fluorescent light which is then

quantified in relative fluorescent units (RFU) for each corresponding well in the sampling plate (Bio-Rad Laboratories, Inc, 2004).

### 3.9.5 Calculation of the Exponential Reaction

A mathematical expression of the DNA amplification was reported by Kochanowski and Udo (1999). Equation 1 allows the determination of the accumulated DNA in each cycle.

$$Y_n = Y_{n-1} * (1 + E_v) \quad 0 \leq E_v \leq 1 \quad (3.1)$$

where,  $Y_n$  is the number of DNA molecules after cycle  $n$ ,  $Y_{n-1}$  is the number of molecules at the beginning of cycle  $n$ , and  $E_v$  is the efficiency of the reaction. Equation 2, obtained from Equation 1, shows the mathematical expression for calculating the total DNA copies accumulated from the beginning to the end of the linear amplification phase. The  $X$  value represents the DNA copies at the beginning of the amplification reaction, and  $E_e$  is the efficiency value from 0 to 1.

$$Y = X(1 + E_e)^n \quad (3.2)$$

In a best case scenario, the amplification of a starting DNA quantity ( $X$ ) must double in each cycle in order to get an efficiency of 1, thus  $\log Y$  should be twice  $\log X$  if  $n$  is equal to 1 (Bio-Rad Laboratories, Inc, 2004). Since Equation 2 is only applicable during the exponential growth amplification, it was concluded that the efficiency value is a good indicator of the reproducibility and precision of the amplification reaction and it depends on the primer/target hybridization, the relative amounts of reactants, as well as sample-to-sample and tube-to-tube variations.

The authors also suggest that DNA quantification with external standards is usually a good method to determine the molecules or copy number of the DNA being studied. Standards which are often a plasmid or genomic DNA, have known DNA concentrations and are run in parallel with the samples of interest. Serial dilutions of the standards provide the linear relation between the Ct value and the known copies of DNA molecules as shown in Figure 3.5, where  $n_a$  and  $n_b$  are the Ct values of two DNA starting concentrations  $Y_a$  and  $Y_b$ , obtained from 10-fold dilution of a DNA template. Replicates of each standard dilution also give information about the precision of the assay.

The slope in Figure 3.5 can be described by Equation 3.3.

$$\text{slope} = \frac{\text{Log}(n_a) - \text{Log}(n_b)}{Y_a - Y_b} \quad (3.3)$$

Finally, the efficiency can be written as a function of the slope as shown in Equation 3.4.

$$\% E_e = (10^{-1/\text{slope}} - 1) * 100 \quad (3.4)$$

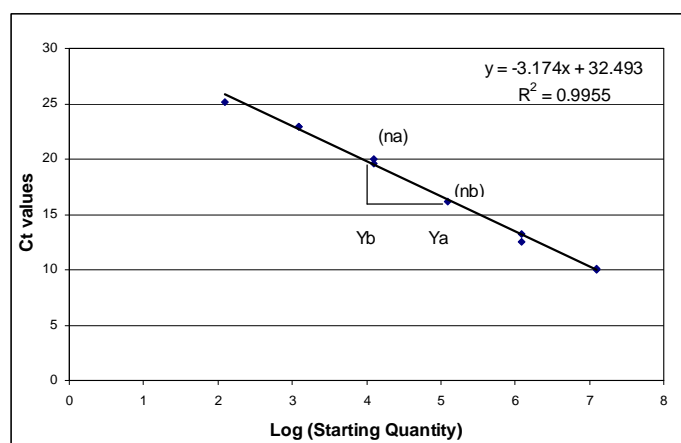


**FIGURE 3.5** Regression line of seven serial dilutions of a DNA template with known standard quantity concentration. Ct values of each dilution are plot against log of the DNA starting concentrations.

Consequently, this method provides two quality control values to evaluate the amplification reaction of the entire assay: the efficiency and the coefficient of determination ( $R^2$ ) of the standard curve. In this study, an optimized qRT-PCR was required to have an efficiency of 85-115% and an  $R^2$  of 0.98-1, although manufacturer recommendations suggest efficiencies from 95-105% are desired (Bio-Rad Laboratories, Inc, 2004).

### 3.10 The OU 5 Area of Hill Air Force Base

The OU 5 site investigation and characterization has been reported by Montgomery Watson Harza (2001). Hill Air Force Base (HAFB) is located in the north part of Utah, approximately 8 km south of Ogden. The OU 5 area is located in the northwest part of HAFB. It is one of the 13 operable units at HAFB listed on the National Priority List of the most hazardous sites in the US because of the presence of chlorinated solvents in the soil and groundwater. The mission of HAFB is to support a variety of industrial operations such as metal plating, degreasing, paint stripping, painting, sanding and other operations related to aircraft, missile, vehicle and railroad engine repair and maintenance. A variety of chemical compounds were generated from those industrial operations including chlorinated and non-chlorinated compounds, petroleum hydrocarbons, acids, bases and metals. During past operations, the waste products were initially placed at the Industrial Wastewater Treatment Plant, chemical disposal pits, landfills and other facilities on the Base.

Tooele Army Rail Shop (TARS), Zone 16 and a Former Wastewater Treatment Plant are the suspected sources of the three contaminated plumes in the OU 5 area that are located underneath the cities of Sunset, Roy, and Clinton outside the Base. The main

contaminant of concern in the OU 5 plumes is trichloroethene (TCE) that is found above the MCL of 5 µg/L. Other hazardous volatile organic compounds (VOCs) in the plumes are 1,1,1-trichloroethane (1,1,1-TCA), tetrachloroethene (PCE), cis-1,2-dichloroethene (cis-1,2-DCE), 1,1-dichloroethene (1,1-DCE), vinyl chloride (VC) and carbon tetrachloride.

Figure 3.6 shows the extent of the TARS plume with three different concentration ranges of TCE; from 5-10 µg/L located at the outside border of the TARS plume, from 10-100 µg/L which has the biggest area inside the TARS plume, and from 100-1000 µg/L located from the source area to the boundary between Sunset and Clinton City.

### **3.11 Site Characterization of OU 5**

#### **3.11.1 Site Hydrogeology**

The Sunset and Delta aquifers are the two principal aquifers under OU 5 area. They are confined aquifers located between 76 to 122 m and 152 to 213 m depth, respectively, and are categorized as current sources of drinking water or Class IIA according to the Guidelines for Groundwater Classification under the EPA Groundwater Protection Strategy.

#### **3.11.2 Geology of the OU 5 Shallow Aquifer**

The stratigraphy of the OU 5 area reported by Montgomery Watzon Harzal (2001) is based on data from 224 monitoring wells that are in the OU 5 area, where the TCE was found in the upper portion of the shallow unconfined, aquifer. The subsurface stratigraphy is composed of interbedded and laterally discontinuous silty sands, sandy silts, silt and clay.

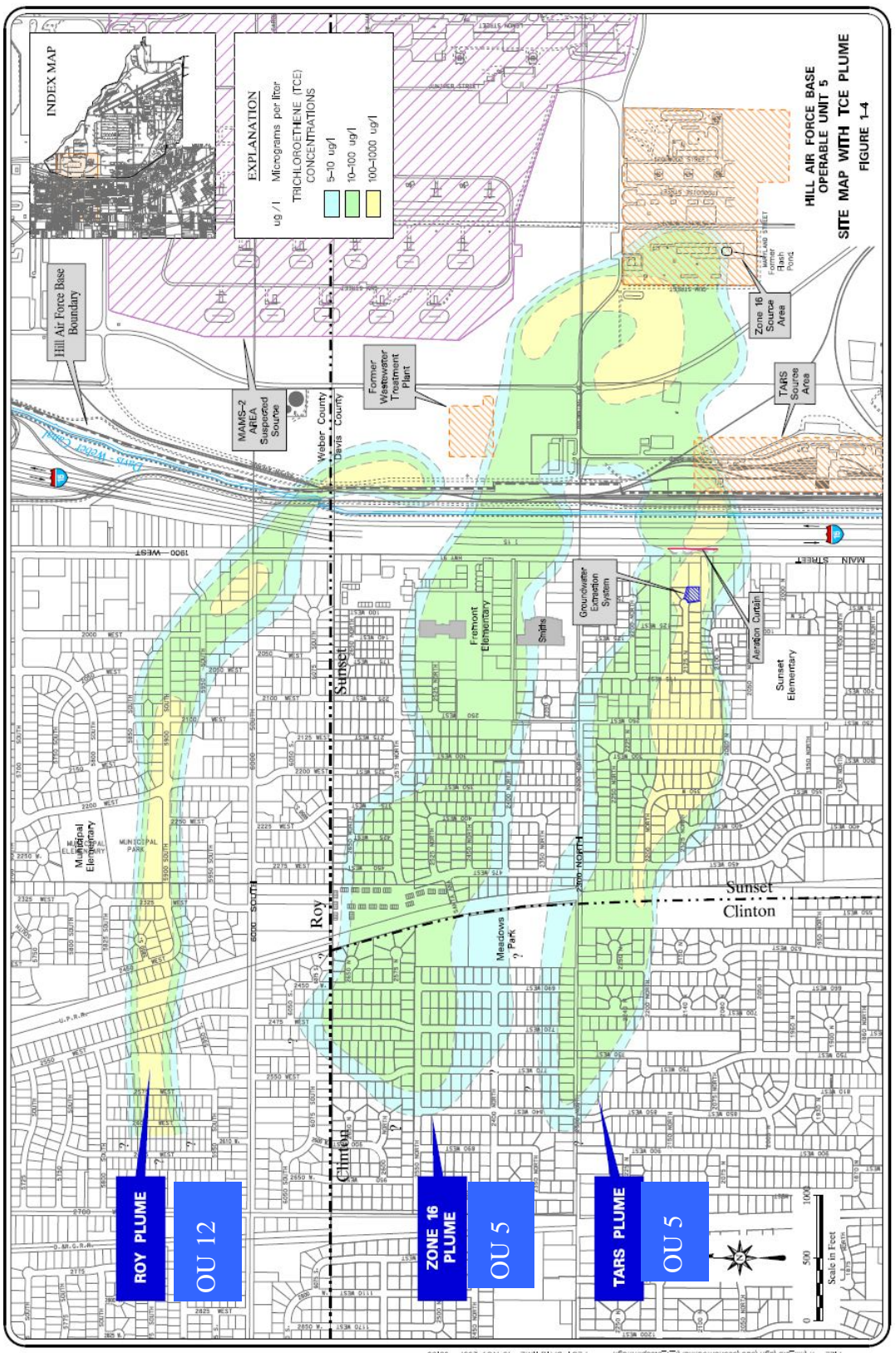


**FIGURE 3.6** Location of the two OU 5 plumes flowing northwesterly from the source area and their respective source of contamination.

The shallow, unconfined aquifer is composed of silt, and fine-grained sand interbedded with silt. The silt content increases with depth until the transition zone which is mostly silty with discontinuous fine sand layers. Beyond this transition zone, there is a low permeability, clayey silt unit which does not show a clear differentiation. The thickness of the transitional zone ranges from 0.61 to 1.5 m across the TARS plume. The low permeability unit is found from 9 to 15 m bgs with a thickness of 5.7 m. TCE contamination from the TARS source area entered the vadose zone and then migrated into the shallow, unconfined aquifer of the TARS plume. No TCE contamination has been found below the low permeability unit.

### **3.11.3 Shallow Groundwater in the OU 5 Area of HAFB**

The water depth in OU 5 ranges from the ground surface to approximately 32 m bgs. Off-Base groundwater depths are from 0.2-1 m bgs. The reported horizontal hydraulic gradient varies between 0.01 and 0.05 m/m across all of the OU 5 area with an average horizontal hydraulic gradient of 0.03 m/m. Vertical hydraulic gradients are from an upward gradient of 0.07 to a downward gradient of 0.04 across OU 5. The estimated horizontal hydraulic conductivity in TARS plume ranges from 0.06 to 37.8 m/day and the vertical hydraulic conductivity values in OU 5 range from  $4.6 \times 10^{-10}$  m/s to  $6.3 \times 10^{-5}$  m/s. The estimated groundwater velocity varies between  $6.1 \times 10^{-3}$  and 4.541 m/day in the TARS plume. The low permeability as well as the heterogeneous particle size of the aquifer material causes a tortuous flow for contaminant transport. In addition, the presence of the low permeability unit stops vertical groundwater flow and contaminant transport causing a more defined vertical extent of the contaminant at the OU 5 site.

#### 3.11.4 TARS TCE Plume

The TARS TCE plume area is about 44.1 hectares and extends 1.5 km toward the west from the TARS source area, as shown in Figure 3.6. The TARS TCE plume is located in the off-base area of OU 5 underneath the cities of Clinton and Sunset. The TARS plume was included in the interim remedial actions implemented in 1997. They were an aeration curtain and groundwater-extraction system. The aeration curtain includes air sparging (AS) and the soil vapor extraction (SVE) systems. Both systems are located across the TARS plume. The AS and SVE systems extend 121.9 m from north to south. The second remedial action operating at the TARS plume was a groundwater extraction system which was installed in September 1997 with five groundwater extraction wells. Operation of this system was discontinued in 2003 due to poor efficiency.

The aeration curtain was installed to stop and diminish groundwater contamination in downstream areas. The clean-up goal of this system was to prevent groundwater-contamination with TCE at the area where the TCE plume reaches concentrations greater than 1000 µg/L. This zone is located at the Sunset residential area.

The vertical distribution of TCE in the TARS plume goes generally from higher concentrations, usually located above the low permeability clayey silt unit, to lower concentrations found in the low permeability unit. No contamination was found below that unit. Vertical distribution in the off-Base area of OU 5 is opposite compared to the source area where TCE concentrations are lower in the upper sand unit due to the dilution effect of the precipitation and irrigation activities in the area. Again, TCE groundwater contamination does not occur below the low permeability clayey silt unit.

## CHAPTER 4

### MATERIALS AND METHODS

#### 4.1 Aquifer Sampling in OU 5 Area of HAFB

An initial investigation of the OU 5 site was performed in October 2005 to gain familiarity with the target genes and the physical/chemical properties of the aquifer material. This investigation included a transect sampling along the TARS plume, the transect length was 1300 m from monitoring wells OU5 2259 and 2260 located within the source area to monitoring well OU5 2257 located near the western edge of the plume. Two cores outside of the plume were considered as controls, they were near monitoring well OU5 2252 and 2257. Figure 4.1 shows the nine sampling locations.



**FIGURE 4.1** Transect sampling across TARS plume with nine sampling points done in October 2005.

All nine aquifer cores were analyzed with qRT-PCR to determine the distribution of selected dechlorinating and iron reducing bacterial 16S genes. Texture and elemental composition were also evaluated in the aquifer samples.

Based on the results of the transect sampling and monitoring data from existing wells located near the aeration curtain which showed detectable concentrations of vinyl chloride (evidence of TCE dechlorination), a portion of the OU 5 area was selected for more intense study. The area was approximately 139 000 m<sup>2</sup>. The area was bounded by Main Street in Sunset on the east, on the west by 350 West Street, on the north by 2300 North Street and on the south by 2050 North Street (Figure 4.2). The TARS plume was chosen because the aquifer material near the selected area had been previously used in microcosm and column studies at the Utah Water Research Laboratory.

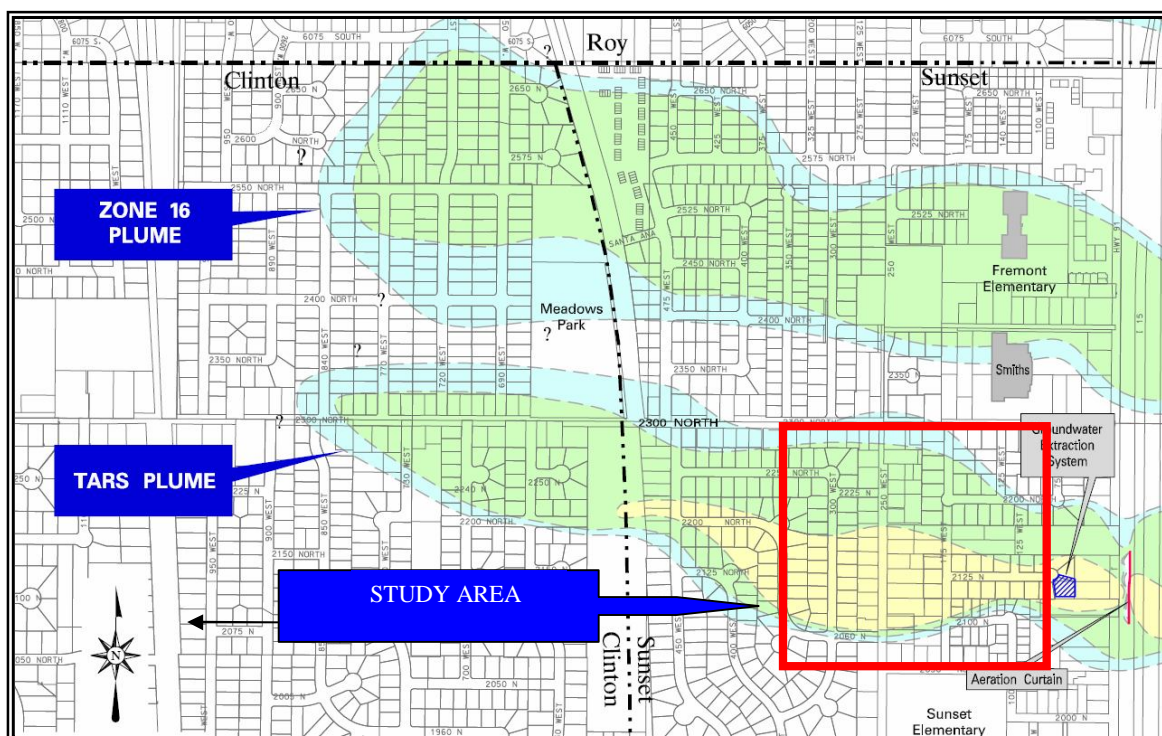


**FIGURE 4.2** Location of the study area in OU 5 of Hill Air Force Base.



Fifteen sampling points were spread in three different TCE concentration zones: the outside plume containing TCE between 5-10 µg/L, the middle part of the plume between 10-100 µg/L and the inside plume between 100-1000 µg/L. In addition, five sampling points were within the no contamination zone.

#### 4.2 **Sample Collection, Handling, and Storage**

A geoprobe was used to obtain the OU 5 aquifer core samples. This equipment was a hydraulically-powered, probing machine designed for use in the environmental field. This equipment applied a “direct push” technique, also known as a soil probing technique, to obtain an intact soil core. The equipment pushed a probe cylinder by using static and percussion forces to advance sampling tools into the subsurface. The probe pushed 1.8-2.4 m into the ground until it reached the groundwater table then 1.2-1.8 m deeper into the aquifer material to obtain the core sample for analysis in this study.

The extraction of the aquifer material cores was via a plastic cylinder tube of about 1.5 m length and 3.5 cm diameter. The sampler tube containing the core was divided into sections of 30 cm. The top and the bottom of each section were covered with a plastic cap and wrapped with tape to preserve the soil cores intact until the end of the field work.

The samples were transported to the Utah Water Research Laboratory in insulated chests and stored under anaerobic conditions. In the anaerobic chamber, all soil core sections from one core were mixed and stored in double Ziploc plastic bags. All plastic bags were labeled with the well location number, sampling date and depth of the water table and were stored under anaerobic conditions at  $16 \pm 2^\circ \text{C}$  until processed.

#### 4.3 **Soil DNA Extraction of OU5 Aquifer Core Samples**

The aquifer material DNA isolation was done using the Ultra Clean Soil DNA Kit from MO BIO Laboratories (Carlsbad, CA). The DNA extraction followed the kit protocol. This extraction method extracted the DNA by adding the soil to a bead beating tube for rapid and thorough homogenization. Cell lysis occurred by mechanical and chemical methods. The DNA extraction was done on six, ~1 g replicates from each soil core sample; resulting in 120 total extractions. The number of replicates was chosen in order to have a good representation of the frequency of occurrence of the target DNA molecule in the core sample.

#### 4.4 **Real-Time PCR Detection of the Target DNA in the OU 5 Soil Cores**

This study applied the qRT-PCR method to quantify the starting quantity of the target 16S rDNA and functional genes in the OU 5 core samples. Table 4.1 shows the primers that were used in the qRT-PCR for amplification of the 16S rDNA target in the aquifer material of OU 5.

It is important to note that the *Rhodoferox* 16S rRNA gene primer amplified 16S rDNA from a range of microorganisms including *Rhodoferox ferrireducens* T118 (Finneran et al., 2003). Table 4.2 shows all known microorganisms that could be amplified in qRT-PCR DNA when the *Rhodoferox* primers were used. This primer was based on a clone library developed from an OU 5 core by the US Department of Energy's Joint Genome Institute. In this library 22 % of the 260 clones were similar to *Rhodoferox ferrireducens*.

**TABLE 4.1 Primer List for Organisms and Functional Genes Quantified in This Study**

Primer Name	DNA Target	Primer Sequence	References
DHC10F DHC10R	<i>Dehalococcoides</i> 16S rDNA	5'-GGGTTGTAAACCTCTTTTCAC-3' 5'-TCAGTGACAACCTAGAAAAC-3'	Major et al., 2002
vcrA2F450 vcrA2R892	Vinyl Chloride reductase gene, <i>vcrA</i>	5'-TGAGGAAGGGCACGGACTAT-3' 5'-GTGGTTGAGGTAGGGTGAAAGT-3'	Müller et al., 2004
DmichF DmichR	<i>Desulfuromas michiganensis</i> 16S rDNA	5'-CATTGAAACTGGGCGGCTT-3' 5'-CTTAATGCGTTAGCTTCGGC-3'	Zhou, 2008
PRBA338F PRUN518R	<i>Bacteria</i> 16S rDNA	5'-ACTCCTACGGGAGGCAGCAG-3' 5'-CTTAATGCGTTAGCTTCGGC-3'	Nakatsu et al., 2000
561F 825R	<i>Geobacter</i> 16S rDNA	5'-GCGTGTAGGCGGTTTCTTAA-3' 5'-TACCCGCACACCTAGTTCT-3'	Cummings et al., 2003
RodoferrinF R.ferr639R	<i>Rhodoferrax</i> 16S rDNA	5'-ACGGAACGAAACGGTCTGCCTT-3' 5'-CTATACAGTCACAAATGCAGGT-3'	Zhou, 2008
TceA923F TceA1116R	Trichloroethene reductive dehalogenase gene, <i>tceA</i>	5'-GCTTTGGCGGTGATGATAAG-3' 5'-GTTATAGCCAAGGCCTGCAA-3'	Magnuson et al., 2000

**TABLE 4.2 Twenty Possible Bacteria Amplified in qRT-PCR by *Rhodoferrax* 16S rDNA Primer Set (Data from Ribosomal Data Base Project II)**

Ribosomal Data Base ID	Genus/species	GenBank access No
S000125063	Antarctic bacterium	AJ440986
S000138085	uncultured beta proteobacterium	AJ421940
S000270888	uncultured beta proteobacterium	AJ575699
S000339023	uncultured Antarctic bacterium	AF173821
S000340933	uncultured beta proteobacterium	AF289168
S000341112	uncultured Green Bay ferromanganous micronodule bacterium	AF293004
S000354524	uncultured bacterium	AY050575
S000354549	uncultured bacterium	AY050600
S000356620	uncultured bacterium	AY218550
S000356657	uncultured bacterium	AY218587
S000356677	uncultured bacterium	AY218607
S000356705	uncultured bacterium;	AY218635
S000356712	uncultured bacterium;	AY218642
S000356718	uncultured bacterium	AY218648
S000356796	uncultured bacterium	AY218726
S000372736	uncultured bacterium	AY662012
S000380535	uncultured bacterium	AY706423
S000391844	beta proteobacterium Wuba139	AF336363
S000394152	<i>Rhodoferrax ferrireducens</i> (T)	AF435948
S000401956	uncultured bacterium	AY212596

The amplification reaction had a final volume of 25  $\mu\text{L}$  and included 12.5  $\mu\text{L}$  of Bio-Rad SybrGreen Master Mix, 7.38  $\mu\text{L}$  of autoclaved deionized water, 0.06  $\mu\text{L}$  of the primer and 5  $\mu\text{L}$  of the sample DNA. Previous qRT-PCR assays using OU 5 transect core samples supported the concentrations of the primer and sample DNA in the 25  $\mu\text{L}$  reaction volume. Since the total number of samples is 120 including the six replicates for each soil, the test was divided into two PCR events. Run 1 had 10 different core samples from soil core 2261 to 2270 with six replicates. Run 2 had the other 10 cores from 2271 to 2280 with their six replicates.

A total of 60 DNA samples were analyzed in each PCR event. All qRT-PCR analyses included standard, target DNA for the primer set. Table 4.3 shows the standards that were used in the study as well as the source from where they were obtained. Standard DNA was used in qRT-PCR as positive controls and to calibrate known concentrations of DNA with the detectable threshold fluorescence cycle (Ct).

**TABLE 4.3 Source of the Standard DNA Material used in This Study**

DNA Target	Standard name	Standard Source
<i>Dehalococcoides</i> 16S rDNA	<i>Dehalococcoides</i>	Genomic DNA
Vinyl Chloride reductase gene ( <i>vcrA</i> )	<i>vcrA2</i>	Plasmid DNA (Cloning product)
<i>Desulfuromas michiganensis</i> 16S rDNA	<i>Michiganensis</i>	Genomic DNA
<i>Bacteria</i> 16S rDNA	<i>Escherichia coli</i>	Genomic DNA
<i>Geobacter</i> 16S rDNA	<i>Geobacter sulfurreducens</i>	Genomic DNA from ATCC
<i>Rhodoferrax</i> -like 16S rDNA	<i>Rhodoferrax</i> JT	Plasmid DNA (Cloning product)
Trichloroethene reductive dehalogenase gene ( <i>tceA</i> )	<i>tceA</i>	Genomic DNA

For calibration, the known concentration of the standard DNA was diluted in at least 10-fold consecutive dilutions. All serial dilutions were run in duplicates. The test had two negative controls and six quality control checks. The negative controls had 5  $\mu$ L of autoclaved reagent grade deionized water instead of the DNA sample. The quality control checks were 3  $\mu$ L of DNA core sample spiked with the 3  $\mu$ L of the standard dilution # 3. The spike samples were analyzed in duplicate.

Once the strip PCR tubes (Phenix Research Products) were filled with SybrGreen Master Mix, water and primer, the DNA sample was added to the mix. Figure 4.4 shows the distribution of the standards, samples, spiked samples and negative controls in the 96 well plate of the PCR instrument.

The PCR program used for the 16s rDNA amplification had the following steps: one cycle for initial denaturation at 95° C for 10 minutes; then 40 cycles for denaturation at 95° C for 15 seconds, annealing at the corresponding primer annealing temperature (see Table 4.4) for 45 seconds, extension at 72° C for 1 minute, a second extension at 82° C for 15 seconds to avoid the formation of dimmers (Avrahami and Bohannan, 2007); followed by one cycle of final extension at 72° C for 10 minutes.

	1	2	3	4	5	6	7	8	9	10	11	12
A	1	1	1	2	3	4	5	6	7	8	9	10
B	2	2	1	2	3	4	5	6	7	8	9	10
C	3	3	1	2	3	4	5	6	7	8	9	10
D	4	4	1	2	3	4	5	6	7	8	9	10
E	5	5	1	2	3	4	5	6	7	8	9	10
F	6	6	1	2	3	4	5	6	7	8	9	10
G	7	7	2	11	12	13		14			15	16
H	8	8	3	11	12	13		14			15	16

**FIGURE 4.4** Distribution of the samples in the 96 well-plate (squares from 1- 10), standards (circles), spikes (squares from 11-16) and negative controls (diamonds).

**TABLE 4.4 QRT-PCR Program Used in This Study**

Cycle #	Steps	Rx Temp.	Time
Cycle 1	Initial DNA denaturation	95°C	10 min
Cycle 2	Denaturation	95°C	15 sec
	Primer annealing	57°C	45 sec
	Chain extension	72°C	60 sec
	Second extension	82°C	15 sec
Cycle 3	Final extension	82°C	10 min
Cycle 4	Melting curve gradient	55-95°C	10 sec

Finally, the melting curve step was after the 41st cycle from 55° C to 95° C, increasing by 1 degree for 10 seconds at each temperature. The annealing temperatures (T<sub>m</sub>) for each primer target were optimized according to a primer gradient optimization assay. Table 4.5 shows the following optimal annealing temperatures.

**TABLE 4.5 Optimized Annealing Temperatures (T<sub>m</sub>)**

DNA Target	Optimized Annealing Temperature
<i>Dehalococcoides</i> 16S rDNA	55°C
Vinyl chloride reductase gene ( <i>vcrA</i> )	60°C
<i>Desulfuromas michiganensis</i> 16S rDNA	61°C
Bacteria 16S rDNA	62°C
<i>Geobacter</i> 16S rDNA	56°C
<i>Rhodoferrax</i> -like 16S rDNA	57°C
Trichloroethene reductive dehalogenase gene ( <i>tceA</i> )	56°C

#### 4.5 **Physical and Chemical Analysis of the OU 5 Aquifer Material**

Approximately 500 g of each core sample was taken to the Soil Testing Laboratory at the Plants, Soil and Climate Department of Utah State University.

The following analyses were used to describe the physical and chemical characteristics of the OU 5 aquifer material:

- Texture analysis: Particle size by hydrometer
- pH
- Electrical conductivity
- Available nitrate and ammonia extracted with 2N KCl. Nitrate and ammonia nitrogen content was determined by using a flow injection analyzer instrument, methods S-3.10 and S-3.50 in Gavlak et al. (2003), respectively.
- Soil organic carbon by the Walkley-Black method (Walkley and Black, 1934)
- Saturation paste extract to determine water soluble Ca, Mg, K, S, Cl<sup>-</sup>, and NO<sub>3</sub><sup>-</sup>-N. Where Ca, Mg, and K were determined by inductively coupled argon plasma emission spectrophotometry (ICP), methods S-1.0 and S-1.60. Chloride from saturation paste was determined via a chloridometer, methods S-1.0 and S-1.40. Nitrate from the saturation paste extract was analyzed via a flow injection analyzer using the cadmium reduction spectrophotometric method (methods S-1.0 and 1.80). All cited methods were from Gavlak et al. (2003).
- Total element composition by acid digestion (US EPA 3050) and ICP analysis (US EPA 6010)
- Total As/Se by ICP/Mass spectrometry (US EPA 6020)

#### 4.6 TCE and Dissolved Oxygen Concentrations in the OU5 Study Area

The most recently measured TCE concentrations were provided by Mark Roginske who was the OU5 site manger. TCE concentrations used in the data analysis were those from the monitoring well nearest the sampling point. The TCE concentration in the wells shown in Table 4.6 was assumed to be the groundwater TCE concentration in the sample core. Dissolved oxygen concentration data were obtained in the same way.

#### 4.7 Arsenic and Iron Extraction Methods from the OU 5 Aquifer Material

A gram of soil aquifer material was extracted with 0.5 M HCl to determine Fe (II+III) and Fe (II) the OU 5 aquifer material.

**TABLE 4.6 Assigned Closest Well to Each Sampling Point in the Study Area and the Sampling Data of TCE, cis-DCE, and VC Concentrations**

Sample OU 5	Closest Monitoring Well in OU 5	Sampling date
2261	137	6-Feb-07
2262	138	7-Feb-07
2263	1072	6-Feb-07
2264	1069	19-Jan-07
2265	144	17-Jan-07
2266	144	17-Jan-07
2267	166	5-Feb-07
2268	1073	2-Feb-07
2269	1034	31-Oct-01
2270	135	2-Feb-07
2271	1026	31-Jan-07
2272	160	24-Jun-99
2273	1029	19-Jan-07
2274	1071	19-Jan-07
2275	166	5-Feb-07
2276	1070	6-Mar-07
2277	159	5-Feb-07
2278	1067	7-Feb-07
2279	142	14-Feb-07
2280	1025	6-Dec-01

This HCl extraction accounts for the acid soluble Fe (III) oxides, sorbed Fe (II) and Fe (III) iron carbonates, one portion of the extractant solution was used to measure Fe (II+III) by flame atomic absorption spectroscopy (Perkin Elmer, AAnalyst 800, Standard Method 3125 (APHA, 1998). The remaining extractant solution was used to measure Fe (II) by using the ferrozine procedure (Lovley and Phillips, 1987) with a spectrophotometer (Milton Roy 601) at 562 nm.

Another gram of material was extracted with 25 mL of 0.25 M hydroxylamine hydrochloride (HA-HCl) in 0.25 M HCl to obtain Fe (II+III). The poorly crystalline iron oxides are reduced to Fe (II) by this acidic reducing agent. This procedure, developed by Lovley and Phillips (1987), allows the rapid determination of microbially reducible Fe (III), called Bio Fe III, which is the HA-HCl in HCL extractable Fe (II+III) minus the HCl extractable Fe (II).

In addition, the OU 5 aquifer material cores were analyzed for arsenic by the two extraction methods, HCl and HA-HCl in HCl. The first extraction was the 0.5 M HCl, described above, to release As into solution. The next extraction, also the same as was used for Fe, used 5 ml of 0.25 M HA in 0.25 M HCl. This extraction method was more selective for dissolving the non-crystalline Fe (III) oxides which bind the bioavailable forms of arsenic.

By the above procedures, six variables were obtained according to the type of extraction method and the extractable form of iron and arsenic: HCl Fe(II+III), HCl Fe(II), HA-HCl+HCl Fe(II+III), Bio Fe(III), HCl As (III+V), HA-HCl+HCl total As. Those variables were further analyzed for their relationship to the target bacteria and functional gene densities.

#### 4.8 QRT-PCR Quality Control Criteria

After the qRT-PCR instrument had finished the program for DNA amplification, all standards, samples and spikes were analyzed with the following analytical and quality control criteria: linear regression model of standards, samples and spikes; threshold cycles no greater than the tolerance limit of the respective primer; threshold cycles no less than five cycles; distinctive peak in the melting curve at the corresponding melting temperature of the target DNA; recovery efficiency of the spikes in the acceptable range and no amplification of the blank samples.

##### 4.8.1 Linear Regression Model

The IQ 5 Optical System software, version 2.0 sorted the data from standards, spikes and samples onto a linear regression line with the threshold cycle in the 'y' axis and the log of copy numbers of the target DNA on the 'x' axis. The efficiency of the assay and the coefficient of determination of the standard curve were calculated based on the linear regression curve. All qRT-PCR tests were required to have efficiency values between 85-115 % as well as a coefficient of determination ( $R^2$ ) of 0.95-1 in order to qualify as an acceptable qRT-PCR assay.

The system software showed amplification curves similar to those in Figure 3.3, which have the number of cycles on the 'x' axis and the RFU on the 'y' axis. Again, perfect amplification must double the starting DNA in every cycle. In a 10-fold dilution of the standards, each standard is related by a factor of 10 to the next standard. Thus, the number of cycles to increase the DNA 10 times must be about 3.32. Consequently, amplification curves for all standards samples should be evenly separated by 3.32 cycles in order to obtain an efficiency of 100%.

#### **4.8.2 Tolerance Limit Method for Quantitation Limits in qRT-PCR**

The results of the qRT-PCR analyses from the transect study in October 2005, indicated that target microorganisms existed in the aquifer material of OU 5 but in very low concentrations. Consequently, it was important to determine the minimum, reliable DNA copy numbers detectable by the procedure. A tolerance limit method was used to evaluate the limit below which the quality of the DNA amplification was not acceptable.

The upper, one sided tolerance limit for the maximum acceptable Ct was determined using Equation 5 (Ostle, 1963)

$$\bar{X} + Ks \quad (4.1)$$

where,  $\bar{X}$  was the mean of seven replicate Ct values which are considered to be near the maximum reliable Ct value; s is the standard deviation and K is the one-sided tolerance factor (Ostle, 1963). The near-maximum Ct was selected based on the apparent departure from linearity of the Ct values based on linear regression of the standards and the existence of amplified products (e.g., primer dimer) other than the anticipated product in the melting temperature analysis. The quality control check of the tolerance limit method was that the copy numbers in any sample and the most dilute standard in the linear regression curve must yield Ct values less than the tolerance limit of the respective DNA target.

#### **4.8.3 The Melting Temperature Analysis**

The next quality control evaluation of the qRT-PCR was done using the melting curve analysis, which was required to show a significantly higher RFU derivative of the target DNA compared to other existing DNA products in the standards, samples and

spikes. The first derivative of the melt-curve RFU with time must indicate melting in a narrow temperature range, usually from 5 to 10 °C and should have similar temperature to that of the DNA amplified from the standards. The existence of other amplified products was shown as peaks before the peak of the target DNA. Amplified products melting early (at low temperatures) in the melting curve analysis were most likely primer-dimers and they appeared when there was poor primer design and/or when the concentration of target DNA was vanishingly low.

Samples with Ct values higher than the tolerance limit may have shown primer-dimer melt peaks along with a relatively small melt peak within the anticipated temperature range of the target DNA product. Such samples were considered to have positive but not quantifiable results since the quantifiable number given by the instrument is out of the detectable range. All positive not quantifiable (PNQ) results in the same soil core sample were counted to calculate the frequency of the PNQ from the six replicate samples.

In summary, to qualify as a positive, quantifiable (P) result the sample must meet two criteria: (1) Ct values less than the tolerance limit of the primer, and (2) the right melting temperature peak. PNQ results were considered when Ct values were higher than the tolerance limit but there was a noticeable peak at the anticipated melting temperature of the PCR product. Negative results occurred when there was no peak at the anticipated melt temperature of the PCR product.

#### **4.8.4 Spikes**

The spiked samples were done under the same conditions as the rest of the samples. Six OU 5 core samples were spiked in duplicates to measure the recovery

efficiency qRT-PCR analytical method. Acceptable qRT-PCR events showed percent recoveries between 80 to 110%.

## CHAPTER 5

### ANALYSIS OF THE DATA

All data were sorted in 57 variables and 20 OU 5 core-observations. The variables included all measured physical and chemical properties, maximum quantifiable copy numbers of target DNA, frequency of PNQ results for the target bacteria, concentration of TCE and other chlorinated products, dissolved oxygen concentration reducible As and Fe concentration forms and released Fe(II) for all of the sampling points. The exploratory statistical analyses included three different multivariate methods: clustering, linear discriminant analysis and the tree classification method.

Clustering can classify non-normal distributed data but linear discriminant analysis assumes a normal distribution of the data. The Shapiro-Wilk test was used to evaluate the normality assumption of the data (Chambers et al., 1991). Table 5.1 shows the results of the test applied to each variable. The test was computed in R software version 2.5.1. (R Development Core team, 2007) A log transformation of the data was attempted if the normality hypothesis was rejected. Variables such as TCE, EC, soluble  $K^+$ , soluble  $Cl^-$ , total Na, total P, and total Zn were not included in the clustering and discriminant analysis tests because they were not normally distributed after log transformation. Bacteria gene copy numbers and *vcrA* functional gene copy numbers were included in both tests; other target genes were not in the analysis because of the high frequency of censored data. The Fe(II) and total Sr data were transformed to logarithms before inclusion in the statistical analyses. The clustering and linear discriminant analysis included 31 variables.

TABLE 5.1 All Measured Variables Included in Each Multivariate Method

Label	Variables	Raw data		Data with Logarithm transformation		Variable Included in the analysis	
		Shapiro-Wilk	Normality Assumption	Shapiro-Wilk	Normality Assumption	Clustering	Discriminant analysis
Bacmean	Bacteria Average Log copy numbers	0.24	Normal			yes	yes
Bacmin	Bacteria minimum Log copy numbers	0.40	Normal			yes	yes
Bacmax	Bacteria maximum Log copy numbers	0.45	Normal			yes	yes
Dehaloc	Dehalococcoides maximum Log copy numbers	1.02E-07	Not Normal	NT		no	no
D.Mich	D.michiganensis maximum Log copy numbers	1.27E-04	Not Normal	NT		no	no
vcrA	vcrA maximum Log copy numbers	0.14	Normal			yes	yes
tceA	tceA maximum Log copy numbers	2.26E-08	Not Normal	NT		no	no
Geobacter	Geobacter maximum Log copy numbers	2.29E-05	Not Normal	NT		no	no
Rhodo	Rhodoferrax ferrireducens-like maximum Log copy numbers	3.81E-05	Not Normal	NT		no	no
HCl Fe(II+III)	Fe(II+III) with HCl method, mg/Kg	0.77	Normal			yes	yes
HA-HCl+HCl Fe(II+III)	Fe(II+III) with HA-HCl+HCl method, mg/Kg	0.66	Normal			yes	yes
HCl Fe(II)	Fe(II) with HCl method, mg/Kg	2.25E-04	Not Normal	0.679802	Normal	yes	yes
Bio FeIII	Microbially available Fe(III), mg/Kg	0.80	Normal, dependency			no	no
HCl As(III+V)	As(III+V) with HCl method, mg/Kg	0.77	Normal			yes	yes
HA-HCl+HCl As(III+V)	As(III+V) with HA-HCl+HCl method, mg/Kg	0.97	Normal			yes	yes
pH	pH	0.93	Normal			yes	yes
EC	Electrical Conductivity, dS/cm	9.40E-04	Not Normal	0.0012	Not Normal	no	no
Sand	Sand, %	0.17	Normal			yes	yes
Silt	Silt, %	0.29	Normal			yes	yes
Clay	Clay, %	0.06	Normal			yes	yes
OM	Organic Matter, %	0.30	Normal			yes	yes
Arsenic	Arsenic, mg/Kg	6.23E-05	Not Normal	0.01341	Normal	yes	yes
Selenium	Selenium, mg/Kg	0.58	Normal			yes	yes
NO3-N	NO3 with 2N KCl, mg/Kg	0.41	Normal			yes	yes
NH4-N	NH4-N with 2N KCl, mg/Kg	0.49	Normal			yes	yes
CaSPE	Soluble Ca, mg/L	0.57	Normal			yes	yes
MgSPE	Soluble Mg, mg/L	0.27	Normal			yes	yes
KSPE	Soluble K, mg/L	1.09E-06	Not Normal	0.000306	Not Normal	no	no
SSPE	Soluble S, mg/L	0.03	Normal			yes	yes
Cl	Soluble Cl, mg/L	2.19E-06	Not Normal	0.000423	Not Normal	no	no
NO3_NSPE	Soluble NO3-N, mg/L	0.61	Normal			yes	yes
TAI	Total Al, %	0.03	Normal			yes	yes
TCa	Total Ca, %	0.96	Normal			yes	yes
TCr	Total Cr	0.94	Normal			yes	yes
TK	Total K, %	0.05	Normal			yes	yes
TMg	Total Mg, %	0.81	Normal			yes	yes
TMn	Total Mn, mg/Kg	0.68	Normal			yes	yes
TMo	Total Mo, mg/Kg	0.09	Normal			yes	yes
TNa	Total Na, %	1.86E-06	Not Normal	1.86E-06	Not Normal	no	no
TP	Total P, %	1.31E-05	Not Normal	1.09E-05	Not Normal	no	no
TSr	Total Sr	5.81E-05	Not Normal	0.218193	Normal	yes	yes
TZn	Total Zn, %	0.009	Not Normal	0.000571	Not Normal	no	no
DO	DO concentration, mg/L	0.28	Normal			yes	yes
TCE	TCE concentration, ug/L	2.17E-05	Not Normal	0.001679	Not Normal	no	no
DCE11	DCE11 ug/L	1.47E-05	Not Normal	NT		no	no
DCE12C	DCE12C ug/L	4.46E-07	Not Normal	NT		no	no
VC	VC, ug/L	3.89E-09	Not Normal	NT		no	no
Total number of variables included in the test						31	31

The clustering analysis grouped the samples into subsets or clusters based on aquifer core properties in such a way that all samples inside a cluster are more closely

related to one another than samples in different clusters (Hastie et al., 2001). The calculations of the clustering and discriminant analysis were done with JMP Software (SAS Institute, 2002). Clustering analysis was represented in a vertical hierarchical tree plot; the plot shows all samples grouping in clusters according to a similarity value which is calculated by the Euclidean distance between two data points as shown in Equation 5.1.

$$(x, y) = \left[ \sum (x_i - y_i)^2 \right]^{1/2} \quad (5.1)$$

By looking at the branches and the joints in the hierarchical tree plot, it was possible to determine the number of clusters for all samples and interpret them for all relationships. Consequently, a new group of data was generated from the clustering analysis; all samples had a single assigned clustering group. The discriminant analysis included this new variable “cluster number” from the clustering analysis to explore the core properties that distinguish each cluster.

The most relevant variables were identified based on the distance to the mean and the associated probability. The software automatically selected the variables that discriminate most among clusters. A two-dimensional canonical plot showed the cluster and the confidence interval of the mean for each group.

The tree classification showed the best splitting variables and the split points based on an algorithm’s decision (Hastie et al., 2001). This method can function with non-normal distributed data so the tree analysis included forty-nine variables. The regression trees were calculated by R computer software version 2.5.1 student edition (R Development Core team, 2007). Six regression trees for each gene were obtained from the analysis. Each tree had one dependent variable which was the frequency of

quantifiable and non-quantifiable results (P+PNQ) of the target genes against all variables including the P+PNQ results of all other target genes.

## CHAPTER 6

## RESULTS

## 6.1 Gene Limits of Quantitation

The limits of quantitation for the qRT-PCR obtained with the tolerance limit method using the target primers are shown in Table 6.1. The efficiencies of all tests were within the acceptable range. The number obtained by Equation 5.1 was the limit Ct value where 95 % of all sample Ct values were below this tolerance limit. Then, the limit Ct value was used to calculate the corresponding logarithm DNA copy numbers using the linear regression equation of the qRT-PCR assay. This result was known as the tolerance limit in units of DNA copies per  $\mu\text{L}$  of soil DNA extract. In order to express the tolerance limit in units of log copies/g of dry aquifer material, the tolerance limit was multiplied by 50  $\mu\text{L}$  (the volume of extract from 1 g wet weight of material) and divided by an average moisture content of 18% (see Appendix A for details of assays).

**TABLE 6.1 Tolerance Limit of 16S rDNA Primers**

DNA Target	Tolerance limit (Copies/ $\mu\text{L}$ )	Log copies/g dry soil (Moisture 18%)	95% of Ct values below the limit of:	Efficiency of the PCR (%)
<i>Dehalococcoides</i> 16S rRNA gene	40	3.4	37	107
Vinyl chloride reductase gene	10	1.8	29	102
<i>D. michiganensis</i> 16S rRNA ( <i>vcrA</i> ) gene	115	3.8	37	100
<i>Bacteria</i> 16S rRNA gene	15	3	32	100
<i>Geobacter</i> 16S rRNA gene	47	3.5	36	90
<i>Rhodofera</i> -like 16S rRNA gene	131	3.9	34	90
Trichloroethene dehalogenase ( <i>tceA</i> ) gene	24	3.2	38	102

## 6.2 Gene Distribution and Population Density

All reported qRT-PCR samples obtained efficiencies in the acceptable range of 85-115%. Standards used at each qRT-PCR event followed the quality control criteria of the linear regression model, threshold cycles were no greater than the Ct tolerance limit but higher than 5 cycles, the melting curve had a recognizable RFU derivative within a ten degree C- temperature range, and there were no peaks of other amplified DNA products. Spiked samples showed recovery efficiencies in the acceptable range and melting curves similar to the standards at each qRT-PCR event. Blank samples in all assays did not show any amplification during the qRT-PCR (data shown in Appendix B1-B7).

### 6.2.1 Bacterial 16S rRNA Genes

The bacterial 16S rRNA gene was quantified in all OU 5 aquifer core samples. The *Bacteria* primer (a domain directed primer) was used to measure the population density of all types of bacteria at each sample location of the study area. Table 6.2 shows the *Bacteria* density in units of DNA copies/g dry soil at each sample location. The average *Bacteria* density was  $9.29\text{E}+05$  DNA copies/g dry soil in the study area (See Appendix B-1 for results of the assay).

Transect qRT-PCR results collected in 2005 showed an average *Bacteria* density of  $9.33\text{E}+06$  copies/g dry soil from the seven inside-plume core samples along the transect. Control OU 5 core samples 2252 and 2257 located outside of the TCE-plume obtained  $2.14\text{E}+08$  and  $4.36\text{E}+04$  copies/g dry soil, respectively.

**TABLE 6.2 Density of *Bacteria* in the OU 5 Study Area in DNA Copies/g Dry Soil**

Soil core Sample in OU5	Geom mean (copy #/g dry soil)
2261	2.86E+05
2262	1.97E+06
2263	4.74E+04
2264	1.23E+06
2265	1.10E+05
2266	2.89E+06
2267	1.18E+05
2268	2.43E+06
2269	2.46E+05
2270	5.25E+05
2271	3.35E+05
2272	1.56E+06
2273	4.28E+05
2274	2.17E+06
2275	9.32E+05
2276	3.17E+04
2277	1.93E+06
2278	4.43E+05
2279	4.95E+05
2280	4.02E+05

Figure 6.1 shows the *Bacteria* 16S gene distribution in the OU 5 study area. The distribution in the area was relatively uniform ranging over less than one order of magnitude. The average log DNA copies/g was 5.70; the highest population (6.46 log DNA copies/g dry soil) was found in Core 2266 at the north of the area. The lowest (4.5 Log DNA copies/g dry soil) was found in the Core 2276 located at the south western side of the study area. Groundwater flow direction was toward the western side of the site as shown in Figure 6.1.

### 6.2.2 Dechlorinating Bacteria

The qRT-PCR results from the preliminary transect sampling showed positive, quantifiable results of *Dehalococcoides* bacteria in the OU 5 cores 2252, 2253, and 2255 with a frequency of one out of three replicate samples.

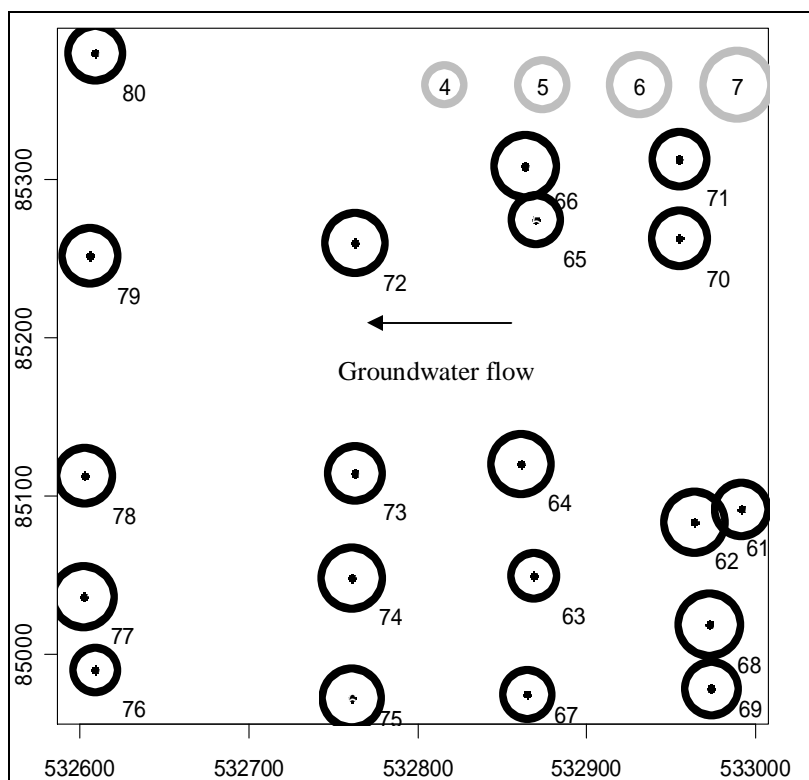


**FIGURE 6.1** *Bacteria* distribution in the OU 5 study area, X and Y axes are N-E coordinates (m). Number in black circle is the maximum log DNA copies per g dry soil at each core location. Core identification number is at the right bottom of each circle. Circle dimensions from 4 to 7 indicate the scale from the lowest to the highest log copy numbers.

They were located at 155, 264, and 298 m, respectively, from the eastern monitoring well within the TCE-source area. The analysis produced a noticeable peak in the curve dRFU/dT at the correct melting temperature and Ct values lower than the detection limit of 37 cycles. PNQ results were obtained in one out of three replicate samples from Core OU 5 2256. This core was located at 823 m from the source point.

*Dehalococcoides* bacteria were found in three cores in the grid study area. As shown in Table 6.3, cores 2273, 2274, and 2275 yielded positive, quantifiable *Dehalococcoides* 16S rRNA gene copy numbers with frequencies of one out of six and three out of six replicate samples.

**TABLE 6.3 Frequency of Quantifiable, Positive not Quantifiable (PNQ), and Negative Results for *Dehalococcoides* sp in the OU 5 Study Area**

OU5 22-	61	62	63	64	65	66	67	68	69	70	71	72	73	74	75	76	77	78	79	80
Negative	6	6	6	6	6	6	6	6	6	6	6	6	5	5	3	6	6	6	5	6
Quantifiable													1	1	3					
PNQ																			1	
Quant +PNQ													1	1	3				1	
Max Log DNA/ g dry soil													3.9	4.5	4.3					
Min Log DNA/ g dry soil													3.9	4.5	4.0					

P+PNQ is the summation of the quantifiable plus PNQ results. Max and Min are the maximum and minimum quantifiable results within the six replicate samples of each core.

The highest frequency (three out of six) of quantifiable results was observed in core 2275. Positive but not quantifiable (PNQ) results were detected in the Core 2279 in one out of 6 replicate samples. All quantifiable results obtained a peak in the curve of dRFU/dT versus temperature at 84-85° C and Ct values lower than the Ct tolerance limit during the qRT-PCR assay. (See Appendix B-2 for details of the assays.) Figure 6.2 shows the maximum *Dehalococcoides* bacteria distribution in the study area in units of log DNA copy numbers per g dry soil. The highest positive result was found in Core OU5 2274 where TCE concentration in the closest monitoring well was 76 µg/L.

Table 6.4 shows the frequencies of the results for *Desulfuromonas michiganensis* 16S rDNA at each core location. Quantifiable results were observed in six OU 5 cores (2262, 2263, 2264, 2267, 2268, and 2270) with frequencies of one and two out of six replicate samples. The highest frequencies of quantifiable results were observed in cores 2263, 2264, and 2268. Negative results were observed in all cores with an average frequency of five out six samples. PNQ results were observed in eight OU 5 cores, the highest frequency (three out of six) of PNQ was observed in the cores 2269 and 2270. (Appendix B-3 shows detailed results of the qRT-PCR assays.)

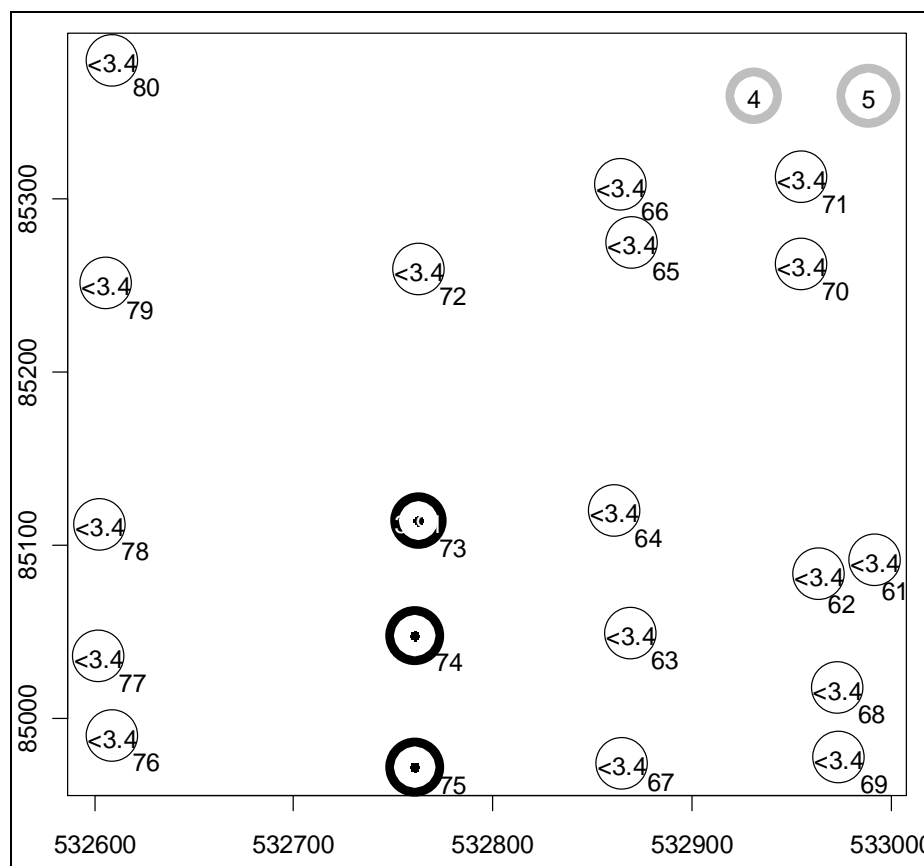


**FIGURE 6.2** Maximum *Dehalococcoides* bacteria distribution in the OU 5 study area, X and Y axes are N-E coordinates (m). Number in black circle is the log copy number per g dry soil at each well location; well identification number is at the right bottom of each circle. Circle dimensions from 4 to 5 indicate the scale from the lowest to the highest log copy numbers.

**TABLE 6.4** Frequencies of Quantifiable, Positive not Quantifiable (PNQ), and Negative Results for *D. michiganensis* in the OU 5 Study Area

OU5 22-	61	62	63	64	65	66	67	68	69	70	71	72	73	74	75	76	77	78	79	80
Negative	5	4	4	3	6	5	5	4	3	2	5	5	6	6	6	5	6	6	5	6
Quantifiable		1	2	2			1	2		1										
PNQ	1	1		1		1			3	3	1	1								
P+PNQ	1	2	2	3		1	1	2	3	4	1	1			1					
Max Log DNA/ g dry soil	<3.8	4.0	3.9	5.0		<3.8	4.2	4.6	<3.8	4.7	<3.8	<3.8				<3.8				
Min Log DNA/ g dry soil	<3.8	4.0	3.8	4.2		<3.8	4.2	3.9	<3.8	4.7	<3.8	<3.8				<3.8				

P+PNQ is the summation of the quantifiable plus PNQ results.

Max and Min are the maximum and minimum quantifiable results within the six replicate samples of each core.

Figure 6.3 shows the distribution of the maximum *D. michiganensis* density measured in each core. The site-wide maximum density was found in Core 2264 with 5 log DNA copy numbers per g dry soil. The core was located near the monitoring well U5-1069 with a TCE concentration of 360  $\mu\text{g/L}$ .

### 6.2.3 Iron-Reducing Bacteria

Quantifiable results for the presence of *Geobacter* sp. in the OU 5 study area were obtained in eight cores: 2262, 2263, 2264, 2265, 2271, 2273, 2277, and 2279, with frequencies of one, two, and three out of six replicate samples.

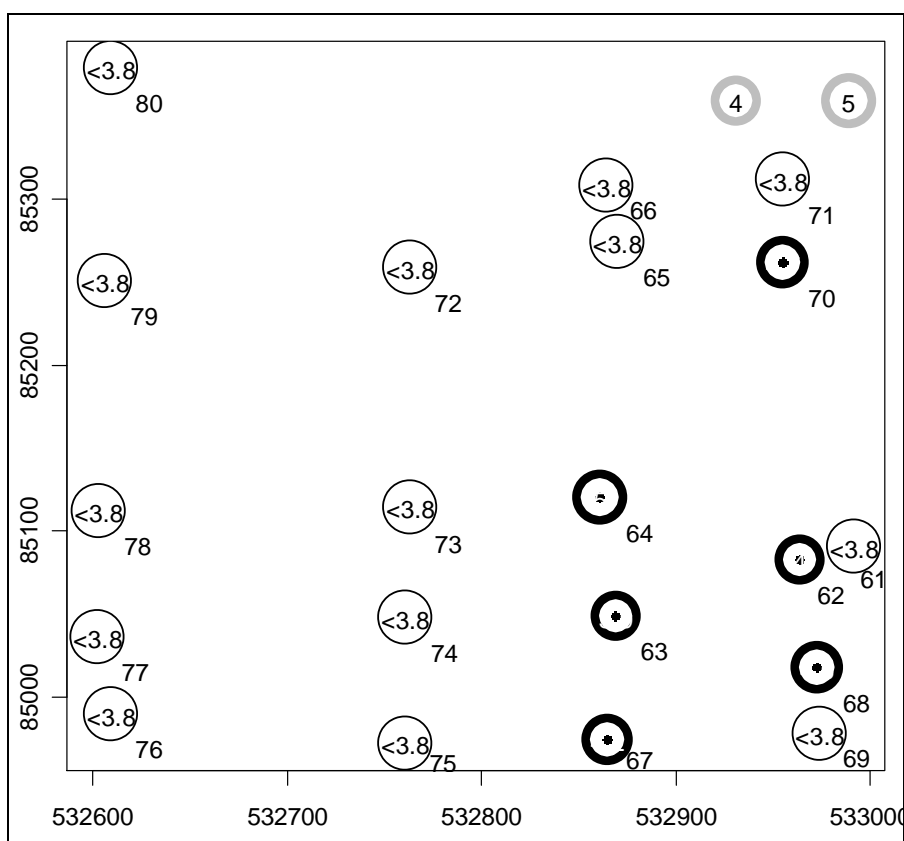


**FIGURE 6.3** Maximum *Desulfuromonas michiganensis* 16S rRNA gene distribution in the OU 5 study area, X and Y axes are N-E coordinates (m). Number in black circle is the log copy number per g dry soil at each core location. Core identification number is at the right bottom of each circle. Circle dimensions from 4 to 5 indicate the scale from the lowest to the highest log copy numbers.

Negative results occurred in all cores with an average frequency of 5 out of 6 replicate samples. PNQ results were observed in three cores with frequencies of 1 out of 6 replicate samples. Table 6.5 shows the summation of the positive quantifiable (P) plus the PNQ results. Appendix B-4 shows results of the qRT-PCR assays.

Figure 6.4 shows the distribution of the maximum *Geobacter* 16S rRNA genes in log copy number per g dry soil. The highest quantifiable concentration was observed in Core 2271, which is located near a monitoring well with a relatively low TCE concentration of 2.9 µg/L.

The determination of the concentration of *Rhodoferrax ferrifeducens*-like bacteria showed positive results in 14 core samples with frequencies from one to four out of six replicate samples (Table 6.6). The highest frequency of positive results (four out of six replicate samples) was observed in cores 2271, 2275, 2278, and 2280. PNQ results were observed in one core with a frequency of one out of six subsamples. Negative results were observed in all cores with an average frequency of four out of six replicate samples). Appendix B-5 shows detailed results of the qRT-PCR assays.

**TABLE 6.5 Frequency of Quantifiable, Positive not Quantifiable (PNQ), and Negative Results for *Geobacter* sp. in the OU 5 Study Area**

OU 5 22-	61	62	63	64	65	66	67	68	69	70	71	72	73	74	75	76	77	78	79	80
Negatives	6	4	3	4	5	6	6	6	6	5	4	6	4	6	6	6	4	6	5	6
Quantifiable		2	3	2	1						2		1				1		1	
PNQ										1			1				1			
P + PNQ		2	3	2	1						2		2				2		1	
Max Log DNA/ g dry soil		5.2	5.1	5.3	3.7						6.1		4.1				3.8		3.6	
Min Log DNA/ g dry soil		4.7	4.6	4.4	3.7						3.7		4.1				3.8		3.6	

P+PNQ is the summation of the quantifiable plus PNQ results.

Max and Min are the maximum and minimum quantifiable results within the six replicate samples of each core.

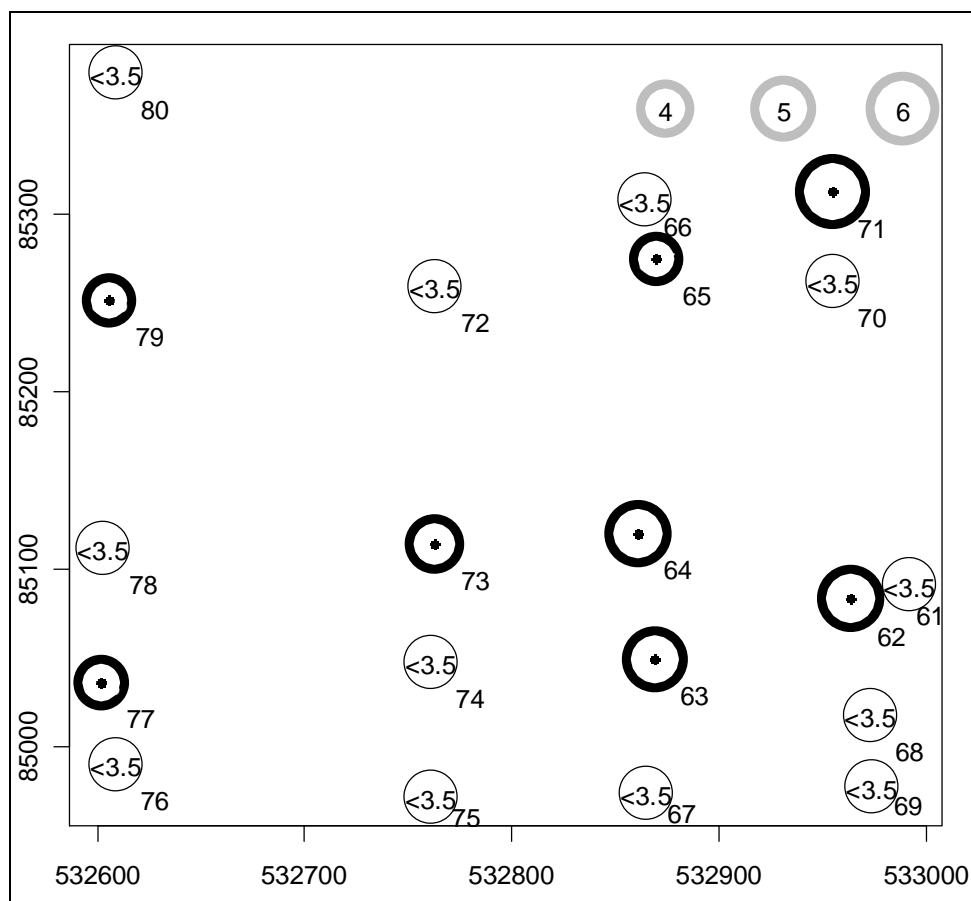


**FIGURE 6.4** Maximum *Geobacter* sp. bacteria distribution in the OU 5 study area. X and Y axes are N-E coordinates (m). Number in black circle is the log copy number per g dry soil at each well location; well identification number is at the right bottom of each circle. Circle dimensions from 4 to 6 indicate the scale from the lowest to the highest log copy numbers.

**TABLE 6.6** Frequency of Positives, Positive not Quantifiable (PNQ), and Negative Results for *Rhodoferrax Ferrireducens*-like Bacteria in the OU 5 Study Area

OU 5 22-	61	62	63	64	65	66	67	68	69	70	71	72	73	74	75	76	77	78	79	80
Negative	5	6	6	4	6	2	6	3	5	6	2	3	5	4	2	6	3	2	4	2
Quantifiable	1			2		3		3	1		4	3	1	2	4		3	4	2	4
PNQ						1														
P+PNQ	1			2		4		3	1		4	3	1	2	4		3	4	2	4
Max Log DNA/ g dry soil	7.5			7.7		7.3			6.2		7.2	7.2	7.2	6.7	6.6		7.1	6.8	6.6	8.2
Min Log DNA/ g dry soil	7.5			6.5		7.0			6.2		6.6	6.8	7.2	6.2	5.7		6.2	6.2	5.9	5.3

P+PNQ is the summation of the quantifiable plus PNQ results.

Max and Min are the maximum and minimum quantifiable results within the six replicate samples of each core

Figure 6.5 shows the maximum bacteria distribution of *Rhodoferax ferrireducens*-like bacteria in log DNA copy number per g dry soil. The highest maximum log DNA copy number was observed in Core 2280 located in an area with no TCE contamination.

#### 6.2.4 Reductase Functional Genes

The vinyl chloride reductase functional gene frequency is shown in Table 6.7. Fourteen OU 5 cores had positive quantifiable counts, with frequencies from one to four out of six subsamples. The highest quantifiable results were observed in Core 2262 where the closest monitoring well registered a TCE concentration of 83  $\mu\text{g/L}$ .

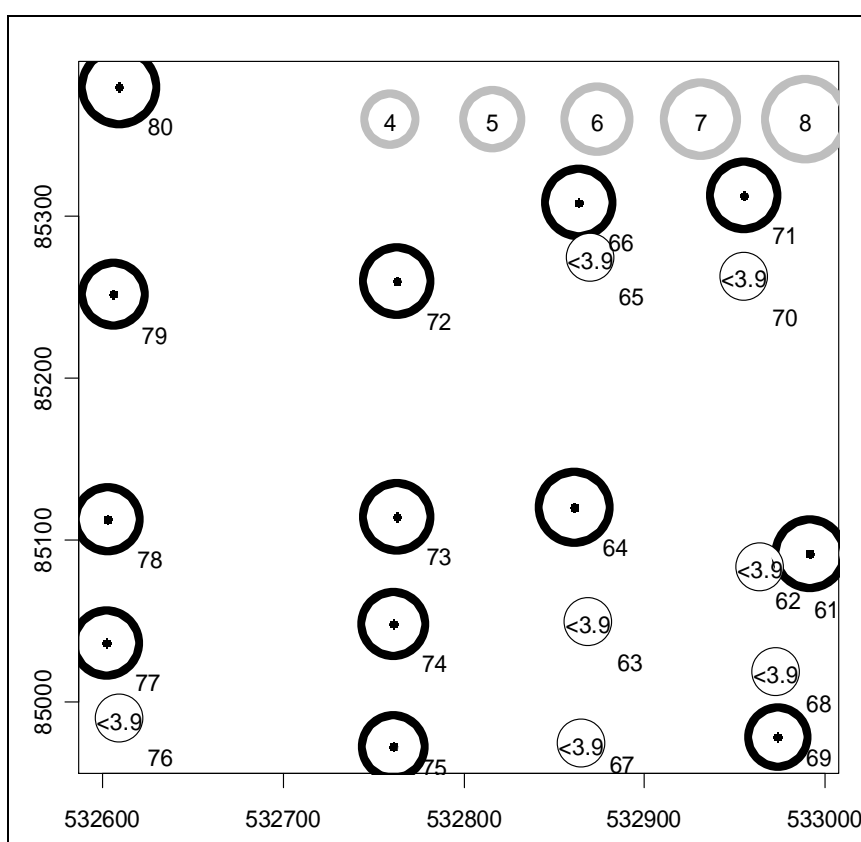


**FIGURE 6.5** Maximum *Rhodoferax ferrireducens*-like bacteria distribution in the OU 5 study area; X and Y axes are N-E coordinates (m). Number in black circle is the log copy number per g dry soil at each well location; well identification number is at the right bottom of each circle. Circle dimensions from 4 to 8 indicate the scale from the lowest to the highest log copies numbers.

**TABLE 6.7 Frequency of Positives, Positive not Quantifiable (PNQ), and Negative Results for *vcrA* Functional Gene in the OU 5 Study Area**

OU5 22-	61	62	63	64	65	66	67	68	69	70	71	72	73	74	75	76	77	78	79	80
Negative	3	2	2	3	5	4		2	4	2	2		1	4	2	2	2		4	3
Quantifiable	3	4	2		1	1	3		1	2		1		1	1		1		1	3
PNQ			2	3		1	3	4	1	2	4	5	5	1	3	4	3	6	1	
P + PNQ	3	4	4	3	1	2	6	4	2	4	4	6	5	2	4	4	4	6	2	3
Max Log DNA/ g dry soil	2.7	3.1	2.8	<1.8	2.0	2.2	2.7	<1.8	2.4	3.1	<1.8	2.7	<1.8	2.1	2.5	<1.8	2.5	<1.8	1.9	2.9
Min Log DNA/ g dry soil	2.2	2.1	2.6	<1.8	2.0	2.2	2.1	<1.8	2.4	2.7	<1.8	2.7	<1.8	2.1	2.5	<1.8	2.5	<1.8	1.9	2.1

P+PNQ is the summation of quantifiable plus PNQ results; maximum and minimum quantifiable result within the 6 replicate samples of each core.

Negative results were observed in 17 cores with frequencies from one to five out of six replicate samples. PNQ results of the *vcrA* gene obtained frequencies from one to six out of six replicate samples. Appendix B-6 shows detailed results of both assay batches.

Figure 6.6 shows the maximum bacteria distribution of the *vcrA* gene in the study area. This functional gene was found at low but relatively uniform concentrations in the study area. The highest observations were observed in Cores 2262 and 2270 with 3.1 log DNA copies/g dry soil in both cases. They were located in areas with different TCE concentrations of 1.7 and 83 µg/L, respectively.

The qRT-PCR results for the *tceA* functional gene showed negative results in all core samples with an average frequency of 5.7 out of 6 replicate samples as shown in Table 6.8. The numbers of replicates in Cores 2261 and 2268 were four and in Core 2263 was five. Positive quantifiable results were found in Cores 2268 and 2274 in one out of six replicate samples for both cases. No PNQ results were observed in the samples. Appendix B-7 shows detailed results of the assay batches.

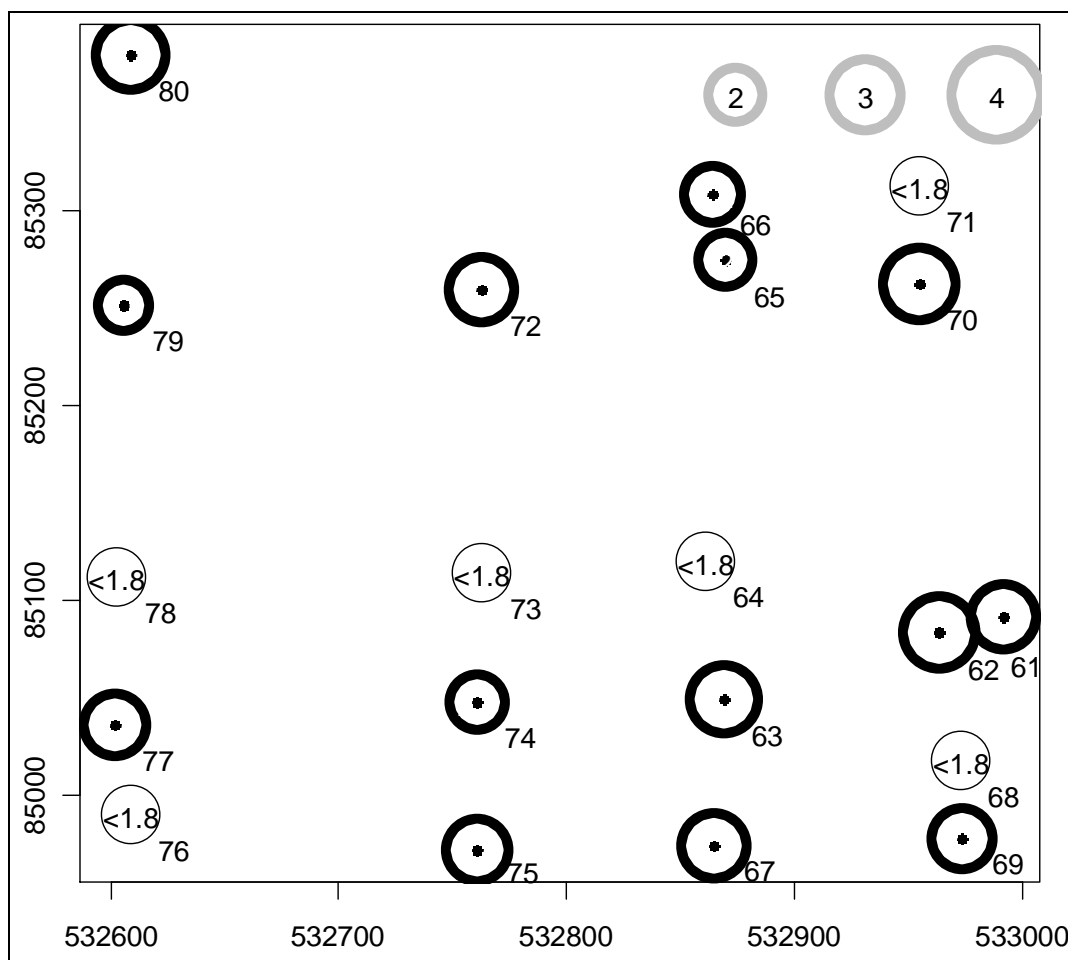


**FIGURE 6.6** Distribution of *vcrA* functional gene in the OU 5 study area, X and Y axes are N-E coordinates (m). Number in black circle is the log copy number per g dry soil at each well location; well identification number is at the right bottom of each circle. Circle dimensions from 2 to 4 indicate the scale from the lowest to the highest log copy numbers.

**TABLE 6.8** Frequency of Positives, Positive not Quantifiable (PNQ) and Negative Results for *tceA* Functional Gene in the OU 5 Study Area

OU 5 22-	61	62	63	64	65	66	67	68	69	70	71	72	73	74	75	76	77	78	79	80
Negative	4	6	5	6	6	6	6	4	6	6	6	6	6	5	6	6	6	6	N/T	6
Quantifiable								1						1					N/T	
PNQ																			N/T	
P +PNQ								1						1					N/T	
Max Log DNA/ g dry soil								4.2						3.3						
Min Log DNA/ g dry soil								4.2						3.3						

P+PNQ is the summation of quantifiable plus PNQ results; maximum and minimum quantifiable result within the replicate samples of each core.

Figure 6.7 shows the maximum observed gene concentration distribution of *tceA* in log DNA copies per g dry soil. The highest copy number was found in Core 2268 where the TCE concentration of the closest monitoring well was 1 µg/L.

### 6.3 Physical and Chemical Properties of the OU 5 Aquifer Material

Table 6.9 shows the total concentration of selected elements in the aquifer material samples. Table 6.10 shows the results of the texture, pH, electrical conductivity, available  $\text{NO}_3^-$ -N and  $\text{NH}_4^+$ -N, soil organic carbon, total arsenic and selenium and the soluble elements such as Ca, Mg, K, S, Cl<sup>-</sup>,  $\text{NO}_3^-$ -N.

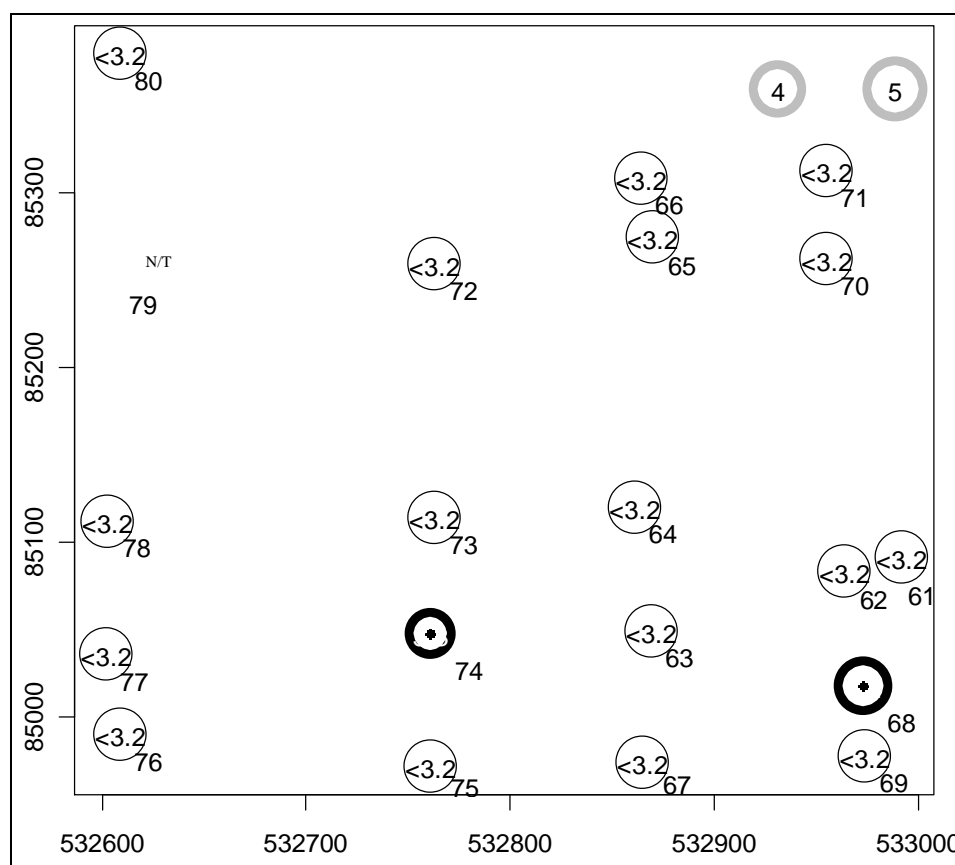


**FIGURE 6.7** Distribution of *tceA* functional gene in the OU 5 study area; X and Y axes are N-E coordinates. Number in black circle is the log copy number per g dry soil at each well location; well identification number is at the right bottom of each circle. Circle dimensions from 4 to 5 indicate the scale from the lowest to the highest log copy numbers. Core 2279 was not tested (N/T).

**TABLE 6.9 ICP Analysis for Total Element Composition of the OU 5 Core Aquifer Samples**

OU 5 Well	Al	Ca	Cr	K	Mg	Mn	Mo	Na	P	Sr	Zn
	%	%	mg/kg	%	%	mg/kg	mg/kg	%	%	mg/kg	mg/Kg
U5 2261	0.41	3.28	6.86	0.09	0.62	148.9	17.5	0.01	0.06	29.6	19.0
U5 2262	0.43	3.44	7.53	0.09	0.64	125.4	17.7	0.01	0.05	34.7	19.3
U5 2263	0.37	3.81	6.9	0.08	0.64	175.6	16.8	0.01	0.06	43.2	18.8
U5 2264	0.52	4.17	8.95	0.11	0.73	214.8	20.9	0.01	0.06	43.3	23.2
U5 2265	0.40	3.26	6.51	0.08	0.60	192.6	16.0	0.01	0.06	29.7	17.5
U5 2266	0.21	2.01	5.75	0.04	0.27	58.16	10.2	0.01	0.06	19.5	10.1
U5 2267	0.51	4.63	9.48	0.10	0.78	238.2	17.7	0.02	0.06	58.1	20.8
U5 2268	0.47	3.88	7.95	0.10	0.72	165.6	17.4	0.01	0.06	40.1	19.9
U5 2269	0.45	3.97	8.05	0.09	0.70	234.8	17.5	0.01	0.06	44.7	19.8
U5 2270	0.29	2.66	5.76	0.06	0.46	149.4	12.3	0.01	0.06	23.7	13.4
U5 2271	0.45	3.54	8.94	0.10	0.65	185.4	19.9	0.02	0.06	30.7	21.3
U5 2272	0.41	3.78	6.74	0.09	0.66	172.4	16.4	0.01	0.06	35.7	18.6
U5 2273	0.24	2.71	5.54	0.06	0.49	124.2	13.7	0.01	0.05	27.7	14.7
U5 2274	0.47	4.41	7.84	0.11	0.89	175.9	16.2	0.02	0.06	71.7	20.5
U5 2275	0.47	5.60	7.74	0.10	1.02	200.3	13.7	0.02	0.05	135.3	19.8
U5 2276	0.46	4.15	7.34	0.10	0.75	191.2	16.6	0.02	0.06	56.7	19.6
U5 2277	0.42	3.20	6.92	0.09	0.75	146.7	16.3	0.01	0.06	39.3	19.0
U5 2278	0.55	4.58	9.97	0.12	0.89	215	21.1	0.02	0.07	51.0	24.5
U5 2279	0.22	2.72	4.12	0.05	0.47	110.7	7.70	0.01	0.05	23.7	9.72
U5 2280	0.40	3.26	7.52	0.09	0.60	161.3	18.9	0.01	0.06	31.1	19.9
<b>Average</b>	0.41	3.65	7.32	0.09	0.67	169.33	16.21	0.01	0.06	43.47	18.48
<b>St deviation</b>	0.10	0.83	1.42	0.02	0.17	43.94	3.34	0.00	0.00	25.29	3.80
<b>CV</b>	24%	23%	19%	23%	25%	26%	21%	31%	8%	58%	21%
<b>Reporting Limits:</b>	0.01	0.01	2.0	0.01	0.01	1.0	2.0	0.01	0.01	1.0	2.0

The average texture of the aquifer material core samples was 64 % sand, 30 % silt and 8 % clay. The highest sand content was found in Core 2266. The highest clay content was found in Cores 2264, 2267, and 2275. The average pH and EC of the aquifer cores was 8.17 and 0.6 dS/m, respectively. The average soil organic matter was 0.4 % and the highest percent of organic matter was found in Core 2275. The average total arsenic and selenium was 4.71 and 0.73 mg/kg, respectively. Total arsenic showed the highest coefficient of variation (CV) of 47%. The average  $\text{NO}_3^-$ -N and  $\text{NH}_4^+$ -N in the 2N KCl extract was 1.74 and 1.42 mg/kg with a CV of 8% and 38% respectively. The average Ca, Mg, K, S, Cl<sup>-</sup> and  $\text{NO}_3^-$ -N was 48, 27, 12.2, 28, 153, and 3.9 mg/L, respectively, with a range of CV values from 17 to 41 %.

TABLE 6.10 Physical and Chemical Properties of the OU 5 Core Aquifer Samples

OU 5 Well	pH	EC	Particle-Size by Hydrometer				Walkley-Black Organic Matter ---%---	TOTAL		2N KCl Extract			Saturated Paste Extract					
			Sand ---%---	Silt ---%---	Clay ---%---	Texture		Arsenic mg/kg	Selenium mg/kg	NO3-N mg/kg	NH4-N mg/kg	Ca mg/L	Mg mg/L	K mg/L	S mg/L	Cl mg/L	NO3-N mg/L	
2261	8.04	0.6	64	28	8	SL	0.3	3.31	0.882	1.80	0.74	56.0	21.2	11.1	18.3	164	3.07	
2262	8.07	0.6	64	28	8	SL	0.4	2.86	0.898	1.84	0.61	47.0	23.4	13.9	21.9	173	3.92	
2263	8.14	0.5	64	28	8	SL	0.3	4.23	0.688	1.53	0.33	46.4	23.5	12.4	26.4	129	3.50	
2264	8.13	0.8	53	36	11	SL	0.5	6.11	0.752	1.69	1.17	53.1	41.4	9.62	24.6	176	2.56	
2265	8.05	0.6	64	29	7	SL	0.3	3.44	0.897	1.69	1.19	58.8	28.6	11.7	38.7	129	3.76	
2266	8.28	0.5	89	7	4	S	0.1	3.60	0.845	1.51	1.52	55.9	20.9	9.76	18.9	130	2.83	
2267	8.12	0.7	48	41	11	L	0.6	6.10	0.748	1.57	1.47	52.3	32.5	7.78	39.6	122	3.07	
2268	8.18	0.5	58	34	8	SL	0.5	4.00	0.607	1.58	1.90	41.8	21.9	12.0	19.2	101	4.98	
2269	8.19	0.5	60	32	8	SL	0.4	4.37	0.611	1.92	2.19	32.3	14.5	12.9	20.5	148	4.16	
2270	8.17	0.5	78	15	7	LS	0.2	3.48	0.774	1.53	1.06	51.2	21.0	9.16	22.0	116	3.83	
2271	8.12	0.6	59	31	10	SL	0.5	4.39	0.773	1.75	1.65	44.4	16.3	8.49	24.9	119	4.56	
2272	8.22	0.5	64	28	8	SL	0.4	2.92	0.541	1.68	0.90	46.1	27.5	10.6	36.0	174	4.90	
2273	8.34	0.5	43	50	7	SL/L/SL	0.3	12.33	0.724	1.84	1.48	48.2	37.8	11.7	36.6	128	5.00	
2274	8.31	0.5	58	33	9	SL	0.4	8.04	0.638	1.92	1.68	36.1	21.5	12.3	24.7	129	5.16	
2275	8.24	0.8	56	33	11	SL	0.8	5.87	0.734	2.00	1.97	33.6	31.5	8.95	22.0	176	3.88	
2276	8.15	0.8	55	36	9	SL	0.5	4.13	0.533	1.83	2.17	60.5	35.0	12.9	42.6	147	4.34	
2277	8.16	0.7	58	32	10	SL	0.5	3.68	0.638	1.93	1.76	46.0	37.7	13.0	34.5	137	3.97	
2278	8.21	0.7	48	42	10	L	0.4	3.96	0.688	1.80	1.94	43.5	47.0	12.1	35.2	150	3.97	
2279	8.32	0.5	83	13	4	LS	0.2	4.35	0.579	1.69	1.80	47.0	27.0	11.9	21.8	134	3.36	
2280	7.97	0.6	71	22	7	SL	0.3	3.01	0.960	1.74	0.87	61.4	20.2	32.3	31.3	382	3.23	
<b>Average</b>	8.17	0.6	62	30	8		0.4	4.71	0.73	1.74	1.42	48.08	27.52	12.23	27.99	153.08	3.90	
<b>St deviation</b>	0.10	0.11	11.49	10.01	2.00		0.16	2.22	0.12	0.15	0.54	8.31	8.75	5.02	7.94	58.06	0.76	
<b>CV</b>	1%	19%	19%	33%	24%		40%	47%	17%	8%	38%	17%	32%	41%	28%	38%	19%	
<b>Reporting Limits</b>	0	0.1	0	0	0		0	0.01	0.01	1.25	0.05	0.08	0.007	0.46	0.07	3	0.25	

#### 6.4 Concentration of TCE and Other Chlorinated Compounds in the Study Area

As shown in Table 6.11, TCE concentrations higher than 10 µg/L were found in wells nearest Cores 2261, 2262, 2263, 2264, 2273, 2274, 2277, and 2278. Furthermore, 1,1-DCE and 1,2-cisDCE were only found in eight wells where the TCE concentrations were higher than 10 µg/L.

The majority of DCE isomer concentrations were below 4 µg/L. Vinyl chloride was found only in the well nearest Core 2262; a core near the source, the aeration curtain and the center of the plume. This core was located about 115 m from the aeration curtain system. As shown in Figure 6.8, TCE concentrations higher than 10 µg/L were mostly oriented to the south-central part of the study area.

**TABLE 6.11 Concentration of TCE, 1,1-DCE, 1,2-cisDCE, and VC in the OU 5 Study Area**

Sample OU 5	N coord	E coord	Closest Monitoring Well in OU 5	TCE	DCE11	DCE12C	VC
	m	m		µg/L	µg/L	µg/L	µg/L
2261	85091	532992	137	32	<1	2.3	<1
2262	85083	532964	138	83	0.75	19	4.1
2263	85049	532869	1072	270	2.30	3.8	<1
2264	85120	532861	1069	360	2.20	6.7	<1
2265	85274	532870	144	2.7	<1	<1	<1
2266	85308	532864	144	2.7	<1	<1	<1
2267	84974	532865	166	<1	<1	<1	<1
2268	85018	532973	1073	1	<1	<1	<1
2269	84978	532974	1034	<1	<1	<1	<1
2270	296712	532955	135	1.7	<1	<1	<1
2271	85312	532955	1026	2.9	<1	<1	<1
2272	85259	532763	160	2	<1	<1	<1
2273	85114	532763	1029	71	<1	2.8	<1
2274	85048	532761	1071	76	<1	1.5	<1
2275	84972	532761	166	<1	<1	<1	<1
2276	84990	532609	1070	<1	<1	<1	<1
2277	85036	532602	159	150	1.10	2.1	<1
2278	85112	532603	1067	220	<1	2.1	<1
2279	85251	532606	142	10	<1	<1	<1
2280	85379	532609	1025	<1	<1	<1	<1

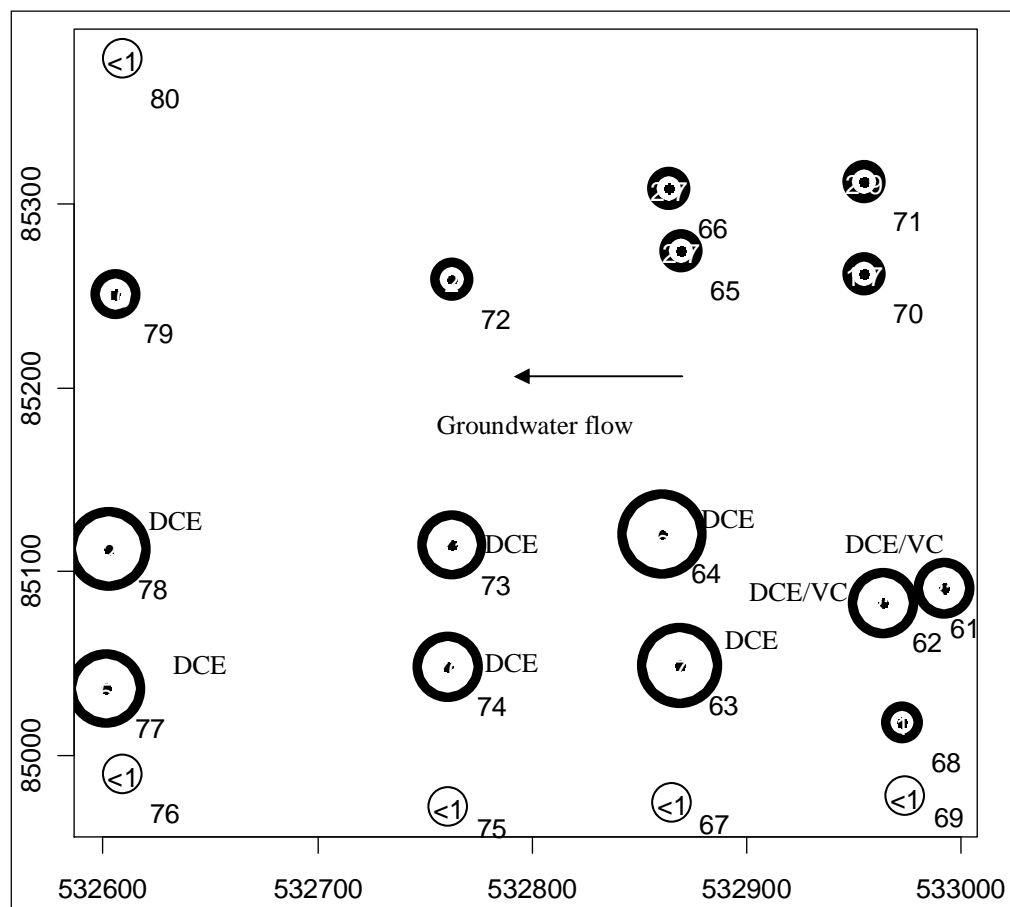


**FIGURE 6.8 TCE distribution in the OU 5 study area. Number in the circle is the TCE concentration in  $\mu\text{g/L}$ . Soil core sample identification is at the right bottom of each circle. DCE/VC indicates the locations where cis-DCE and VC concentrations have been reported in the nearest monitoring well. Arrow indicates the groundwater direction towards the western side of the study area and the OU 5 plume. 1 mg/L is the detection limit for all chlorinated compounds.**

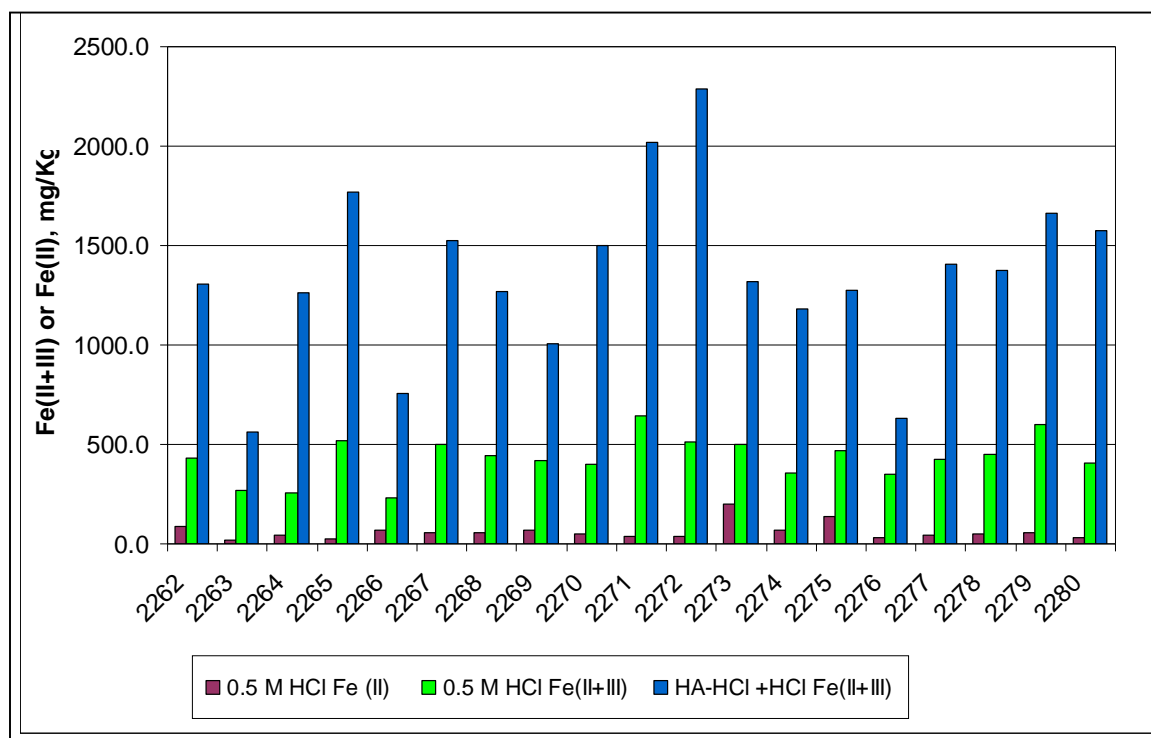
DCE isomers were also detectable in the south-central part of the area. TCE concentrations lower than 3  $\mu\text{g/L}$  were oriented to the northern and southern-most parts of the area.

### 6.5 Iron and Arsenic Reducible Forms

The concentrations of HCl extractable Fe (II) were small compare to the concentrations of HA-HCl + HCl extractable Fe (II+III). The average HCl extractable Fe

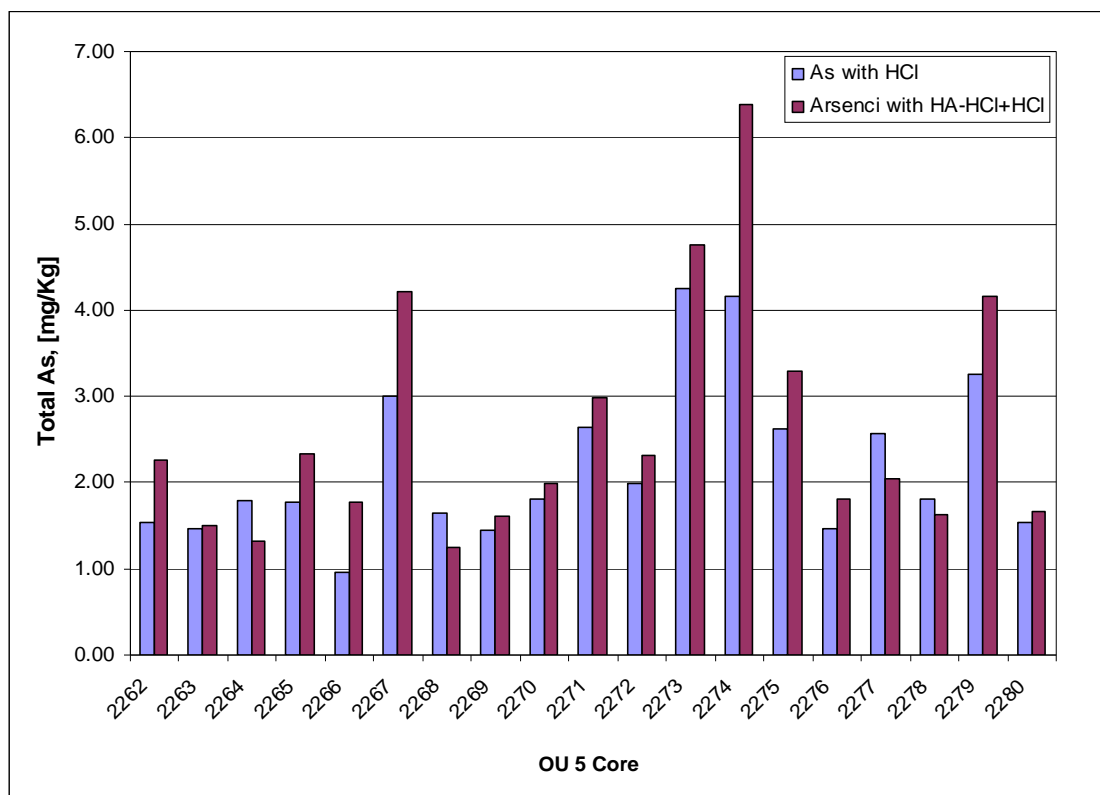
(II) was 61 mg/kg and the highest concentration of HCl extractable Fe (II) was observed in Cores 2273 and 2274. The average concentration of HCl extractable Fe (II+III) was 431 mg/kg and the average concentration of HA-HCl + HCl extractable Fe (II+III) was 1353 mg/kg. CV values were 71%, 25% and 32% for HCl extractable Fe(II) and Fe(II+III), and HA-HCl + HCl extractable Fe(II+III) (Data shown in Appendix C-1).

Figure 6.9 compares the concentrations of Fe (II+III) extracted by the two extraction methods and the concentration of Fe (II) by the HCl extraction for each soil core sample. The distribution of HA-HCL + HCl extractable Fe (II+III) was not uniform. The large quantity of the Fe (II+III) extracted by HA-HCl + HCl suggested the availability of non crystalline Fe (III) oxides which is related to the microbially reducible Fe (III) (Bio Fe III data is in Appendix C-1).



**FIGURE 6.9 Fe (II+III) by two extraction methods: HCL and HA-HCl + HCl. Released Fe (II) extracted by HCl, all measured concentrations are in mg/kg.**

This is also an indication of the generally oxidizing conditions present in the OU 5 aquifer material. Figure 6.10 shows the released total arsenic by the two extraction methods. Unlike the HA-HCl + HCl extractable Fe (II+III), there were no significant amounts of total As extracted by the HA-HCl + HCl solutions, suggesting that the majority of the arsenic forms were not removed from the non-crystalline iron oxides, which are considered to be the more microbially reducible form of iron. Total As was similarly removed from the HCl soluble Fe (III) oxides and the HA-HCL+HCl extractable, non crystalline iron oxides. Measurement errors in both methods explain the apparently higher concentration of HCl extractable total As compared to HA-HCl +HCl extractable total As in samples from cores 2264, 2268, 2277, and 2278 (Appendix C-2)



**Figure 6.10 Total arsenic by two different extraction methods.**

Further analysis of iron and arsenic by the two extraction methods were done to see if there was a linear relationship between the bacteria and functional genes and the five variables obtained in this section. Plots, shown in Appendix C-3, suggested that there was not a linear relationship between P+PNQ results and the forms of iron and arsenic by the two extraction methods.

#### **6.6 Dissolved Oxygen Concentration in the OU 5 Study Area**

The approximate saturation concentration of the groundwater, in contact with an atmosphere of 21% O<sub>2</sub>, would be 8.7 mg/L at an average altitude of 1288 m and water temperature of 15° C. The well water dissolved oxygen (DO) concentrations varied from 0.04 to 7.1 mg/L. Figure 6.11 shows different DO concentrations at each well location. The highest DO was found in the well nearest Core 2279. DO concentrations lower than 0.6 mg/L were found in three wells nearest Cores 2264, 2274, and 2280.

#### **6.7 Clustering Analysis**

Figure 6.12 shows the clustering classification of the area physical and chemical data. Three major cluster groups were selected to simplify the identification of major discriminating factors. The first cluster, indicated by the square symbol, contains six soil core samples, the next cluster, indicated by the cross sign, contains two soil cores and the last cluster labeled with the plus sign includes 12 cores.

#### **6.8 Discriminant Analysis**

Thirty-one measured variables plus the clustering group designation were used in discriminant analysis.

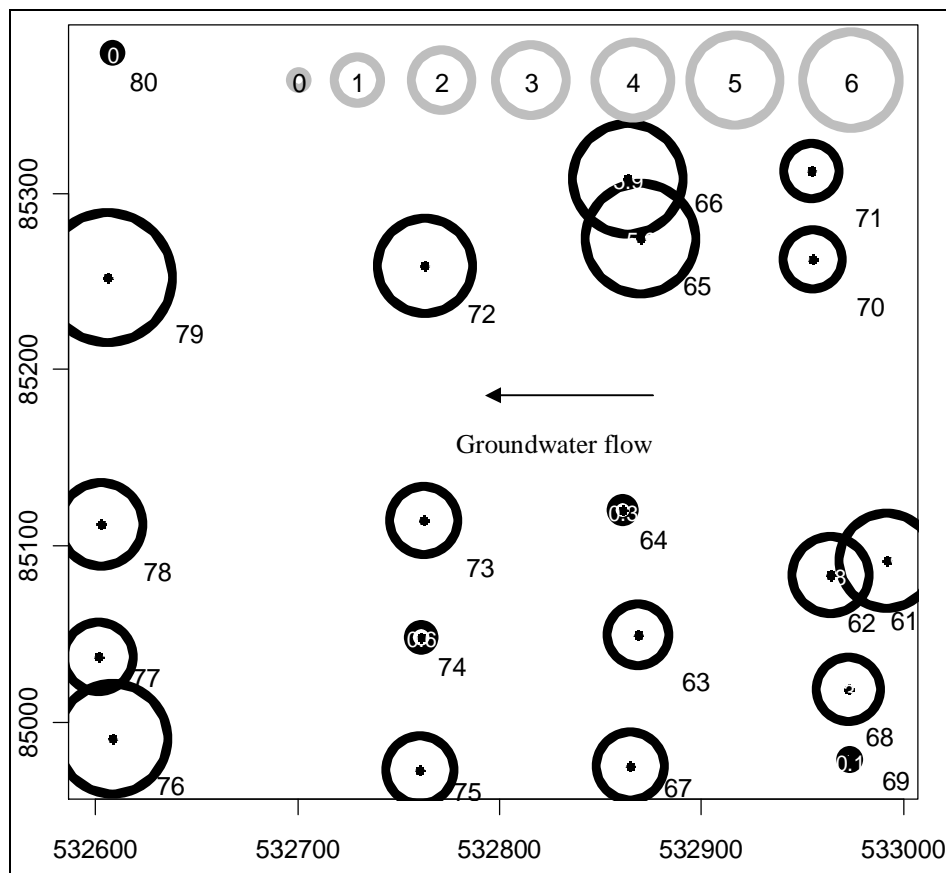


**FIGURE 6.11** Dissolved oxygen concentrations (mg/L) in the OU 5 study area.

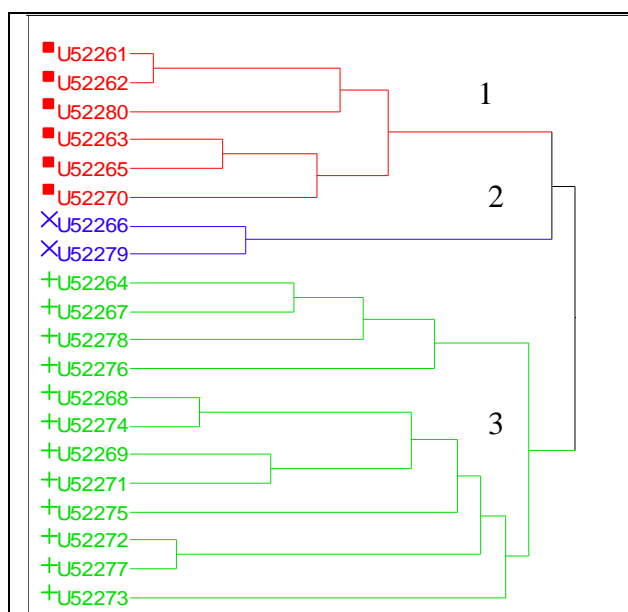


**FIGURE 6.12** Hierarchical tree classification plot of the OU 5 soil core samples. Cluster 1: square signs, Cluster 2: cross signs, Cluster 3 plus sign.

The discriminant analysis identified the five most discriminating variables based on the calculated F ratio and the associated probability of a greater F ratio. The variables that discriminated most among the three clusters were sand and silt content, KCl extractable  $\text{NH}_4^+\text{-N}$ , pH and  $\text{NO}_3^-\text{-N}$  from the saturated paste extraction ( $\text{NO}_3^-\text{-NSPE}$ ). The selected variables included in the applied model obtained high F ratios and probabilities of a greater F ratio of less than 0.05 (Appendix D-1 shows the associated probabilities and F ratios for all variables).

The canonical plot from the discriminant analysis in Figure 6.13 shows the three cluster groups bounded with a circle indicating the 95 % confidence interval for the mean, where the mean is the multivariate mean of each cluster group. The clusters were significantly different since the circles did not intersect. The canonical Axes 1 and 2 represent the linear combination of variables that best discriminate among the clusters.

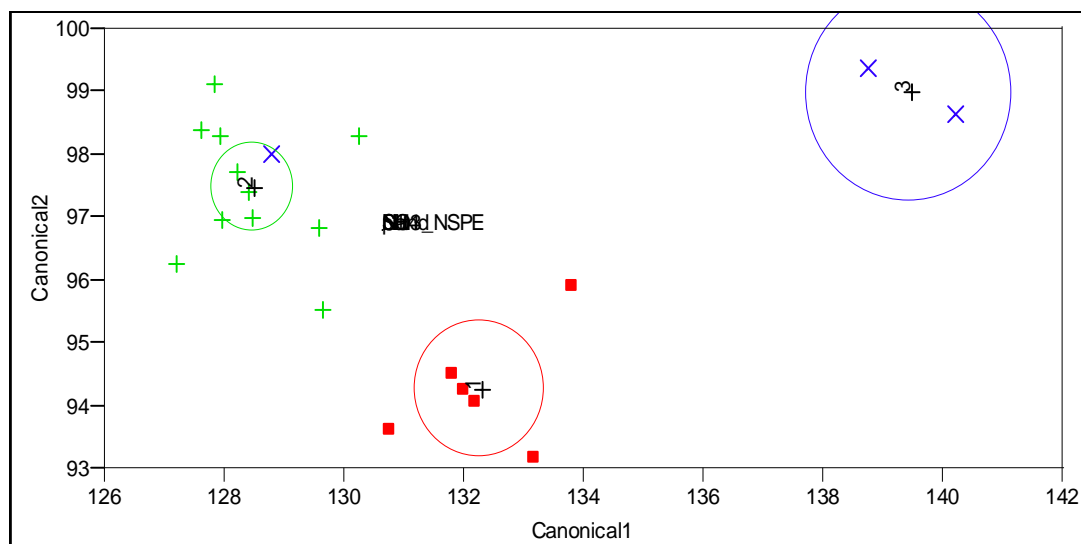


**FIGURE 6.13** Canonical plot of the discriminant analysis showing three different clusters with the 95 % confidence interval.

Table 6.12 contains the mean, standard deviation and confidence interval (CI) for the mean for the five most discriminating variables grouped in Clusters 1, 2 and 3. Cluster 3 showed the highest values of pH and sand content but the lowest value of silt and  $\text{NO}_3^-$ -N. Cluster 3 is intermediate in  $\text{NH}_4^+$ -N. Cluster 2 showed the highest silt,  $\text{NH}_4^+$ -N and  $\text{NO}_3^-$ -N, while pH and sand were intermediate and low, respectively. Cluster 1 is intermediate in sand, silt and  $\text{NO}_3^-$ -N, but is the lowest in pH and  $\text{NH}_4^+$ -N.

Table 6.13 shows the P+PNQ results of the target genes *vcrA*, *D. michiganensis*, *Geobacter* sp., and *Rhodoferrax ferrireducens*-like bacteria in the three clusters. Other genes showed a large fraction of data that were censored. The three 16s rRNA genes showed more P+PNQ and quantifiable log DNA copies to make comparisons among the clusters. According to a one-way analysis of variance (ANOVA) and assuming the conditions of independence, normality and unequal variances for the three cluster groups, the frequency means for each bacteria are not significantly different among clusters at the 95% confidence level ( $F_{2,17,0.05}$  value of 4.45), suggesting that there was no particular pattern between the genes and the discriminating variables. In addition, an ANOVA done with the *Bacteria* log DNA copies showed no significant differences among the three clusters, suggesting the similar Bacteria distribution in the three clusters (detail data and ANOVA test shown in Appendix D-2). Figure 6.14 indicates the distribution of the Clusters 1, 2, and 3 in the OU 5 study area.

**TABLE 6.12 Mean of the Discriminating Variables in Each Clustering Group**

Variables	Cluster 1 (n=6)				Cluster 2 (n=12)				Cluster 3 (n=2)			
	Mean	Stdev	95% C.I. (t=2.57)		Mean	Stdev	95% C.I. (t=2.201)		Mean	Stdev	high value	low value
pH	8.07	0.07	8.15	8.00	8.20	0.07	8.24	8.15	8.30	0.03	8.32	8.28
Sand	67.50	5.86	73.64	61.36	55.00	6.00	58.81	51.19	86.00	4.24	89.00	83.00
Silt	25.00	5.51	30.78	19.22	35.67	6.02	39.49	31.84	10.00	4.24	13.00	7.00
NH4	0.80	0.31	1.13	0.47	1.69	0.39	1.94	1.44	1.66	0.20	1.80	1.52
NO3_NSPE	3.55	0.34	3.91	3.19	4.21	0.80	4.72	3.71	3.10	0.37	3.36	2.83

TABLE 6.13 P+PNQ Results of the Target Genes in Each Clustering Group

Cluster	OU5 core	<i>D. Mich</i> P+PNQ	<i>vcrA</i> P+PNQ	<i>Geobacter</i> P+PNQ	<i>R. ferrireducens</i> like P+PNQ	Bacteria (log DNA copies/g dry soil)
1	61	1	3	0	1	5.5
1	62	2	4	2	0	6.3
1	63	2	4	3	0	4.7
1	65	0	1	0	0	5.0
1	70	4	4	0	0	5.7
1	80	0	3	1	4	5.6
2	64	3	3	1	2	6.1
2	67	1	6	0	0	5.1
2	68	2	4	2	3	6.4
2	69	3	2	1	1	5.4
2	71	1	4	0	4	5.5
2	72	1	6	2	3	6.2
2	73	0	5	0	1	5.6
2	74	0	2	2	2	6.3
2	75	0	4	0	4	6.0
2	76	1	4	0	0	4.5
2	77	0	4	0	3	6.3
2	78	0	6	2	4	5.6
3	66	1	2	0	4	6.4
3	79	0	2	0	2	5.5

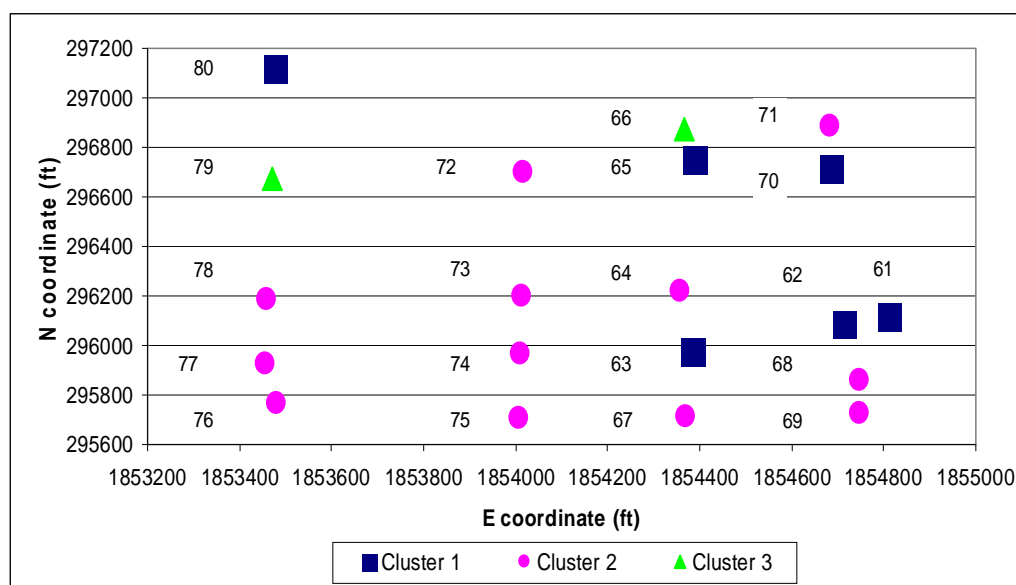


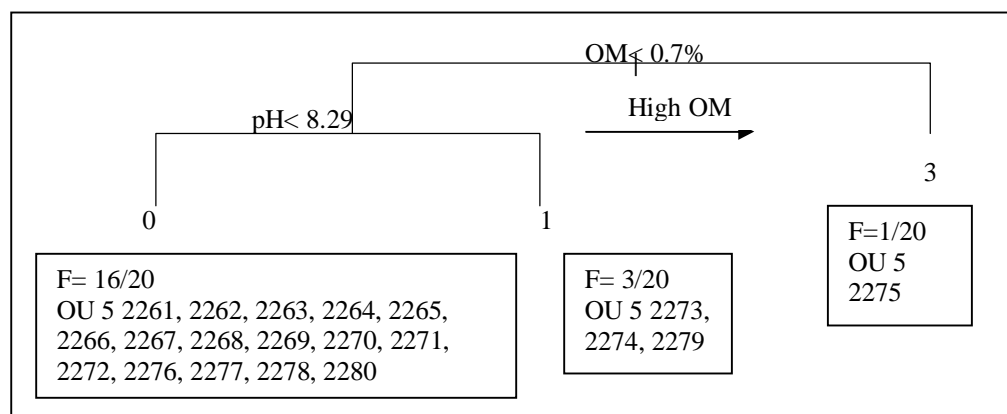
FIGURE 6.14 Location of the three clusters in the OU 5 study area.

## 6.9 Regression Tree Classification

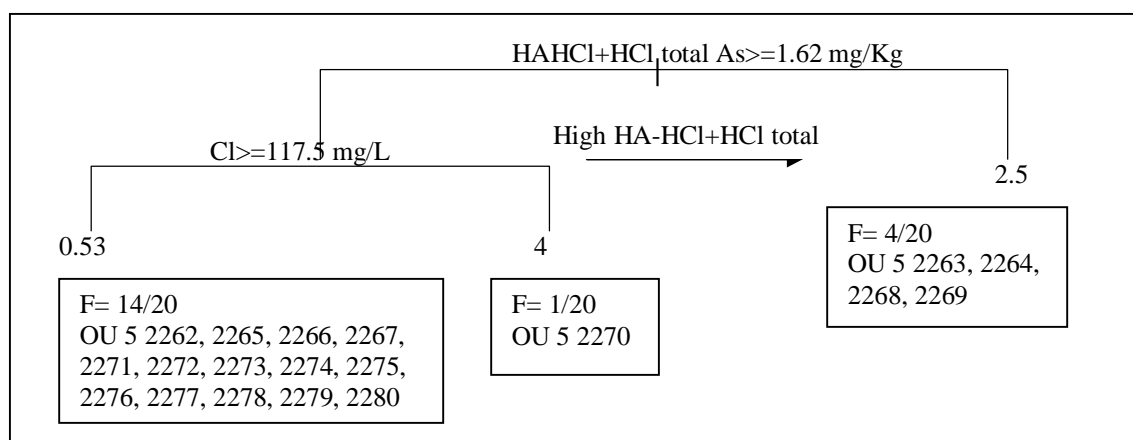
The regression tree method used all the variables shown in Table 5.1 to describe the influence of the physical-chemical properties in the 16S rRNA and functional genes frequencies. The results were not intended to be used as a predictive model between gene frequencies and the physical/chemical properties of the OU 5 aquifer material because of the limited number of non-censored observations.

Figure 6.15 shows the tree classification of the *Dehalococcoides* P+PNQ results. The method distinguished two splitting variables: organic matter and pH. Only one medium frequency of *Dehalococcoides* was observed when organic matter was higher than 0.7%. Two groups of *Dehalococcoides* frequencies were differentiated at pH 8.29; the group with no *Dehalococcoides* was found at pH values lower than 8.29 and the second group with three observations at pH higher than 8.29.

Figure 6.16 shows the tree classification for *D. michiganensis* P+PNQ results. Three groups of *D. michiganensis* frequency were obtained by the method. The first splitting point is at HAHCl+HCl total As equal to 1.62 mg/kg, cores with an average frequency of 2.5 P+PNQ were found at HAHCl+HCl total As lower or equal than 1.62 mg/kg. A single core with a frequency of 4 P+PNQ was found when HAHCl+HCl total As was higher than 1.62 mg/kg and Cl<sup>-</sup> was less than or equal to 118 mg/L. The majority of the cores, with an average frequency of 0.53 P+PNQ, were found when HAHCl+HCl total As concentrations were higher than 1.62 mg/L and Cl<sup>-</sup> concentrations were higher than 118 mg/L. The core 2261 was not classified due to the lack of measurement of HAHCl+HCl total As.



**Figure 6.15** Regression tree classification using *Dehalococcoides sp.*, P+PNQ results as the dependent variable; numbers in the branches are the splitting points and numbers at the end of the branches are the average of the P+PNQ results of the corresponding cores.



**FIGURE 6.16** Regression tree classification using *D. michiganensis* P+PNQ results as the dependent variable; numbers in the branches are the splitting points and numbers at the end of the branches are the average of the P+PNQ results of the corresponding cores.

The presence of the *vcrA* functional gene was found to be related to the amount of sand and Fe (II+III) extracted with HA-HCl in HCl, as shown in Figure 6.17. Higher frequencies of detection of the *vcrA* gene were found when sand percentages were lower than 50.5%. P+PNQ, which occurred when sand is higher than 50 % and HA-HCl+HCl Fe (II+III) was lower than 2156 mg/kg.

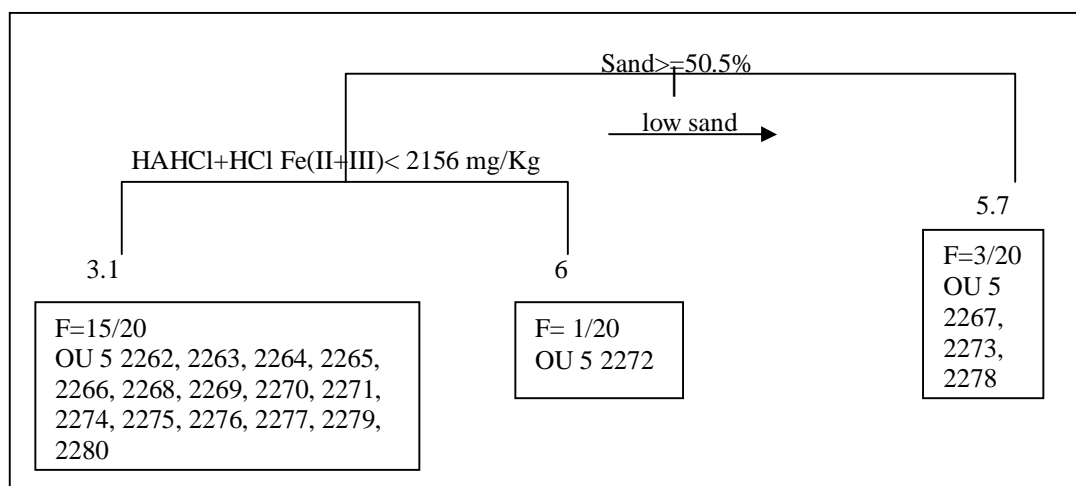


**FIGURE 6.17** Regression tree classification using *vcrA* functional gene P+PNQ results as the dependent variable; numbers in the branches are the splitting points and numbers at the end of the branches are the average of the P+PNQ results of the corresponding cores.

However, the majority of the cores fall in the group with an average of 3.1. A single core had the highest frequency of P+PNQ and it was observed when sand was higher than 50% and HA-HCl+HCl Fe (II+III) was higher than 2156 mg/kg.

The regression tree shown in Figure 6.18 indicates that 1,2 cis-DCE is the best splitting variable to classify the *Geobacter sp.* data. The regression tree indicated that frequencies of about 2.2 P+PNQ for *Geobacter sp.* occurred when concentrations of cis-DCE were higher than 2.5  $\mu\text{g/L}$ . The lowest frequency of *Geobacter sp.* occurred when 1,2 cis-DCE was lower than 2.5.

Figure 6.19 shows the tree classification of *Rhodoferrax ferrireducens*-like bacteria P+PNQ results as the dependent variable. The regression tree suggested that medium frequencies (3.3) of P+PNQ results of *Rhodoferrax ferrireducens*-like bacteria were obtained when minimum *Bacteria* concentrations were higher than 5.5 log DNA copy numbers/g.

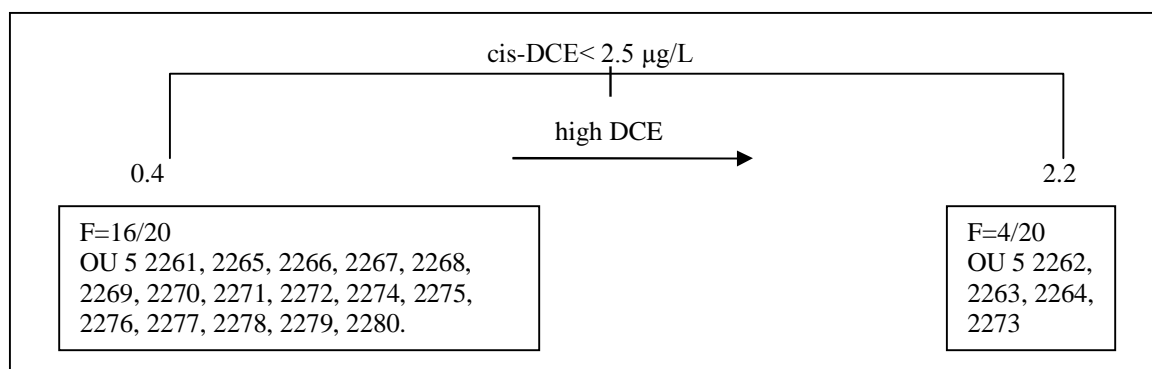


**FIGURE 6.18** Regression tree classification using *Geobacter* P+PNQ results as the dependent variable; numbers in the branches are the splitting points and numbers at the end of the branches are the average of the P+PNQ results of the corresponding cores.

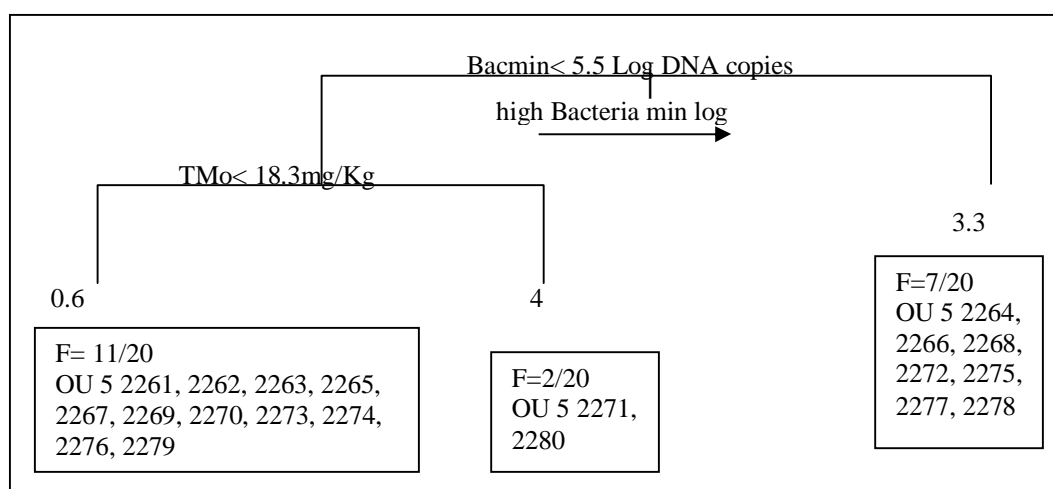


**FIGURE 6.19** Regression tree classification using *Rhodoferrax ferrireducens*-like bacteria as the dependent variable; numbers in the branches are the splitting points and numbers at the end of the branches are the average of the P+PNQ results of the corresponding cores.

The cores with lower frequencies (0.6) of P+PNQ results were found when minimum observed *Bacteria* 16S rRNA genes were lower than 5.5 log copy numbers/g and total molybdenum was lower than 18.3 mg/kg. A group with two cores was identified when minimum *Bacteria* 16S rRNA genes were lower than 5.5 log copy numbers/g and total molybdenum was higher than 18.3 mg/kg.

Figure 6.20 shows the tree classification of *tceA* functional gene P+PNQ results based on the maximum observed *Bacteria*. A group with a frequency of 1 P+PNQ results was found when maximum *Bacteria* were higher than 7.36 log DNA copies per g. The second group with undetectable P+PNQ results was found when observed maximum *Bacteria* was lower than 7.36 log DNA copies per g.

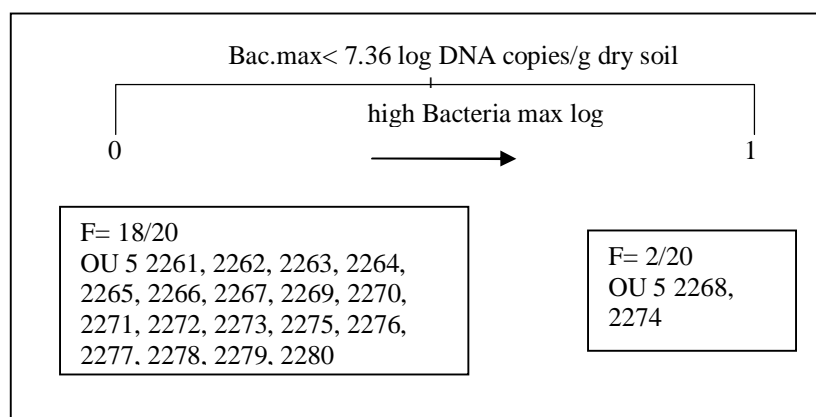


**FIGURE 6.20** Regression tree classification using *tceA* functional gene P+PNQ results as the dependent variable; numbers in the branches are the splitting points and numbers at the end of the branches are the average of the P+PNQ results of the corresponding cores.

## CHAPTER 7

## DISCUSSION

Based on the limits of quantitation for qRT-PCR developed in this study the qRT-PCR results were classified into two categories: positive and quantifiable or PNQ. This approach made all of the results useful for further analysis. The 16S rRNA gene targets had lower tolerance limits or method detection limits of between 10 and 131 copies/ $\mu$ L (Table 9). Translation of these limits to concentration per gram dry weight of aquifer material indicated a range of from 60 to  $7.9 \times 10^3$  copies/g dry weight. These detection limits are similar to those found in other studies, for example, *Geobacter lovleyi* strain SZ had a detection limit of 30 16S rRNA gene copies per  $\mu$ L (Amos et al., 2007), *Dehalococcoides* quantification with probe/primer pairs indicated a detection range of 1 to 20 and from 50 to 100 *tceA*, *bvcA* and *vcrA* gene targets per  $\mu$ L PCR volume (Ritalahti et al., 2006).

The average *Bacteria* population densities measured in the initial transect study done in 2005 were about one log higher than the average *Bacteria* density of the more recent area study. The transect results were from seven OU 5 core samples from the source area (inside HAFB Base) through the end of the plume with the highest TCE concentration.

Based on the bacterial distribution, there is a partial and low dechlorination potential in the OU 5 study area since *Dehalococcoides* sp, *D. michiganensis* and the functional gene *tceA*, the major indicator of dechlorination, were detectable but had uneven distribution and very low densities. Because of these low concentrations, improved methods of detection for 16s rRNA target genes will be required to characterize

the distribution and fate of the dechlorinating microorganisms. *Dehalococcoides* distribution was concentrated in the south-central, part of the area inside the TCE-plume and *D. michiganensis* distribution was oriented to the southeast side of the area in and outside of the plume, indicating different spatial distributions of both target genes in the study area. *Dehalococcoides sp.* was not found in cores where *D. michiganensis* was present, which may suggest that both groups of bacteria were growing independently due to the different major electron donor used during the dechlorination reaction.

However, the broader but uneven distribution of the functional gene *vcrA* in the area might suggest dechlorination capability from cis-DCE to VC in spite of the low densities of this gene. The physiological activity of this gene has been observed in the production of VC in two OU 5 monitoring wells near cores that also had the highest densities of this gene per g dry material. The distribution of *vcrA* functional gene appeared to be ubiquitous in the area irrespective of the concentration of TCE, cis-DCE and VC in the plume or the distribution of detectable *Dehalococcoides sp* in the area. The distribution of the *tceA* functional gene also suggested a similar independent distribution as the *vcrA* gene; however, the relatively high limit of detection of this gene in qRT-PCR made it difficult to further characterize its distribution.

*R. ferrireducens*-like bacteria distribution was ubiquitous with the highest densities among all studied bacteria. *Geobacter* showed a broad distribution but not everywhere as was the case for the *R. ferrireducens*-like bacteria distribution. It is important to notice that the higher densities of *Rhodoferrax ferrireducens*-like bacteria compared to other 16S genes was possibly due to the wider specificity of the primer set used in the qRT-PCR amplification.

It was expected that for natural groundwater systems, *Geobacter* sp., would be an important iron reducing competitor with dechlorinating bacteria (Lovley, 1991), but they did not seem to be a major component of the microbial community in many locations and the observed densities were close to the detection limit. Improved sensitivity for this gene will be required to further evaluate the presence and influence of these bacteria. The distribution of the two iron reducing bacteria, *Geobacter* sp. and *R. ferrireducens*-like, were spread around the entire area of study and their distribution did not appear to influence the distribution of *Dehalococcoides* and the functional genes *vcrA* and *tceA*. The differences in the spatial distribution between *R. ferrireducens*-like and *D. michiganensis* bacteria, suggest the independence of these two bacterial populations.

From the physical and chemical analysis, it is important to point out that the OU 5 site was characterized as having mainly sandy loam aquifer material with lower organic matter content typical of sandy loam soils (Paul and Clark, 1996).

The clustering and discriminant analysis multivariate methods were applied to evaluate the influence of all physical and chemical properties of the OU 5 cores in the three cluster groups. The most discriminating variables were: pH, sand, silt,  $\text{NH}_4^+$ -N and  $\text{NO}_3^-$ -N. It is noteworthy, that the observed properties of cluster 2 (higher concentrations of  $\text{NH}_4^+$ -N,  $\text{NO}_3^-$ -N and silt but lower in sand) can be related to the higher cation exchange capacity of the clay particles and SOM, that allows the accumulation of  $\text{NH}_4^+$ -N and  $\text{NO}_3^-$ -N influenced by the slow groundwater movement typical in clay-dominated aquifers. Accumulated  $\text{NH}_4^+$ -N may be converted to  $\text{NO}_3^-$ -N in the aerobic process of nitrification and denitrification, converting  $\text{NO}_3^-$ -N to  $\text{N}_2$ , may also occur if anaerobic conditions are present in the aquifer (Paul and Clark, 1996). However, the higher

concentration of  $\text{NO}_3^-$ -N in cluster 2 may indicate slow denitrification, possibly energy source (organic matter) limited, and more accumulation of  $\text{NO}_3^-$ -N in solution due to the slow-moving groundwater conditions and some nitrification.

Based on the ANOVA test, it was observed that the discriminating variables did not seem to highly influence the distribution of the bacteria and functional genes in each cluster; the distribution of the bacteria/genes appeared to be similar in the three clusters. It is important to mention, that the ANOVA test was not a very powerful tool for testing the variance among the clusters when the data did not have a normal distribution.

Multivariate methods did not completely agree on the effect of certain physical/chemical properties in the bacterial distribution; however they both indicated that pH and sand were influencing variables in the data distribution. The tree classification method showed that lower sand content best described the higher densities of the *vcrA* gene. Other splitting variables selected by the method were log *Bacteria* densities, cis-DCE concentration and organic matter. Total *Bacteria* were related to higher densities of *Rhodoferrax ferrireducens*-like bacteria and *tceA*. Cis-DCE concentrations best described to relatively higher densities of *Geobacter* sp., and organic matter described the observations of *Dehalococcoides*.

The tree classification method indicated that soluble  $\text{Cl}^-$  and total Mo were important aquifer soil components that influenced the distribution of *D. michiganensis* and *Rhodoferrax ferrireducens*-like bacteria. It is important to mention that, those components naturally exist in the OU 5 soil sediments from ancient times and their presence is related to the type of mineralogy, especially to the sandy mineral composition abundant in this aquifer. The two forms of As and Fe extracted by the HA-HCL +HCL

were also distinguishing by the tree classification method. They were related to the distribution of the *D. michiganensis* bacteria and *vcrA* functional gene, respectively. Similar to the Cl<sup>-</sup> and Mo elements, As naturally exists in the sediments and it is more related to the sandy mineral composition of the soil than to the clay fraction. Lower As indicated the relatively higher densities of *D. michiganensis*. In the opposite way, the two forms of iron are related to amount of clay minerals of the sediments, for that reason higher concentration of iron described the higher densities of the *vcrA* gene in the study area.

Multivariate statistical methods provided the tools for the evaluation of the physical/chemical properties in the study area. A larger number of observations will be required to confirm the influence of the physical/chemical properties in the bacterial and functional gene densities.

## CHAPTER 8

### CONCLUSIONS

The first project objective was to determine the limits of quantitation in qRT-PCR of the bacterial genes which were enumerated. It could be concluded that there was a low potential for dechlorination because all dechlorinating target genes had low densities, near the limits of quantification. This finding supports hypothesis 3 that there would be low concentrations of the target dechlorinating bacteria and functional genes.

The second objective was to estimate the distributions and population densities of the 16S rRNA genes of *D. ethenogenes*, *D. michiganensis*, *Geobacter spp.*, and *Rodoferax ferrireducens*-like bacteria and the functional genes *tceA* and *vcrA* in the OU 5 aquifer material. The limited area of detectable populations of *D. michiganensis* and the even more limited distribution of detectable *D. ethenogenes* suggested that biostimulated dechlorination in the study area would happen only in certain areas and that the onset of dechlorination may be delayed while dechlorinating bacteria population densities increase. The population density and distribution of the *tceA* gene could also support this conclusion. However, the broader and more uniform distribution of the *vcrA* functional gene in the study area suggests that dehalogenation capability was widely distributed in the study area and an appropriately designed application of biostimulation treatment would result in the complete dehalogenation of TCE in the site. Again, these findings support hypothesis 3.

From the determination of *Geobacter spp.*, and *Rodoferax ferrireducens*-like bacteria distribution called in objective 2, the data suggested the little or no influence of the iron reducing bacteria on *D. ethenogenes* because there was no effect on the

distribution of *D. ethenogenes* and the dehalogenation functional genes apparent from the iron-reducing bacteria distribution. Contrarily, a possible interaction (e.g., niche separation) between *R. ferrireducens*-like and *D. michiganensis* may have existed based on the different spatial distribution between these bacteria. The relatively wide distribution of the iron reducing bacteria did not support the hypothesis of low and non-uniform distribution of the iron-reducing bacteria.

The goal of Objective 3 was to evaluate the influence of Fe(II) and bioavailable Fe(III) in the aquifer material of OU 5 on the dechlorinating and iron-reducing bacteria distribution in the OU 5 plume. This study did not find any effect in the two iron-reducing bacteria distributions. This may have due to the existing oxidizing conditions of the site evidenced by the relatively high amounts of bioavailable Fe(III).

Finally, the purpose of Objective 4 was to evaluate the influences of soil texture, water soluble elements, elemental composition, pH, electrical conductivity, dissolved oxygen in well water, organic carbon,  $\text{NO}_3^-$ -N,  $\text{NH}_4^+$ -N, TCE, cis-DCE and VC in the OU 5 aquifer material on the dechlorinating and iron reducing bacteria distributions. The distributions and densities of the dechlorinating and iron-reducing bacteria in the OU 5 study area were related to the sand mineralogy and salinity of the site as described by the concentrations of soluble  $\text{Cl}^-$ , total As and Mo; the reducible Fe(III); the lower total *Bacteria*; pH and the low percent of organic matter. Three findings support this conclusion: (1) properties such as OM, pH, As and  $\text{Cl}^-$  influenced the observed densities of the two dechlorinating bacteria; (2) total *Bacteria* and the bioavailable Fe (III) affected the densities of the two functional genes and (3) cis-DCE, total *Bacteria* and Mo influenced the observed distribution and densities of the two iron-reducing bacteria.

In conclusion, the selection of the target gene with its particular detection limit plus the physical/chemical properties in a biostimulated study of a TCE-contaminated site will likely affect the outcome of the evaluation of the site dechlorinating capability using the procedures of this study.

## CHAPTER 9

### ENGINEERING SIGNIFICANCE

Dechlorinating capabilities of this site are strictly related to the presence of influencing factors listed by Zhou (2008), to achieve bioremediation by bioaugmentation. Those factors include the physical and chemical properties, the available carbon donor, the native microbial community and its enzymatic diversity, the potential competition for electron donors and the microbial and enzymatic properties of the added microbial community, if there is bioaugmentation.

The site evaluation done in this study included the microbial dechlorinating populations which were in low densities or not detectable in many locations; the low organic matter that it is believed does not enhance the microbial growth of the existing dechlorinating bacteria; the wide-spread enzymatic properties for dechlorination from cis-DCE to VC (i.e, *vcrA* functional gene) but the low availabilities for TCE reduction to ethene (i.e, *tceA* functional gene); the physical and chemical properties directly related to the sandy mineralogy, salinity and pH; and the existence of oxidizing conditions that can support iron-reducing bacteria. From this evaluation, the characterized factors in OU 5 did not completely match the factors listed by Zhou (2008), which suggest the reasons of the actual incomplete dechlorination of TCE in the OU 5 site even with the biostimulation that occurred accidentally when the air sparge treatment was installed. However, complete dechlorination to ethene by bioaugmentation can be achieved if biostimulation by a carbon and energy (hydrogen) donor is applied in the OU 5 area.

This study has enhanced our understanding of the importance of knowing the physical/chemical/biological properties of a TCE-contaminated plume before the implementation of the bioaugmentation with biostimulation design in a TCE groundwater contaminated site. Cost-effective decisions based on the correct application of the bioaugmentation where engineered, near optimal physical/chemical conditions exist are the key for successful implementation of the treatment design and usefulness of the biostimulation/bioaugmentation during bioremediation of sites with low dechlorinating capabilities as was the case in the OU 5 study area.

## CHAPTER 10

### FUTURE STUDIES

Improved molecular biology techniques are needed to decrease the detection limits of the studied genes. Those molecular tools will help to efficiently characterize the bacterial distribution of a TCE-contaminated plume as well as quantify all microbial communities present in the aquifer with confidence and minimum detection limits.

A systematic differentiation between quantifiable and PNQ values is required in order to make PNQ values more useful and meaningful. One approach could be determining the area under the melting curve dRFU/time for the PNQ samples and comparing it with the area under the curve of a standard with a concentration very near the detection limit. Consequently, every PNQ result will be represented by a ratio less than one. Similarly, quantifiable results can have a ratio by doing the calculation with their own areas. This ratio will be higher than 1. With this approach, one core with six replicate samples can have descriptive values like the mean and standard deviation. This then would allow using PNQ and quantifiable results on the same scale for future statistical analysis.

The inclusion of other *Dehalococcoides* strains such as FL2 and BAV1 as well as other genes such as those from methanogens and sulfate-reducing microorganisms is very important to further characterize the bacterial community in the OU 5 site. The inclusion of methanogens and sulfate reducing bacteria will help clarify the hydrogen utilization system in the aquifer as well as the redox conditions of the site. The knowledge of the other *Dehalococcoides* strains will help determine the dominant pathway of VC reduction occurring in the site.

## REFERENCES

- Adrian, L., U. Szewzyk, J. Wecke, and H. Görisch. 2000. Bacterial dehalorespiration with chlorinated benzenes. *Nature* 408:580-583.
- Amos, B., Y. Sung, K.E. Fletcher, T.J. Gentry, W. Wu, C. S. Criddle, J. Zhou, and F. Löffler. 2007. Detection and quantification of *Geobacter lovleyi* strain SZ: implications for bioremediation at tetrachloroethene-(PCRE) and uranium-impacted sites. *Appl. Environ. Microbiol.* 73:6898-6904.
- AFCEE and NFESC. 2004. Principles and practices of enhanced anaerobic bioremediation of chlorinated solvents. Force Center for Environmental Excellence, Brooks Air Force Base, Texas and Naval Facilities Engineering Service Center (NFESC), Port Hueneme, CA.
- APHA. 1998, *American Public Health Association: Standard Methods for the examination of water and wastewater*. Washington, DC: GPO.
- Applied Biosystems. 2006. Real-time PCR vs. traditional PCR, posting as the technical support services in June 2006, <http://www.appliedbiosystems.com/support/apptech/>.
- Avrahami, S., and B. J. M. Bohannan. 2007. Response of *Nitrosospira* sp. strain AF-like ammonia oxidizers to changes in temperature, soil moisture content and fertilizer concentration. *Appl. Environ. Microbiol.* 73:1166-1177.
- Bio-Rad Laboratories, Inc. 2004a. iCycle iQ™ Real Time PCR detection system, instruction manual, posting to the Bio-Rad literature index, July 21, 2008, <http://www.bio-rad.com/B26/BioRad/literature/>.
- Bio-Rad Laboratories, Inc. 2004b. Real time PCR application guide. Bulletin 5279 US/EG Rev A. Hercules, CA.
- Bitton, G. 2005. *Wastewater microbiology*. New Jersey: John Wiley & Sons, Inc.
- Cantor, Ch., and C. Smith. 1999. *Genomics the science and technology behind the human genome project*. New York: John Wiley & Sons, Inc.
- Chang, Y. C., M. Hatsu, K. Jung, Y. S. Yoo, and K. Takamizawa. 2000. Isolation and characterization of a tetrachloroethylene dechlorinating bacterium, *Clostridium bifermentans* DPH-1. *J. Biosci. and Bioengineering* 89:489-491.
- Chambers, J., R. Becker, and A. Wilks. 1991. *The new S language*. New York: Chapman & Hall.

- Coppi, M., V. Ching Leang, S.J. Sandler, and D.R. Lovley. 2001. Development of a genetic system for *Geobacter sulfurreducens*. *Appl. Environ. Microbiol.* 67:3180-3187.
- Cummings, D.E., O.L. Snoeyenbos-West, D.T. Newby, A.M. Niggemyer, D.R. Lovley, L.A. Achenbach, and R.F. Rosenzweig. 2003. Diversity of *Geobacteraceae* species inhabiting metalpolluted freshwater lake sediments ascertained by 16S rDNA analyses. *Microb. Ecol.* 46:257-269.
- Dupont, R.R., D.L. Sorensen, J.E. McLean, W.J. Doucette, and M. Loucks. 2003. Enhancement of trichloroethylene degradation via carbon donor and microbial amendment addition. Paper presented at the seventh international in situ and on-site bioremediation symposium, June 2-5, in Orlando, Florida.
- Evans, P. J., and S.S. Koenigsberg. 2001. A bioavailable ferric iron assay and relevance to reductive dechlorination. Paper presented at the sixth international in situ and on site bioremediation symposium, June 4-7, in San Diego, CA.
- Finneran, K.T., C.V. Johnsen, and D.R. Lovley. 2003. *Rhodoferrax ferrireducens* sp. nov., a psychrotolerant, facultatively anaerobic bacterium that oxidizes acetate with the reduction of Fe(III). *International J. Systematic Evol. Microbiol.* 53:669-673.
- Gavlack, R., D. Horneck, R.O. Miller, and J. Kotuby-Amacher. 2003. *Soil, plant and water reference methods for western region*. Second edition. [http://cropandsoil.oregonstate.edu/nm/WCC103/Soil\\_Methods.htm](http://cropandsoil.oregonstate.edu/nm/WCC103/Soil_Methods.htm) [accessed July 18, 2008].
- Gerritse, J., V. Renard, T.M. Pedro Gomes, P.A. Lawson, M.D. Collins, and J. C. Gottscha. 1996. *Desulfitobacterium* sp. strain PCE1, an anaerobic bacterium that can grow by reductive dechlorination of tetrachloroethene or ortho-chlorinated phenols. *Archives of Microbiology* 165:132-140.
- Gerritse, J., O. Drzyzga, G. Kloetstra, M. Keijmel, L.P. Wiersum, R. Hutson, M.D. Collins, and J.C. Gottschal. 1999. Influence of different electron donors and acceptors on dehalorespiration of tetrachloroethene by *Desulfitobacterium frappieri* TCE1. *Appl. Environ. Microbiol.* 65:5212-5221.
- Hastie, T., R. Tibshirani, and J. Friedman. 2001. *The elements of statistical learning data mining, inference and prediction*. New York: Springer-Verlag.
- He, J., K.M. Ritalahti, K.L. Yang, S.S. Koenigsberg, and F.E. Löffler. 2003. Detoxification of vinyl chloride to ethene coupled to growth of an anaerobic bacterium. *Nature* 424:62-65.
- He, J., Y. Sung, R. Krajmalnik-Brown, K.M. Ritalahti, and F.E. Löffler. 2005. Isolation and characterization of *Dehalococcoides* sp. strain FL2, a trichloroethene (TCE) - and 1,2-dichloroethene-respiring anaerobe. *Appl. Environ. Microbiol.* 71:1442-1450

- Hendrickson, E.R., J. Payne, R.M. Young, M.G. Starr, M.P. Perry, S. Fahnestock, D.E. Ellis, and R.C. Ebersole. 2002. Molecular analysis of *Dehalococcoides* 16S ribosomal DNA from chloroethene-contaminated sites throughout North America and Europe. *Appl. Environ. Microbiol.* 68:485-495
- Holliger, C., G. Wohlfarth, and G. Diekert. 1998. Reductive dechlorination in the energy metabolism of anaerobic bacteria. *FEMS Microbiol. Reviews* 22:383-398.
- Holliger, C., D. Hahn, H. Harmsen, W. Ludwig, W. Schumacher, B. Tindall, F. Vazquez, N. Weiss, and A.J.B. Zehnder. 1999. *Dehalobacter restrictus* gen. nov., a strictly anaerobic bacterium that reductively dechlorinates tetra- and trichloroethene in an anaerobic respiration. *Archives of Microbiology* 169:313-321.
- Hyman, M., and R.R. Dupont. 2001. *Groundwater and soil remediation: Process design and cost estimating of proven technologies*. City, VA: American Society of Civil Engineers Press.
- Kochanowski, B., and R. Udo. 1999. *Quantitative PCR Protocols*. City, NY: Humana Press.
- Krajmalnick-Brown, R. 2005. Genetic identification of reductive dehalogenase genes in *Dehalococcoides*. PhD Dissertation, Georgia Institute of Technology.
- Kästner, M. 1991. Reductive dechlorination of tri- and tetrachloroethylenes depends on transition from aerobic to anaerobic conditions. *Appl. Environ. Microbiol.* 57:2039-2046.
- Krumholz, L. R. 1997. *Desulfuromonas chloroethenica* sp. nov. uses tetrachloroethylene and trichloroethylene as electron acceptors. *International J. Systematic Bacteriol.* 47:1262-1263.
- Lee, M.D., J.M. Odom, and R.J. Buchanan. 1998. New perspectives on microbial dehalogenation of chlorinated solvents: Insights from the field. *Annual Review of Microbiol.* 52:423-452.
- Löffler, F.E., K.M. Ritalahti, and J.M. Tiedje. 1997. Dechlorination of chloroethenes is inhibited by 2-bromoethanesulfonate in the absence of methanogens. *Appl. Environ. Microbiol.* 63:4982-4985.
- Lovley, D., and E.J.P. Phillips. 1987. Rapid assay for microbially reducible ferric iron in aquatic sediments. *Appl. Environ. Microbiol.* 53:1536-1540.
- Lovely, D.R. 1991. Dissimilatory Fe(III) and Mn(IV) Reduction. *Environ. Sci. Technology* 25:1062-1067.

- Lovley, D.R. 1995. Bioremediation of organic and metal contaminants with dissimilatory metal reduction. *Ind. Microbiol.* 14:85–93.
- Lu, X., S. Tao, T. Wilson, and J. Gerritze. 2001. Characteristic hydrogen concentration for various redox processes in batch study. *Environ. Sci. Health* A36:1725-1734.
- Lu, X., J.T. Wilson, and D.H. Kampbell. 2006. Relationship between geochemical parameters and the occurrence of *Dehalococcoides* DNA in contaminated aquifers. *Water Resour. Res.* 42W08427.
- Magnuson, J.K., M.F. Romine, D.R. Burris, and M.T. Kingsley. 2000. Trichloroethene reductive dehalogenase from *Dehalococcoides ethenogenes*: Sequence of *tceA* and substrate range characterization. *Appl. Environ. Microbiol.* 66:5141-5147.
- Magnuson, J.K., R.V. Stern, J.M. Gossett, S.H. Zinder, and D.R. Burris. 1998. Reductive dechlorination of tetrachloroethene to ethene by a two-component enzyme pathway. *Appl. Environ. Microbiol.* 64:1270-1275.
- Major, D.W., M.L. McMaster, E.E. Cox, E.A. Edwards, S.M. Dworatzek, E.R. Hendrickson, M.G. Starr, J. Payne, and L.W. Buonamici. 2002. Field demonstration of successful bioaugmentation to achieve dechlorination of tetrachloroethene to ethene. *Env. Sci. Technol.* 36:5106-5116.
- Maymó-Gatell, X., Y.T. Chien, J.M. Gossett, and S.H. Zinder. 1997. Isolation of a bacterium that reductively dechlorinates tetrachloroethene to ethene. *Science* 276:1568-1571.
- Maymó-Gatell, X., T. Anguish, and S.H. Zinder. 1999. Reductive dechlorination of chlorinated ethenes and 1,2-dichloroethane by “*Dehalococcoides ethenogenes*” 195. *Appl. Environ. Microbiol.* 65:3108-3113.
- Maymó-Gatell, X., I. Nijenhuis, and S.H. Zinder. 2001. Reductive dechlorination of cis-dichloroethene and vinyl chloride by *Dehalococcoides ethenogenes*. *Environ. Sci. Technol.* 35:516-521.
- Miller, E., G. Wohlfarth, and G. Diekert. 1997. Comparative studies on tetrachloroethene reductive dechlorination mediated by *Desulfitobacterium* sp. strain PCE-S. *Archives Microbiol.* 168:513-519.
- MoBio Laboratories. Ultra Clean Soil DNA Isolation Instruction Manual. 2008. Posting to support-protocols list, July 21, 2008, <http://www.mobio.com/support/protocols.php>
- Müller J.A., B.M. Rosner, G. Abendroth, G. Meshulam-Simon, P.L. McCarty, and A.M. Sporman. 2004. Molecular identification of the catabolic vinyl chloride reductase

- from *Dehalococcoides* sp. Strain VS and its environmental distribution. *Appl. Environ. Microbiol.* 70:4880-4888.
- Montgomery Watson Harza. 2001. *Final conceptual model for operable unit 5*. Hill Air Force Base, Utah.
- Nakatsu C.H., V. Torsvik, and L. Øvreås. 2000. Soil community analysis using DGGE of 16S rDNA polymerase chain reaction products. *Soil Sci. Soc. Am.* 64:1382–1388.
- National Primary Drinking Water Regulation. Federal Register 40 C.F.R Section 141.61, US EPA, Washington, DC, 1 July 1, 2002, p. 426.
- Ostle, B. 1963. *Statistics in research*. Ames: Iowa State University Press.
- Paul, E.A., and F.E. Clark. 1996. *Soil microbiology and biochemistry*. City, CA: Academic Press.
- Prescott, L., J. Harley, and D. Klein. 2002. *Microbiology*. New York: McGraw-Hill.
- R: A language and environment for statistical computing. Version 2.5.1 (R 2.5.1). R development Core Team, R Foundation for Statistical Computing, Vienna.
- Ritalahti, K.M., B.K. Amos, Y. Sung, Q. Wu, S.S. Koenigsberg, and F.E. Löffler. 2006. Quantitative PCR targeting 16S rRNA and reductive dehalogenase genes simultaneously monitors multiple *Dehalococcoides* strains. *Appl. Environ. Microbiol.* 72:3784-3790.
- Roden, E.E., and J.M. Zachara. 1996. Microbial reduction of crystalline Fe(III) oxides: Role of oxide surface area and potential for cell growth. *Environ Sci Technol.* 30:1618–1628.
- SAS Institute. 2002. JMP Ver 5. SAS Institute Inc., Cary, NC.
- Sung, Y., K.M. Ritalahti, R.A. Sanford, J.W. Urbance, S.J. Flynn, J.M. Tiedje, and F.E. Löffler. 2003. Characterization of two tetrachloroethene (PCE)-reducing, acetate-oxidizing anaerobic bacteria, and their description as *Desulfuromonas michiganensis* sp. nov. *Appl. Environ. Microbiol.* 69:2964-2974.
- Vogel, T.M., and P.L. McCarty. 1987. Abiotic and biotic transformations of 1,1,1-trichloroethane under methanogenic conditions. *Environ. Sci. Technol.* 21:1208–1213.
- US Environmental Protection Agency (EPA). 1986. Test methods for Evaluating Solid Waste SW 846. Washington, DC.

- Walkley, A., and I.A. Black. 1934. An examination of the Degtjareff method for determining soil organic matter, and a proposed modification of the chromic acid titration method. *Soil Sci.* 37:29–38.
- Wild, A., R. Hermann, and T. Leisinger. 1996. Isolation of an anaerobic bacterium which reductively dechlorinates tetrachloroethene and trichloroethene. *Biodegradation* 7:507-511.
- Zhou J. 2008. The development of molecular tools for the evaluations of the bioremediation of chlorinated solvents. PhD Dissertation, Utah State University.

## APPENDICES

## **Appendix A**

### **Tolerance Limits of the Studied 16S rDNA Primers**

## **Appendix B**

### **qRT-PCR Results of the Target 16S rDNA Primers in the Soil Core Samples**

## **Appendix C**

### **Iron and Arsenic Data in the OU 5 Aquifer Core Samples**

## Appendix C-1

Different Forms of Iron obtained by two extraction methods

Sample Name OU5	0.5 M HCl Fe (II) (mg/kg)	0.5 M HCl Fe(II+III) (mg/kg)	0.5 M HCl Fe (III) (mg/kg)	Ratio Fe(III)/Fe(II) ( )	HA-HCl +HCl Fe(II+III) (mg/kg)	Bio Fe III (mg/kg)	Ratio Fe(III)/Fe(II) ( )
2262	88.2	431.7	343.5	3.9	1308	1220	13.8
2263	16.4	270.7	254.3	15.6	561	545	33.3
2264	43.1	258.4	215.2	5.0	1264	1221	28.3
2265	27.3	516.3	489.0	17.9	1771	1744	63.8
2266	66.3	232.6	166.3	2.5	755	688	10.4
2267	59.1	497.8	438.7	7.4	1523	1464	24.8
2268	53.5	443.4	389.9	7.3	1272	1218	22.8
2269	66.0	419.3	353.4	5.4	1009	943	14.3
2270	47.7	403.0	355.3	7.4	1499	1451	30.4
2271	38.9	646.6	607.6	15.6	2021	1982	50.9
2272	38.0	514.7	476.7	12.6	2290	2253	59.3
2273	199.7	499.6	299.9	1.5	1322	1122	5.6
2274	68.7	354.6	286.0	4.2	1180	1111	16.2
2275	140.1	469.7	329.6	2.4	1273	1133	8.1
2276	28.9	350.9	322.0	11.1	632	603	20.8
2277	41.9	423.1	381.1	9.1	1405	1363	32.5
2278	50.6	447.1	396.5	7.8	1375	1325	26.2
2279	56.7	598.1	541.4	9.5	1661	1604	28.3
2280	30.2	405.7	375.4	12.4	1577	1547	51.2
Mean	61.1	430.7	369.6	8.3	1352.5	1291.3	28.5
stdev	43.1	107.6	108.9	4.8	433.1	437.8	17.0
CV	71%	25%	29%	58%	32%	34%	60%

## Appendix C-2

Arsenic forms obtained by two extraction methods

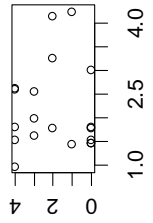
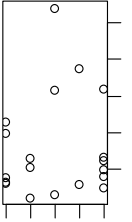
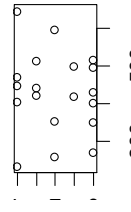
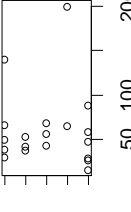
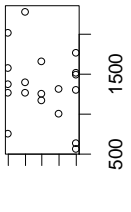
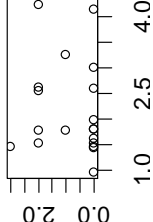
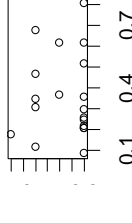
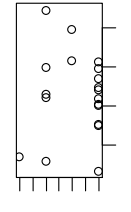
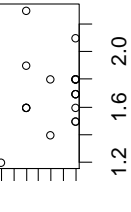
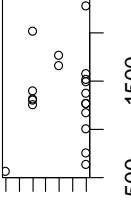
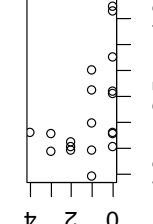
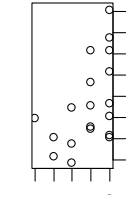
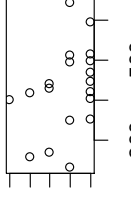
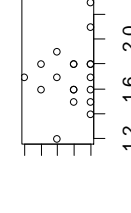
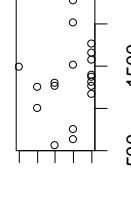
OU 5 core sample	0.5 M HCl	HA-HCl +HCl	ratio
	As(III+V)	As(III+V)	HCl As/HA-HCl+HCl
	mg/kg	mg/kg	As(III+V)
2262	1.54	2.26	68
2263	1.47	1.51	98
2264	1.79	1.31	136
2265	1.78	2.33	76
2266	0.96	1.77	54
2267	3.01	4.21	71
2268	1.64	1.24	132
2269	1.44	1.61	89
2270	1.82	2.00	91
2271	2.64	2.98	89
2272	1.99	2.31	86
2273	4.26	4.76	89
2274	4.16	6.39	65
2275	2.62	3.29	80
2276	1.47	1.81	81
2277	2.57	2.05	126
2278	1.81	1.63	111
2279	3.26	4.16	78
2280	1.55	1.66	93
mean	2.20	2.59	90.23
Stdev	0.93	1.38	22.26
High CI	2.64	3.26	100.96
LowCI	1.75	1.93	79.50

## Appendix C-3

Linear plots between studied bacteria and functional genes as P+PNQ results and the two forms of Iron and Arsenic by the two extraction methods

X	HCl_As (III+V)	HA- HCl+HCl As (III+V)	HCl_Fe (II+III)	HCl_Fe(II)	HAHCl+HCl Fe(II+III)
Y					
<i>Dehalococcoides</i>					
<i>vcrA</i>					
<i>tceA</i>					

## Appendix C-3 cont

X	HCl_As (III+V)	HA-HCl+HCl As (III+V)	HCl_Fe (II+III)	HCl_Fe(II)	HAHCl+HCl Fe(II+III)
Y	HCl_As (III+V)	HA-HCl+HCl As (III+V)	HCl_Fe (II+III)	HCl_Fe(II)	HAHCl+HCl Fe(II+III)
<i>Rhodoferax ferrireducens-like</i>					
<i>Geobacter</i>					
<i>D. michiganensis</i>					

## **Appendix D**

### **Discriminant Analysis and ANOVA Results**

## Appendix D-1

## Most Relevant Variables Obtained in the Discriminatory Data Analysis

Entered	Column	F Ratio	Prob>F
	X	0.149	0.863061
	Y	0.594	0.568752
	EUmean	0.615	0.5582
	Eumin	1.607	0.244231
	Eumax	0.174	0.842469
	vcraA	0.601	0.565076
	DO	2.376	0.138743
	HCLAs	0.605	0.563387
	HAHCLAs	1.346	0.299878
	TFe	0.778	0.48305
	Fe(II)	0.1	0.905764
X	pH	6.262	0.013723
X	Sand	12.418	0.001195
	Clay	.	.
	OM	0.496	0.622079
	Selenium	0.745	0.497375
X	NH4	4.492	0.034977
	CaSPE	0.319	0.733485
	MgSPE	0.091	0.913831
	SSPR	0.101	0.904888
X	NO3_NSP	9.973	0.00281
	TAI	0.156	0.857334
	TCa	0.372	0.697434
	TCr	0.446	0.650975
	TK	0.255	0.779212
	TMg	1.114	0.362539
	TMn	1.052	0.381999
	TMo	1.132	0.357134
	TSr	0.697	0.518897
	NO3	0.415	0.66997
X	Silt	7.647	0.007222

## Appendix D-2

P+PNQ results for the studied bacteria and functional genes

Cluster	OU5 core	Dehaloc	D. Mich	vcrA	tceA	Geobacter	Rhodo	Bacteria log
1	61	0	1	3	1	0	1	5.5
1	62	0	2	4	1	2	0	6.3
1	63	0	2	4	0	3	0	4.7
1	65	0	0	1	0	0	0	5.0
1	70	0	4	4	1	0	0	5.7
1	80	0	0	3	1	1	4	5.6
<b>Average</b>		<b>0</b>	<b>2</b>	<b>3</b>	<b>1</b>	<b>1</b>	<b>1</b>	<b>5.46</b>
<b>Variance</b>		<b>0</b>	<b>2</b>	<b>1</b>	<b>0</b>	<b>2</b>	<b>3</b>	<b>0</b>
2	64	0	3	3	0	1	2	6.1
2	67	0	1	6	0	0	0	5.1
2	68	0	2	4	0	2	3	6.4
2	69	0	3	2	0	1	1	5.4
2	71	0	1	4	0	0	4	5.5
2	72	0	1	6	0	2	3	6.2
2	73	0	0	5	1	0	1	5.6
2	74	1	0	2	0	2	2	6.3
2	75	1	0	4	2	0	4	6.0
2	76	3	1	4	0	0	0	4.5
2	77	0	0	4	0	0	3	6.3
2	78	1	0	6	0	2	4	5.6
<b>Average</b>		<b>1</b>	<b>1</b>	<b>4</b>	<b>0</b>	<b>1</b>	<b>2</b>	<b>5.75</b>
<b>Variance</b>		<b>1</b>	<b>1</b>	<b>2</b>	<b>0</b>	<b>1</b>	<b>2</b>	<b>0</b>
3	66	0	1	2	0	0	4	6.4
3	79	1	0	2	2	0	2	5.5
<b>Average</b>		<b>1</b>	<b>1</b>	<b>2</b>	<b>1</b>	<b>0</b>	<b>3</b>	<b>5.93</b>
<b>Variance</b>		<b>0.5</b>	<b>0.5</b>	<b>0</b>	<b>2</b>	<b>0</b>	<b>2</b>	<b>0.37</b>

ANOVA Tests

Geobacter				
Source of Variation	Sum of squares	Degrees of Freedom	Mean Square	F ratio
Between clusters	1.53	2	0.77	0.61
Within clusters	21.29	17	1.25	
Total	22.83	19		not diiferent
Total average	0.80		F table	4.45

<b>Bacteria</b>				
Source of Variation	Sum of squares	Degrees of Freedom	Mean Square	F ratio
Between clusters	0.47	2	0.23	2.16
Within clusters	1.83	17	0.11	
Total	2.29	19		not diiferent
Total average	5.68		F table	4.45

<b>Rhodoferrax ferrireducens-like</b>				
Source of Variation	Sum of squares	Degrees of Freedom	Mean Square	F ratio
Between clusters	10.72	2	5.36	1.01
Within clusters	90.40	17	5.32	
Total	101.12	19		not different
Total average	1.90		F table	4.45

<b>D. Michiganensis</b>				
Source of Variation	Sum of squares	Degrees of Freedom	Mean Square	F ratio
Between clusters	1.80	2	0.90	0.34
Within clusters	44.52	17	2.62	
Total	46.32	19		not di
Total average	1.10		F table	4.45

<b>vcrA</b>				
Source of Variation	Sum of squares	Degrees of Freedom	Mean Square	F ratio
Between clusters	10.05	2	5.03	1.64
Within clusters	52.02	17	3.06	
Total	62.07	19		not different
Total average	3.65		F table	4.45

<b>Dehalococcoides</b>				
Source of Variation	Sum of squares	Degrees of Freedom	Mean Square	F ratio
Between clusters	1.05	2	0.52	1.17
Within clusters	7.61	17	0.45	
Total	8.66	19		not different
Total average	0.35		F table	4.45

<b>tce A</b>				
Source of Variation	Sum of squares	Degrees of Freedom	Mean Square	F ratio
Between clusters	1.21	2	0.61	1.74
Within clusters	5.93	17	0.35	
Total	7.14	19		not different
Total average	0.43		F table	4.45